REMARKS

Claims 2-3, 6-31, and 33-35 constitute the pending claims in the present application. Claims 1-2, 4-18, 21, and 29 were elected with traverse. Applicants will cancel non-elected claims upon indication of allowable subject matter. Please cancel claims 1, 4, and 32 without prejudice. Claims 2, 6-11, 29, and 31 have been amended. Support for the amendments is found throughout the specification. Dependent claims 33-35 have been added and support for this subject matter can be found in the specification (e.g., page 2, lines 11-16; page 14, lines 7-10). No new matter has been added. Applicants respectfully request reconsideration in view of the following remarks. Issues raised by the Examiner will be addressed below in the order they appear in the prior Office Action.

Applicants note with appreciation that the amendments put forth in Paper 20 (4/8/03) have been entered in full.

Withdrawn rejections

Applicants note that the Examiner has withdrawn the rejection of claims 1-2, 4-18, 21, and 29 under 35 U.S.C. 112, second paragraph, in view of Applicants' amendments.

Claim rejections under 35 U.S.C. 112, first paragraph

Claims 1-2, 4, 6-18, 21, 29, and 31-32 are rejected under 35 U.S.C. 112, first paragraph, as allegedly failing to enable one of skill in the art to practice the claimed invention. Applicants traverse these rejections to the extent that they are maintained in light of the amended claims.

Although the Examiner acknowledges that the specification is enabling "for methods of suppressing or promoting thymic T-cell maturation comprising administering a polypeptide at least 100% identical to the N-terminal autoproteolytic fragment of a hedgehog polypeptide, wherein said peptide binds a naturally occurring patched protein," the Examiner argues that the specification "does not reasonably provide enablement for the broad scope of suppressing or enhancing the immune function or immune system of an animal, nor for modulating T-cell maturation other than in the thymus (e.g. peripheral T-cell maturation), nor for any form of therapy, and nor for the suppression of promotion of T-cell maturation comprising the

administration of a hedgehog agonist thereof other than a polypeptide at least 100% identical to the N-terminal autoproteolytic fragment of a hedgehog polypeptide or [an] antagonistic antibody that binds thereto."

The basis of the rejection appears to have two components. First, the Examiner alleges that although the specification is enabling for methods of suppressing or promoting thymic T-cell maturation, Applicants have allegedly failed to reasonably enable for methods of suppressing or enhancing the immune function or immune system of an animal, methods of modulating T-cell maturation other than in the thymus, or methods of any form of therapy. Second, the Examiner alleges that although a polypeptide 100% identical to the N-terminal autoproteolytic fragment of a hedgehog polypeptide is effective in the methods of the present invention, Applicants have allegedly failed to reasonably provide methods which employ any other polypeptide agonists or non-polypeptide agonists.

In response to the Examiner's first basis, Applicants reiterate the arguments of record and contend that the specification is enabling for the broad scope of the claimed methods. The application teaches that hedgehog agonists/antagonists can be used in suppressing or enhancing the immune function/system of an animal (pages 4, line 21 – page 5, line 25; page 9, line 8 – page 12, line 14), and Applicants provide a working example demonstrating that these hedgehog agonists/antagonists are efficacious in suppressing or promoting thymic T-cell maturation (page 58, line 25 – page 59, line 6).

Nevertheless, solely to expedite prosecution of claims directed to commercially relevant subject matter, Applicants have amended independent claims 2 and 31 to more particularly point out the hedgehog agonists for use in suppressing T cell function of an animal. The amendments are fully supported by the original specification and by the evidence obtained since the filing of the present application (**Exhibit 1**). Applicants submit that amendments are not in acquiescence of the rejection, and Applicants reserve the right to prosecute claims of similar or differing scope.

In response to the Examiner's second basis, Applicants reiterate the arguments of record and contend that the claims are enabled not only for the use of polypeptides comprising a sequence identical to all or a portion of the hedgehog sequences provided in the disclosure (e.g.,

SEQ ID NOs: 10-18), but also for variants of these disclosed sequences and for non-polypeptide agonists (e.g., small molecule agonists). The specification provides a detailed description of hedgehog signaling (page 46, line 14- page 47, line 3), and provides the nucleic acid and amino acid sequences of multiple hedgehog family members isolated from phylogenetically diverse species (page 13, Table 1). Although the hedgehog family members differ in terms of their exact sequence, they share common structural and functional properties.

Nevertheless, to expedite prosecution of claims directed to commercially relevant subject matter, Applicants have amended independent claims 2 and 31 to more particularly point out the structural features of this genus, as well as define the structure and function of the fragments. Applicants submit that one of skill in the art, at the time the application was filed, could readily have prepared and tested hedgehog proteins (e.g., for their ability to bind to a patched polypeptide) satisfying these parameters in the claimed methods or relevant assays without undue experimentation.

The Examiner asserts that "[t]he specification has failed to teach one of skill in the art which amino acid substitutions, deletions, or insertions to make....If a variant of the naturally occurring hedgehog protein is to have a structure and function similar to the naturally occurring hedgehog protein, then the specification has failed to teach one of skill in the art which amino acid substitutions, deletions, or insertions to make that will preserve the structure and function of the naturally occurring hedgehog protein."

Applicants respectfully point out that one of skill in the art could practice the present invention without necessarily knowing which amino acid substitutions, deletions, or insertions to make, as variants of the hedgehog proteins of amended claims 2 are clearly defined structurally and functionally. Applicants submit that the techniques of combinatorial mutagenesis (Reidhaar-Olson and Sauer 1988, enclosed herewith as **Exhibit 2**) and high through-put screening, known in the art at the time of filing, make the identification of variant hedge polypeptides routine, if not trivial. The fields of combinatorial and scanning mutagenesis had trivialized the once complex and painstaking process of making and testing polypeptide variants long before the filing of the present application. These techniques were routinely practiced, and allow a wide range of amino acid substitutions to be made and tested for the maintenance or disruption of

functional properties without undue experimentation. These techniques are described in the specification (pages 27-31). Accordingly, techniques for synthesizing, testing, and identifying sequences which would possess the claimed structures and functions were well known in the art at the time of filing and routinely carried out. Accordingly, one of skill in the art faced with the task of constructing hedgehog polypeptides within the scope of the claims would not approach the problem by trial and error. Instead, the skilled artisan could use combinatorial mutagenesis and would not face undue experimentation.

The Examiner also asserts that "[w]hile it is known that many amino acid substitutions are generally possible in any given protein, the positions within the protein's sequence where such amino acid substitutions can be made with a reasonable expectation of success are limited." The Examiner also cites Bowie et al. to make this rejection.

Although Applicants agree that it is possible to abolish activity of a given protein by changing a critical residue as disclosed by the Bowie reference, Applicants disagree that this fact means that a skilled artisan cannot make functional variants of hedgehog protein without undue experimentation. In fact, Bowie et al. teach that "proteins are surprisingly tolerant of amino acid substitutions" (page 1306, column 2, lines 12-13). Of approximately 1500 single amino acid substitutions, about half of the substitutions were found to be "phenotypically silent." Based on the teachings of Bowie et al., one can expect that a great percentage (about 50%) of the random substitutions in a given protein can produce variant proteins with normal or nearly normal activity. Accordingly, one would expect that even random substitution in hedgehog proteins would give rise to a majority of variants with normal or partial activity.

Applicants further point out that the making of polypeptide variants was and is routinely practiced in the art using common and routine laboratory techniques. One of skill in the art would know to make only conservative changes in a hedgehog protein to avoid the changes in its activity. These substitutions can be made based on both the sequence data and on knowledge of the structure of the twenty amino acids. Amino acid substitutions can be chosen in order to maintain or disrupt the shape and charge density of a region of the protein, and one of skill in the art would have recognized that the choice of an amino acid substitution that would either maintain or disrupt a given region of a protein is highly predictable based on the structure of the

twenty natural amino acids. For example, arginine and lysine are positively charged amino acids and the substitution of one for the other is routinely practiced in the art without affecting the function of the overall sequence (reviewed in detail in specification, pages 26-27).

In addition, Applicants submit a copy of Chang et al. 1994 (**Exhibit 3**). Chang et al. show that Hhg-1, a mouse Sonic hedgehog gene, functions in *Drosophila* in a manner similar to the native *Drosophila* hedgehog protein (pages 3344-3347), despite the fact that these polypeptides are only approximately 46% identical. Accordingly, Applicants submit that variants at least 90% identical to any of these proteins can be used in the presently claimed methods without undue experimentation, as taught by the application at the time of filing. Indeed, Applicants submit that a skilled artisan could have readily produced variants of the recited SEQ ID Nos. or N-terminal fragments thereof using these and other known sequences as a guide to which substitutions would be expected to retain activity.

Furthermore, Applicants submit a copy of Pathi et al. 2001 (**Exhibit 4**). Pathi et al. demonstrate that "the three Hh proteins [Shh, Ihh, and Dhh] have the potential to function similarly, although in certain assays they have different potencies." As depicted in Table 1, all three proteins exhibited similar functions in the various assays performed, although potencies differed. Accordingly, one skilled in the art would appreciate that other than wild-type hedgehog proteins, variants of these hedgehog proteins can be used in the presently claimed methods without undue experimentation, as taught by Applicants at the time of filing.

The Examiner has also cited two references (Lahana R. and Horrobin DF) to assert that "Applicants' confidence in high throughput assays does not appear to be shared by those who practice the art." Applicants submit that these two references are rendered irrelevant in view of the amended claims.

For the reasons set forth above, Applicants submit that the claimed subject matter is enabled throughout its scope. Reconsideration and withdrawal of this rejection is respectfully requested.

In addition, Applicants point out that even if the claims encompass certain inoperative embodiments, that does not undermine the enablement of the operative subject matter. In

accordance with MPEP 2164.08(b), "[t]he presence of inoperative embodiments within the scope of a claim does not necessarily render a claim nonenabled. The standard is whether a skilled person could determine which embodiments that were conceived, but not yet made, would be inoperative or operative with expenditure of no more effort than is normally required in the art." This standard has been upheld in the courts, and permits a claim to encompass a finite number of inoperable embodiments so long as inoperable embodiments can be determined using methodology specified in the application without undue experimentation. See, for instance, *In re Angstadt*, 190 U.S.P.Q. 214 (CCPA 1976).

In view of the arguments and amendments presented above, Applicants submit that all pending claims as amended fully comply with the enablement requirement. Applicants reiterate that the references cited by the Examiner are not applicable to the claimed invention for the reasons made of record, and should not be considered, in particular, in view of the claim amendments. Accordingly, reconsideration and withdrawal of the rejection under 35 U.S.C. 112, first paragraph, is respectfully requested.

Claim rejections under 35 U.S.C. 112, first paragraph

The Examiner maintains the rejection of claims 1-2, 4, 6-18, 21, 29, and 31-32 under 35 U.S.C. §112, first paragraph, as allegedly containing subject matter which was not described in the specification in such a way as to reasonably convey to one skilled in the relevant art that the inventors, at the time the application was filed, had possession of the claimed invention. Applicants traverse this rejection to the extent that it is maintained over the amended claims.

Applicants maintain the arguments of record and contend that the application, as filed, provides ample support for a wide range of hedgehog agonists/antagonists. First, the terms *hedgehog* agonist and antagonist are described in detail throughout the specification such that one of skill in the art could easily envision the polypeptides and small molecules of the invention. Second, a representative number of such compounds are enumerated in the application (e.g., hedgehog polypeptides and PKA inhibitors). Finally, Applicants have even provided several experimental measures which would allow one of skill in the art to readily recognize the claimed subject matter. Finally, Applicants have demonstrated possession of the claimed invention by describing examples of actual reduction to practice of structurally diverse

compounds. The working examples teach at least one hedgehog agonist (e.g., an octyl-modified Shh) and one hedgehog antagonist (e.g., an anti-hedgehog antibody). Accordingly, Applicants contend that claims directed to hedgehog agonists are well supported by the specification and satisfy the requirements under 35 U.S.C. 112, first paragraph.

Nevertheless, solely to expedite prosecution of claims directed to commercially relevant subject matter, Applicants have amended the claims to more particularly point out the hedgehog agonists for use in the subject methods. Applicants submit that the amendments are not in acquiescence of the rejection, and Applicants reserve the right to prosecute claims of similar or differing scope. Reconsideration and withdrawal of this rejection are respectfully requested.

CONCLUSION

In view of the foregoing amendments and remarks, Applicants submit that the pending claims as amended are in condition for allowance. Early and favorable reconsideration is respectfully solicited. The Examiner may address any questions raised by this submission to the undersigned at 617-951-7000. Should an extension of time be required, Applicants hereby petition for same and request that the extension fee and any other fee required for timely consideration of this submission be charged to **Deposit Account No. 18-1945.**

Respectfully Submitted,

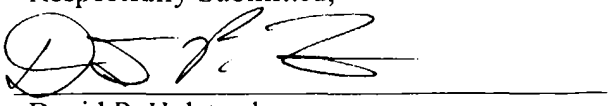

Date: November 12, 2003

David P. Halstead
Reg. No. 44,735

Customer No: 28120
Docketing Specialist
Ropes & Gray LLP
One International Place
Boston, MA 02110
Phone: 617-951-7000
Fax: 617-951-7050

Exhibit 1

The role of morphogens in T-cell development

Alberto Varas[1], Ariadne L. Hager-Theodorides[2], Rosa Sacedón[3], Angeles Vicente[3], Agustín G. Zapata[1] and Tessa Crompton[2]

[1]Department of Cell Biology, Faculty of Biology, Complutense University, 28040 Madrid, Spain
[2]Department of Biological Sciences, Sir Alexander Fleming Building, Imperial College London, South Kensington Campus, London SW7 2AZ, UK
[3]Department of Cell Biology, Faculty of Medicine, Complutense University, 28040 Madrid, Spain

The Hedgehog (Hh) and Wnt family proteins, and the bone morphogenetic proteins (BMPs) 2 and 4, act as morphogens during vertebrate embryogenesis and organogenesis by regulating patterning and cell fate. They have recently been found to have a role in regulating cell fate and determination in self-renewing tissues in adults, such as the immune system and haematopoietic system. This Review presents studies on the role of Sonic Hh (Shh), Wnts and BMP2/4 in the regulation of thymocyte development. Shh and BMP2/4 act as negative regulators of thymocyte development. By contrast, Wnt signalling, through β-catenin, has a positive role in the control of T-cell development, such that an absence or reduction in the Wnt signal leads to a reduction in cell number and cell proliferation rate and differentiation to the $CD4^+CD8^+$ double-positive stage.

Morphogens are secreted signalling molecules produced at a localized source that specify different cell fates in a concentration-dependent manner. The generation of a concentration gradient of the morphogen by diffusion or movement from its source across the target-cell field enables cells to respond according to their position within the field, and patterning signals are thereby generated [1,2]. In *Drosophila melanogaster*, Hedgehog (Hh), Wingless (Wg) and decapentaplegic (dpp) have been identified as morphogens during development [3,4] and their vertebrate orthologs, the Hh family, Wnt family and bone morphogenetic proteins (BMPs) 2 and 4, likewise act as morphogens during vertebrate embryogenesis and organogenesis [1,4]. Recent studies have revealed that these proteins not only determine patterning and cell fate during development but also function in cell-fate determination of self-renewing tissues in the adult, such as the immune system and haematopoietic system. Here, the evidence of a role for these three families of signalling proteins in the control of T-cell development in the thymus is reviewed. The main focus is on the functions of Wnts, Shh and BMP2/4 in the regulation of the development of thymocytes from the earliest $ckit^+CD44^+CD25^-$ ($CD4^-CD8^-$) double-negative (DN) stage through to the $CD4^+$ or $CD8^+$ single-positive (SP) stage [$ckit^+CD44^+CD25^-$DN (DN1) to $CD44^+CD25^+$DN (DN2) to $CD44^-CD25^+$DN (DN3) to $CD44^-CD25^-$DN (DN4) to $CD4^+CD8^+$ double-positive (DP) to $CD4^+$SP or $CD8^+$SP].

Hh signalling pathway

The Hh family of secreted proteins are intercellular signalling molecules that specify cell fate and patterning during the development of many tissues and are highly conserved from flies to mammals. In mammals, there are three family members, Sonic hedgehog (Shh), Indian hedgehog (Ihh) and Desert hedgehog (Dhh) [4]. These proteins have different expression patterns and have essential nonredundant roles during embryogenesis but share a common signalling pathway, summarized in Fig. 1 (reviewed in Ref. [4]). They signal to neighbouring cells by binding to their cell-surface receptor Patched (Ptc). The cell-surface molecule Smoothened (Smo) then transmits the Hh signal into the target cell. In the absence of its Hh ligand, Ptc inhibits the ability of Smo to signal; however, when Hh binds to Ptc, Ptc releases Smo to signal into the cell. The mechanisms by which Smo signals into the cell are still unclear but at the end of the signalling pathway are the Gli family of transcription factors, Gli1, Gli2 and Gli3 [5]. Gli1 is an activator of transcription [6], whereas Gli2 and Gli3 probably function both as positive and negative regulators of transcription [6]. The repressor form of Gli2 has not been detected *in vivo* but Gli3 seems to act predominantly as a repressor [5,6]. Gli1 and Gli2 transcription is positively regulated by Hh signalling, whereas Gli3 transcription is downregulated by Hh [5]. The activator function of Gli2 and Gli3 is Hh dependent and requires complex formation with CBP [cAMP response element-binding protein (CREB)-binding protein] [6]. The repressor form of the Gli proteins is formed by cleavage of the full-length molecule and is promoted by phosphorylation by protein kinase A (PKA) [6].

Components of the Hh signalling cascade, including Shh, Ihh, Ptc, Smo, Gli1, Gli2 and Gli3, are expressed in the murine thymus in both the adult and the foetus [7–9]. Shh is produced by the thymic epithelium, and Ihh expression is mainly associated with blood vessels in the thymic medulla [7]. Cell-surface expression of the signal transduction molecule Smo on thymocytes is largely restricted to the DN cells and Smo is downregulated on

Corresponding author: Tessa Crompton (t.crompton@imperial.ac.uk).

http://treimm.trends.com 1471-4906/03/$ - see front matter doi:10.1016/S1471-4906(03)00033-4

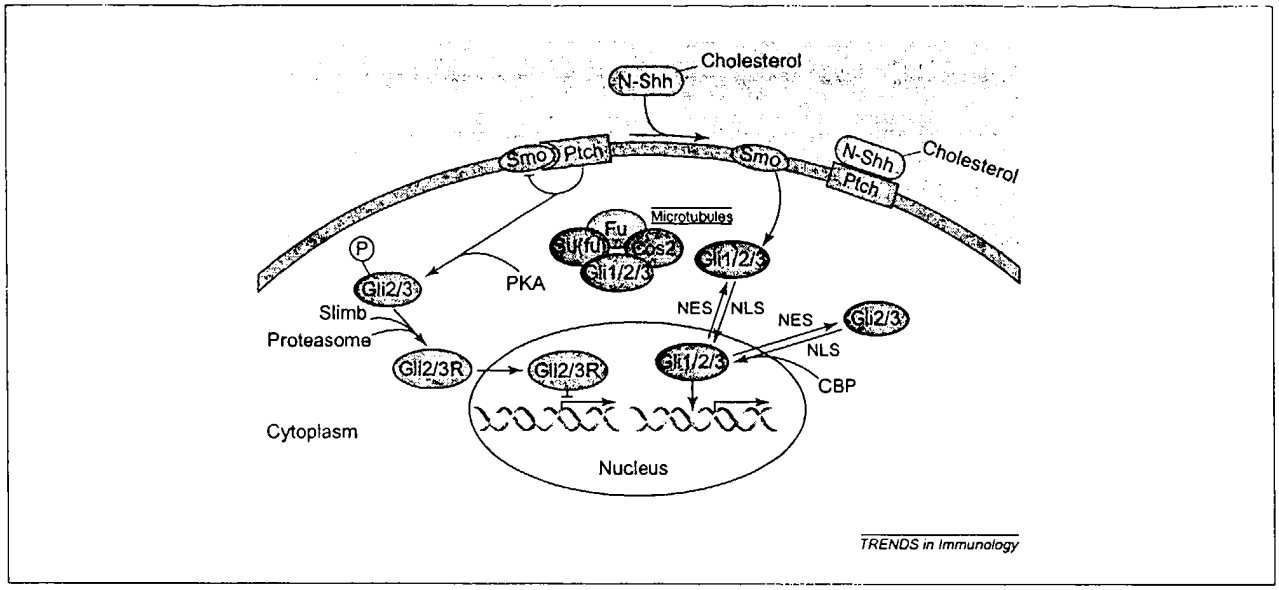

Fig. 1. The Sonic hedgehog (Shh) signalling pathway. In the presence of N-terminal-cholesterol-bearing Shh (N-Shh), Patched (Ptch) allows Smoothened (Smo) to signal into the target cell. The Smo signal, by a mechanism not fully understood, involving the multiprotein complex containing Fused (Fu), Supressor of fused [Su(fu)] and Costal 2 (Cos2), causes the release of Gli1/2/3 proteins that are part of a complex in the microtubules, which then act as gene activators. Gli2 and Gli3 interact with CBP [cAMP response element-binding protein (CREB)-binding protein]. All three full-length Gli proteins possess nuclear localization signals (NLS) and nuclear export signals (NES). In the absence of Shh ligand, Ptch binds to Smo, repressing its signal. This allows Gli2 and Gli3 to be phosphorylated by protein kinase A (PKA) and then be processed to generate repressor Gli2/3R forms. The repressor forms of Gli2/3 only possess NLS. The existence of the Gli2 repressor form is speculative and has not been found endogenously.

the subsequent DP and $CD4^+$SP and $CD8^+$SP populations. Analysis of the DN populations defined by CD44 and CD25 expression shows that the earliest $CD44^+CD25^-$DN1 cells that are not committed to the T-cell lineage [10] do not express significant levels of Smo [7]. In the next compartment of $CD44^+CD25^+$DN2 cells, Smo expression is upregulated whereas, in the subsequent $CD44^-CD25^+$ DN3 and $CD44^-CD25^-$DN4 populations, both the proportions of positive cells and the levels of expression gradually decline. Thus, the thymocyte precursors that are presumably responding to the Hh signal are the $CD25^+$DN cells. These cells are committed to the T-cell lineage and are undergoing rearrangement of the gene encoding the T-cell receptor (TCR)β chain. The function of Hh signalling in these cells is not known and Hh target genes have yet to be identified but it is possible that the Hh signal is involved in T-cell lineage commitment or the regulation of rearrangement of the gene encoding the TCRβ chain.

Evidence for the involvement of Hh in the regulation of T-cell differentiation comes from *in vitro* experiments in which murine foetal thymus organ cultures (FTOCs) were treated with recombinant Shh or with a neutralizing antibody to Shh that blocks Hh binding to Ptc [7]. We found that treatment of FTOCs with anti-Shh increased and accelerated the differentiation of DN to DP cells, and that treatment with Shh arrested thymocyte differentiation at the $CD25^+$ DN stage, after rearrangement of the TCRβ gene. Although Hh signalling regulates the transition from DN to DP cell, neutralization of Shh was unable to replace a pre-TCR signal in $Rag1^{-/-}$ FTOCs. However, the antibody treatment did enhance anti-CD3-induced differentiation in $Rag1^{-/-}$ FTOCs, indicating that termination of Hh signalling can only promote thymocyte differentiation after the pre-TCR complex has transduced its signal. Ligation of CD3 on $Rag1^{-/-}$ thymocytes caused downregulation of *smo* mRNA and cell-surface Smo expression, making the developing thymocytes refractory to Hh within two days of receiving the pre-TCR signal. The fact that pre-TCR signalling downregulates Smo demonstrates a direct link between pre-TCR signalling and Hh signalling in the regulation of differentiation of DN thymocytes. It suggests that the Hh signal might function as a negative regulator, providing a break in thymocyte differentiation and cell-cycle progression until the *TCRβ*

Fig. 2. Signalling by Sonic hedgehog (Shh), bone morphogenetic proteins (BMPs)2/4 and Wnts affects thymocyte development. Developing thymocytes progress from the $CD4^-CD8^-$ double-negative (DN) stage to the $CD4^+CD8^+$ double-positive (DP) stage before differentiating to single-positive (SP) $CD4^+$ or $CD8^+$ T cells that migrate to the periphery. Progression from DN to DP involves four DN stages ($CD44^+CD25^-$DN1 to $CD44^+CD25^+$DN2 to $CD44^-CD25^+$DN3 to $CD44^-CD25^-$DN4) and an immature single-positive (ISP) stage. Green boxes denote a positive effect and red boxes an inhibitory effect. (a) Shh is produced by thymic epithelial cells and the signal is received by developing thymocytes. Smoothened (Smo) expression is downregulated after pre-T-cell receptor (TCR) signalling and Shh signalling is thus blocked, allowing differentiation of DN3 to DN4 thymocytes. (b) BMP2/4, as well as their antagonists Twisted gastrulation (Tsg), Chordin and Noggin, are expressed in the thymic epithelium. BMP2/4 can block differentiation of DN1 to DN2 stage and at the transition from DN to DP. Noggin and Chordin with Tsg can antagonize BMP2/4 *in vitro* and promote differentiation. The expression of Tsg is upregulated after TCRβ rearrangement and TCR signalling. (c) Most thymocyte subsets and mainly thymic epithelial cells produce several Wnt proteins, which function in thymocyte development in both autocrine and paracrine fashions. Wnt molecules promote the proliferation and differentiation of DN thymocytes, although Wnt signalling must be switched-off while the TCRβ chain is being rearranged. The survival of DP thymocytes is also enhanced by Wnt proteins.

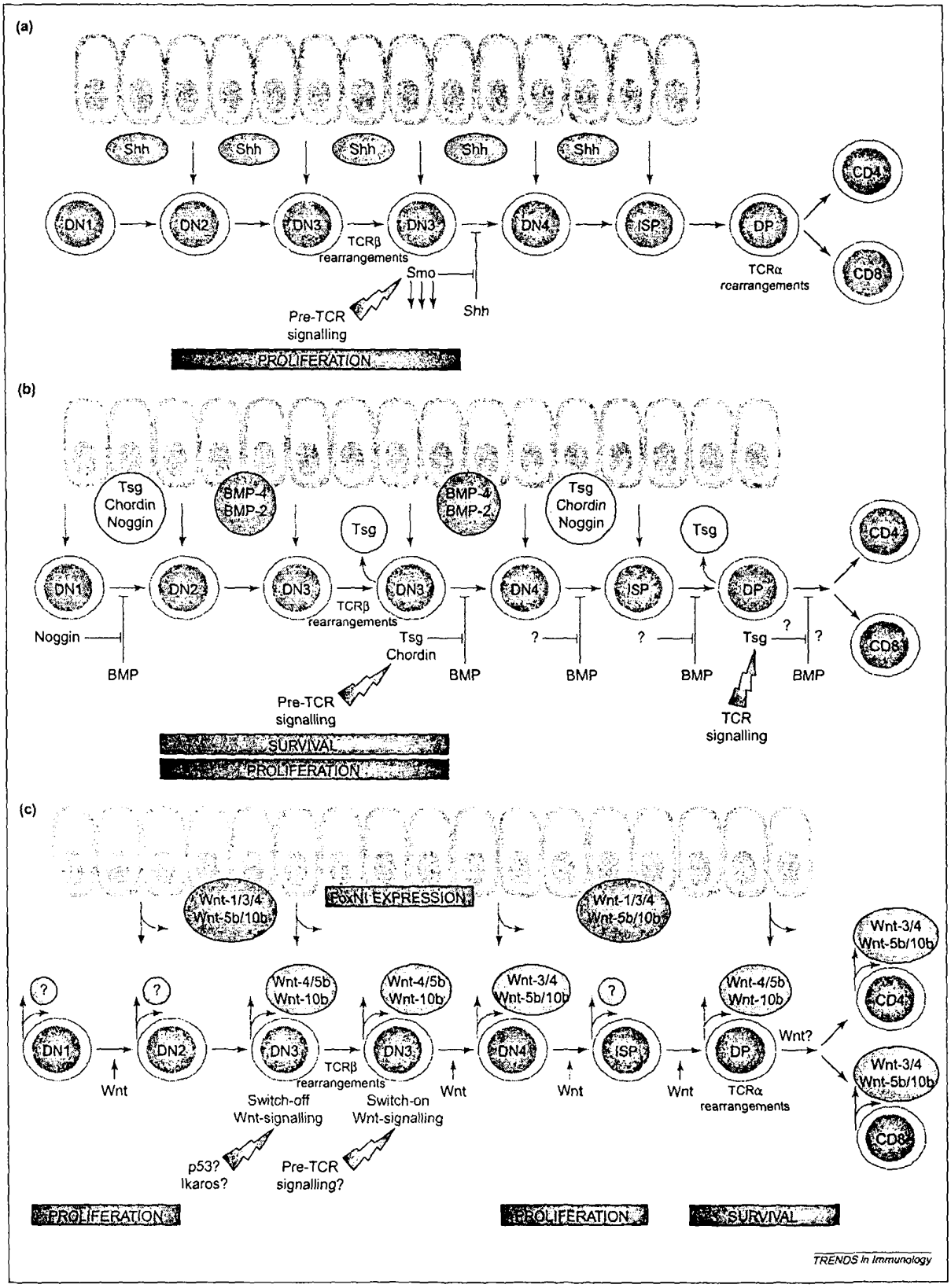
(a)
Shh
DN1
DN2
DN3
TCRβ rearrangements
DN3
DN4
ISP
DP
CD4
CD8
TCRα rearrangements
Smo
Shh
Pre-TCR signalling
PROLIFERATION
(b)
Tsg Chordin Noggin
BMP-4 BMP-2
Tsg
BMP-4 BMP-2
Tsg Chordin Noggin
Tsg
DN1
DN2
DN3
TCRβ rearrangements
DN3
DN4
ISP
DP
CD4
CD8
Noggin
BMP
Tsg Chordin
BMP
?
BMP
?
BMP
Tsg
?
?
BMP
Pre-TCR signalling
TCR signalling
SURVIVAL
PROLIFERATION
(c)
Wnt-1/3/4 Wnt-5b/10b
FoxN1 EXPRESSION
Wnt-1/3/4 Wnt-5b/10b
Wnt-3/4 Wnt-5b/10b
?
Wnt-4/5b Wnt-10b
Wnt-4/5b Wnt-10b
Wnt-3/4 Wnt-5b/10b
?
Wnt-4/5b Wnt-10b
DN1
DN2
DN3
TCRβ rearrangements
DN3
DN4
ISP
DP
Wnt?
CD4
Wnt-3/4 Wnt-5b/10b
CD8
Wnt
Switch-off Wnt-signalling
Switch-on Wnt-signalling
Wnt
Wnt
Wnt
TCRα rearrangements
p53? Ikaros?
Pre-TCR signalling?
PROLIFERATION
PROLIFERATION
SURVIVAL
TRENDS in Immunology

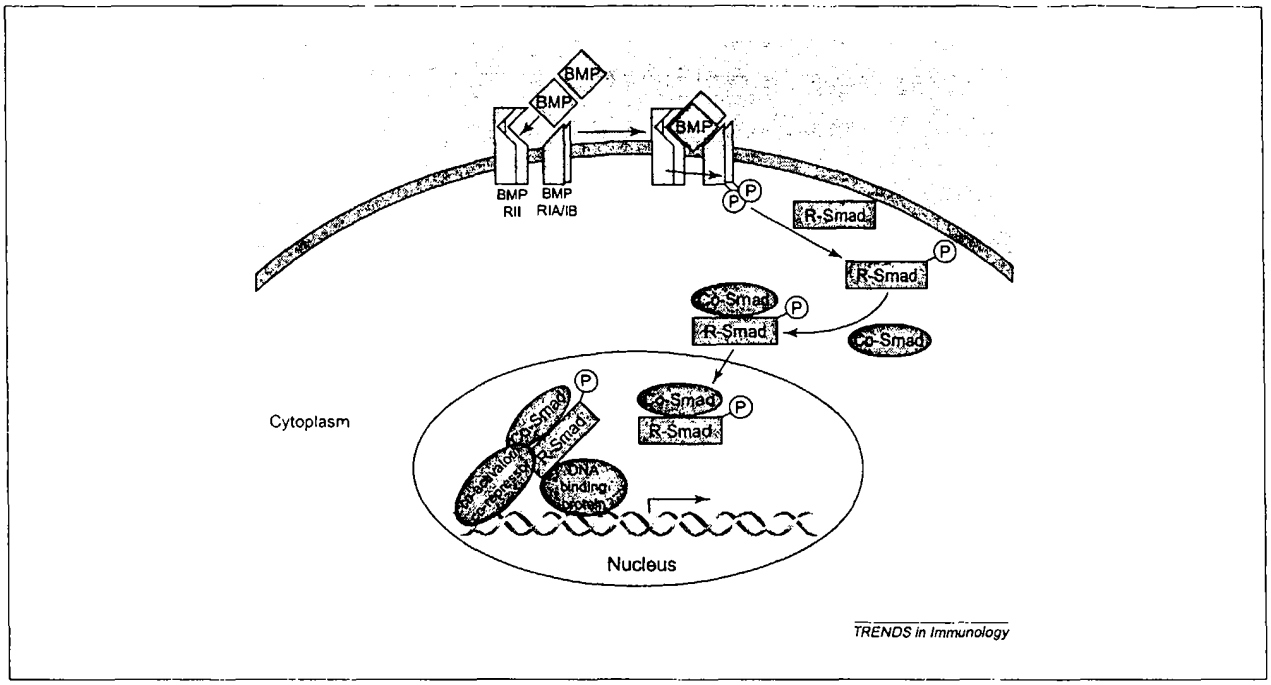

Fig. 3. The bone morphogenetic protein (BMP)2/4 signalling pathway. BMP2/4 ligands attach to type II BMP receptor (BMPR-II), which then recruits and phosphorylates (P) type I BMP receptors (BMPR-IA or BMPR-IB). The phosphorylated BMPR-IA and/or BMPR-IB then phosphorylate the receptor-regulated R-Smads (Smad-1, Smad-5 and Smad-8), which recruit the common mediator Co-Smad (Smad-4) and translocate to the nucleus. In the nucleus, the R-Smad–Co-Smad heterodimers recruit DNA-binding proteins and co-activator or co-repressor proteins, and activate or repress the expression of target genes.

gene has rearranged and the pre-TCR has signalled for differentiation.

The experiments summarized here demonstrate the effects on thymocyte differentiation of modulating the Hh signal at the end of the period of Smo expression (and presumably active Hh signalling, see Fig. 2a). In the future, it will be interesting to investigate a role for Hh signalling on the earlier $CD44^{+}CD25^{+}$ cells. As a negative regulator of thymocyte differentiation, Shh produced by the thymic epithelium might function in controlling the number of thymocytes produced.

BMP2/4 signalling pathway

BMP2 and BMP4, members of the transforming growth factor-β (TGF-β) superfamily of secreted proteins, are closely related, highly conserved homologues of the *Drosophila* protein dpp. Gene sequences for BMP2 and BMP4 cluster together with *dpp* in phylogenetic trees of BMP genes [11], indicating that the function of BMP2/4 might be more similar to that of dpp than any other protein member of the TGF-β superfamily. BMP4 and BMP2 have different expression patterns and have essential non-redundant roles during mouse embryogenesis [12,13] but share a common signalling pathway, summarized in Fig. 3 [14]. BMPs signal through ligation and heterodimerization of type I (BMPR-IA or BMPR-IB) and type II (BMPR-II) serine–threonine kinase receptors that phosphorylate downstream signal transduction/transcription factors, the receptor-regulated pathway-specific R-Smads. The BMP2/4 signal specifically phosphorylates the R-Smads: Smad-1, Smad-5 and Smad-8 [15]. The phosphorylated R-Smads recruit the common-mediator Co-Smad, Smad-4, and translocate to the nucleus, where they form complexes with other transcription factors and DNA-binding proteins.

BMP signalling is regulated by extracellular inhibitors that bind BMPs with high affinity, preventing BMPs from binding to their cell-surface receptors. Such inhibitors of BMP2 and BMP4 include Noggin, Chordin (reviewed in Ref. [16]) and Twisted gastrulation (Tsg) [17–19]. Mouse Tsg can bind to and cleave Chordin, enhancing the ability of Chordin to inhibit BMP4, and can also bind directly to BMP4 [19]. Recently, BMP4 has been shown to regulate the development and proliferation of human haematopoietic stem cells [20,21] and the differentiation of murine thymocytes [22,23].

BMP2 and BMP4 are expressed in the thymus [7] by epithelial cells [22,23]. The BMP receptors BMPR-II [23], BMPR-IA and -IB [23,24], the R-Smads (Smad-1, -5, -8) [23,25,26] and the Co-Smad (Smad-4) [23,26] are also expressed in the thymus, by both the thymic stroma and thymocytes [23]. The antagonists of BMP2/4 signalling have an important role in the modulation of the signal the cells receive. Chordin is expressed in the thymus [19] by the epithelium [22,23], whereas Tsg is expressed by both thymic epithelium and thymocytes [22,23,27]. Interestingly, the transcription of *Tsg* is differentially regulated during thymocyte development [22,27]. *Tsg* transcription is upregulated after pre-TCR signalling, at the transition from DN to DP cell, and after TCR signalling at the transition from DP to SP cell [22]. This suggests that reduction in the BMP2/4 signal is required for differentiation at these two developmental checkpoints. The Smad-interacting transcription factor Schnurri-2 is

required for positive selection of mouse thymocytes, again implicating BMP signalling in the control of differentiation from DP to SP cell [28].

Recently, two studies demonstrated that BMP2/4 signalling acts as a negative regulator of thymocyte differentiation *in vitro*. One study indicated that BMP2/4 inhibit thymocyte differentiation at the transition from DN to DP thymocyte [22], at the same stage as TGF-β [29] and Shh [7]. The other study showed inhibition at the transition from the earliest $CD44^+CD25^-$DN stage of development to the T-lineage-committed $CD25^+$ DN stage [23].

The work of Graf *et al.* [22] showed that treatment of FTOCs with recombinant BMP4 reduced both thymocyte proliferation and differentiation of DN to DP cells. This inhibition of differentiation was not as a result of a delay in TCRβ rearrangement or a reduced response to pre-TCR signalling because the same effect was observed in the development of DP cells in $Rag1^{-/-}$ FTOCs after stimulation with anti-CD3 antibody. The effect of BMP4 treatment was direct because it also inhibited the differentiation of DN cells in suspension cultures. Experiments in which the action of endogenously produced BMP2/4 was neutralized by treatment of FTOCs with soluble BMPR-IA protein or Chordin protein indicated that the proliferation of thymocytes in FTOCs and their transition from DN to DP cell are inhibited by BMPs *in situ*. Anti-CD3-induced differentiation of $Rag^{-/-}$ FTOCs was inhibited by BMP4 but Chordin alone was unable to restore fully the production of DP cells. As shown by the addition of Tsg and Chordin together to such cultures, Chordin and Tsg can synergize to antagonize BMP4-mediated inhibition of differentiation. Graf *et al.* [22] suggest that a balance between BMP2/4, Chordin and Tsg regulates the development of thymocytes and ensures the maintenance of sufficient numbers of immature precursor cells. They argue that the developmentally regulated differential expression of Tsg in thymocytes enables the cells to modulate the morphogen gradient of their environment.

Our own study [23] has identified an earlier stage of thymocyte development at which BMP2/4 signalling can inhibit differentiation. We found that treatment of FTOCs with BMP4 arrested thymocyte differentiation at the $CD44^+$c-kit^+CD25^-DN1 stage, before T-cell lineage commitment. This effect was dose dependent and was reversed by addition of the BMP2/4 antagonist Noggin. BMP4 treatment enhanced thymocyte survival and inhibited thymocyte proliferation. Treatment of FTOCs with only Noggin promoted thymocyte survival and differentiation, increasing the proportion of cells expressing cell-surface CD2, and the percentages of $CD44^-CD25^-$DN4 and DP cells. Thus, Noggin treatment showed that endogenous BMP2/4 in the cultures was inhibiting thymocyte differentiation. Interestingly, Noggin treatment accelerated and promoted differentiation along the T-cell lineage (beyond the $CD25^+$ subset), even though BMP4 arrested differentiation at the earliest $CD44^+CD25^-$DN1 stage. Noggin treatment was insufficient to overcome the developmental block in FTOCs from $Rag1^{-/-}$ and $TCR\beta^{-/-}\delta^{-/-}$ embryos, indicating that neutralization of BMP2/4 signalling is insufficient to overcome the need for a pre-TCR signal.

Taken together with the work of Graf *et al.* [22], these experiments suggest that endogenous BMP2/4 are inhibiting T-cell differentiation throughout thymocyte development (Fig. 2b). Such a negative regulator could provide a way of controlling thymocyte cell numbers (irrespective of TCR specificity), and also of maintaining some precursor cells in a pluripotent state. Interestingly, in human haematopoietic cell cultures, Shh, acting upstream of BMP2/4, increased the survival and proliferation of human haematopoietic stem cells with pluripotent reconstituting ability [21]. The involvement in germline stem-cell survival and proliferation has also been shown for dpp, the *Drosophila* ortholog of BMP2/4, in *Drosophila* ovaries [30]. In this context, taken together with our data from the FTOCs [23], it would not be surprising if BMP2/4 are involved in the survival of pluripotent thymocytes not committed to the T-cell lineage.

Wnt signalling pathway

Wnt genes encode a large family of secreted glycoproteins that are involved in a wide spectrum of cell activities in development (reviewed in Ref. [31]). The Frizzled (Fz) family of serpentine receptors and the low-density lipoprotein receptor-related proteins (LRP)-5 and -6 cooperatively bind Wnt proteins, forming a tripartite unit that initiates Wnt signalling pathways [32,33]. However, Wnt receptor binding is tightly modulated through association with diverse secreted proteins, such as Dickkopf [34], Frzb-1 [35,36] or Cerberus [37], and extracellular or cell-membrane glycosaminglycans [38].

Wnt signals are transduced through at least three different intracellular signalling pathways, including the canonical Wnt pathway, which primarily functions during development (Fig. 4). This Wnt signalling cascade leads to stabilization of β-catenin, which translocates to the nucleus where it engages with the lymphoid enhancer factor (LEF)-1 and the T-cell factors (TCF)-1, TCF3 or TCF4. In the absence of Wnt signals, glycogen synthase kinase (GSK) 3β, through interactions with the product of the adenomatous polyposis coli (APC) gene and Axin (the destruction complex), phosphorylates βcatenin. The phosphorylation of βcatenin leads to its recognition by βtransducin repeatcontaining protein (βTRCP), a component of an E3 ubiquitin ligase, which causes its proteasomal degradation. By contrast, on binding of Wnt proteins to their receptors, the cytoplasmic protein Dishevelled (Dsh) is activated, leading to inhibition of GSK3β and the destruction complex. This, in turn, results in the escape of βcatenin and its movement to the nucleus, where it binds to TCF or LEF (reviewed in Refs [31,39,40]). TCF and LEF are transcription factors that are bound to DNA and, in the absence of βcatenin, interact with transcriptional corepressors, such as Groucho, which impedes transcription [41]. The complex of LEF or TCF with β-catenin promotes expression of genes that modulate cell fate, proliferation and survival during embryonic development as well as T-lymphocyte-specific genes, such as CD3ε, TCRα, CD4, TCRβ and TCRδ (reviewed in Refs [31,42,43]).

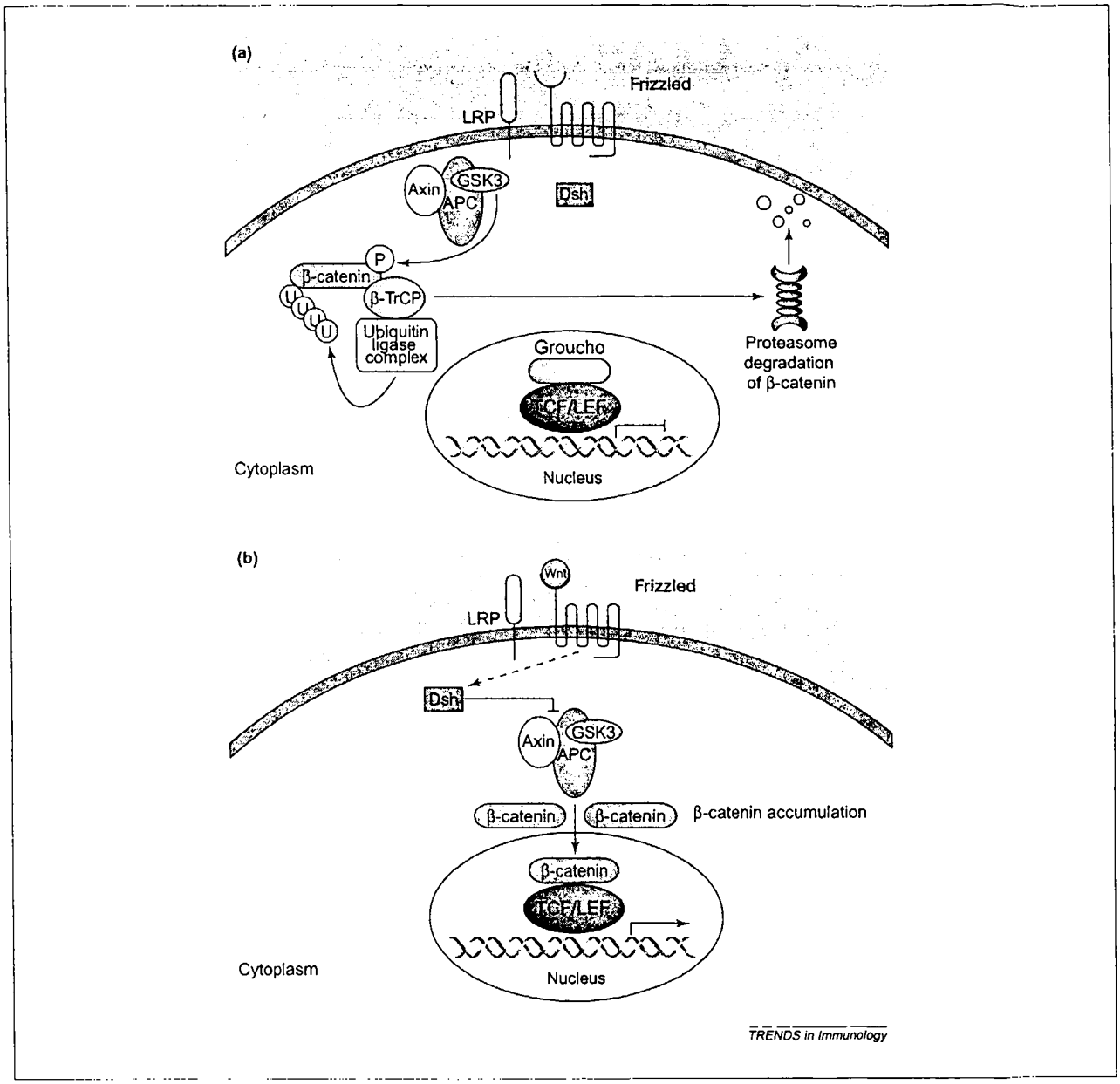

Fig. 4. The Wnt signalling pathway. (a) In the absence of Wnt, the protein complex constituted by the glycogen synthase kinase (GSK)-3, the scaffolding protein Axin and the tumour suppressor adenomatous polyposis coli (APC) protein phosphorylates (P) β-catenin, the central effector of the Wnt signalling pathway. This phosphorylation enables the recognition of β-catenin by β-transducin repeat-containing protein (β-TRCP), a component of E3 ubiquitin ligase, which causes its proteasomal degradation. In the nucleus, the transcription factors T-cell factor (TCF) and lymphoid enhancer factor (LEF) are bound to DNA but transcription of specific genes is impeded by their interaction with the co-repressor Groucho. (b) On binding of Wnt proteins to their receptors, Frizzled and low-density lipoprotein receptor-related protein (LRP), the cytoplasmic protein Dishevelled (Dsh) is activated, which results in the inactivation of GSK-3. Subsequently, β-catenin is stabilized and moves to the nucleus where it binds to TCF and LEF, allowing gene transcription.

However, the Wnt signalling cascade is a more intricate signalling network, not only because Wnt proteins can signal through two other alternative signalling pathways, involving trimeric G proteins/Ca^{2+} [44,45] and Rho proteins [46] but also because the lifespan of β-catenin can be regulated independently of Wnt signalling by other factors, such as p53, which antagonize the canonical Wnt pathway [47]. Furthermore, spliced variants of TCF-1 can be generated that are unable to bind β-catenin yet maintain the DNA- and Groucho-binding domains and, therefore, their inhibitory properties [48,49].

Recently, the Wnt pathway has been shown to be involved in the regulation of T-cell development in the thymus. The transcription factors TCF-1 and LEF-1 were the first components of the Wnt pathway whose expression was demonstrated in the thymus. Although TCF-1 expression is widely distributed in the embryo, after birth it is confined to the T-cell lineage [48,50,51]. Eight

Table 1. Evidence for a role of Wnt signalling in T-cell development[a]

Experimental models	Findings	Refs
TCF-1(V)-knockout mice (carrying a deletion in exon V)	Modest reduction of thymic cellularity and impairment in T-cell development	[50,57]
TCF-1(VII)-knockout mice (carrying a deletion in exon VII encoding part of the DNA-binding domain of TCF-1)	Severe reduction in thymocyte numbers; partial block in thymocyte differentiation at early developmental stages; more-pronounced effects with age; inability of haematopoietic precursors to reconstitute T-cell lineage in normal recipients	[50,52,56]
TCF-1(VII)$^{-/-}$ mice overexpressing p33 TCF-1 isoform (lacking β-catenin interaction site)	Similar phenotype to TCF-1-deficient mice	[52]
TCF-1(VII)$^{-/-}$ mice overexpressing p45 TCF-1 isoform (containing β-catenin interaction site)	Partial restoration of thymus cellularity, cell survival, cell cycling and T-cell differentiation	[52]
LEF-1-knockout mice	No abnormalities in thymocyte differentiation	[71]
LEF-1/TCF-1(V) double-knockout mice	Complete arrest of differentiation at the CD8$^+$ ISP stage; thymic γδ T-cell development unaffected; failure of haematopoietic precursors to reconstitute T- cell development in normal recipients	[57]
Wnt-1/Wnt-4 double-knockout mice	Reduced numbers of thymocytes; normal pattern of T-cell maturation	[58]
Gene-targeted mice showing accumulation of nondegradable β-catenin specifically in thymocytes	Generation of DP and SP thymocytes in the absence of pre-TCR signalling and TCRβ selection; reduced proliferation and survival of DP cells	[53]
Transgenic mice overexpressing Axin	Reduced thymus size; massive apoptosis of cortical thymocytes	[59]
Addition of antisense oligonucleotides for TCF-1 to FTOCs reconstituted with foetal liver lymphoid progenitors	Severe arrest of differentiation at the DN stage	[51]
Re-colonization of FTOCs with foetal liver progenitors transduced with extracellular domains of Frizzled-7 receptor	Complete arrest of differentiation at the DN stage	[55]

[a]Abbreviations: DN, CD4$^-$CD8$^-$ double negative; DP, CD4$^+$CD8$^+$ double positive; FTOCs, foetal thymus organ cultures; ISP, immature single positive; LEF-1, lymphoid enhancer factor-1; SP, CD4$^+$CD8$^-$ or CD4$^-$CD8$^+$ single positive; TCF-1, T-cell factor-1; TCR, T-cell receptor.

spliced variants of TCF-1 are expressed in thymocytes, including isoforms that can exclusively function as repressors [49,52]. β-catenin is also present in thymocytes but, owing to its short lifespan, only low levels of this protein can be detected by flow cytometry in CD44$^+$ CD25$^-$DN1 and CD44$^+$CD25$^+$DN2 populations, and levels decrease through differentiation [53]. More recently, Balciunaite *et al.* [54] demonstrated that CD44$^-$CD25$^+$ DN3, CD44$^-$CD25$^-$DN4, DP and mature SP thymocytes express several *wnt* genes, including *wnt-3*, *wnt-4*, *wnt-5b* and *wnt-10b*. These authors also found a differential transcription of *wnt* genes in immature and mature thymic epithelial cells. Epithelial expression exceeds that found in thymocytes and also includes *wnt-1*. Several different isoforms of the Fz receptor, including Fz5, Fz7 and Fz8, are also expressed in the thymus but there are no data about their regulation during T-cell differentiation [55]. Staal *et al.* [55] demonstrated that the canonical Wnt signalling pathway is active in the thymus by showing that the transduction of Wnt-1 activates the transcription of a TCF-dependent reporter gene in DN and immature SP (ISP) thymocytes.

A pivotal role for the Wnt–β-catenin–TCF-1 signalling cascade in different stages of T-cell development has become apparent from studies using *in vitro* assays and animal genetic models (Table 1 and references therein). Taken together, these complementary gain-of-function and loss-of-function studies clearly indicate that Wnt signalling controls thymic cellularity as well as different stages of thymocyte differentiation. All experimental models that impair Wnt signalling lead to important reductions in thymic cell content [50,56–58]. Thymocyte numbers in Wnt-1$^{-/-}$Wnt-4$^{-/-}$ double-knockout mice are reduced by 50–70% at days 15–16 of gestation and by 40–50% at birth, although other Wnt proteins expressed in the thymus could partially replace the lack of Wnt-1 and Wnt-4 [58]. Similar results are observed in TCF-1$^{-/-}$ mice and the reduction of thymic cellularity is exacerbated with age [50,56]. Conversely, the number of cells obtained from cell suspension cultures of foetal thymocytes transduced with Wnt-1 and Wnt-4 is sevenfold higher than in control cultures [55]. Proliferation and survival are the two parameters that seem to be contributing to the altered thymic cell numbers after Wnt signalling modifications. Cell-cycle analysis of adult TCF-1-deficient mice reveals a major reduction in the proliferation rate in those thymocyte populations representing important cell expansion steps during T-cell development, such as CD44$^+$CD25$^+$ DN2, CD44$^-$CD25$^-$DN4 and ISP cells [52,56]. The reduction of cells in the S and G2/M phases of the cell cycle is 93% for CD44$^-$CD25$^-$DN4 cells, 50% for ISP thymocytes and 50% for uncommitted CD44$^+$CD25$^-$DN1 cells [52,56]. By contrast, the proliferation of DP thymocytes is not altered in TCF-1$^{-/-}$ mice, although TCF–β-catenin signalling promotes their survival by regulating Bcl-x_L expression [52]. In mice in which Wnt signalling is inhibited by overexpression of Axin using an inducible Axin transgene, the thymus is very small and histological analysis reveals massive apoptosis of cortical thymocytes [59], confirming that β-catenin activation promotes thymocyte survival.

Thymocyte differentiation is not affected in Wnt-1$^{-/-}$ Wnt-4$^{-/-}$ double-knockout mice [58], whereas it is severely impaired in the TCF-1$^{-/-}$ thymus [50,56]. In one-month-old TCF-1$^{-/-}$ mice, DP cells represent $<30\%$ of total thymus and the percentages of DN and ISP cell

subsets are concomitantly increased [50,56]. This increase in ISP cells is already detected at 10 days of postnatal life [56]. The analysis of DN subsets in young mice demonstrates the total absence of the $CD44^+CD25^+$DN2 population and a reduction in $CD44^-CD25^-$DN4 cells, which contrasts with the fivefold increase observed in the $CD44^+CD25^-$DN1 subset. This is the main population present in six-month-old TCF-$1^{-/-}$ thymus [56]. In FTOCs from TCF-$1^{-/-}$ LEF-$1^{-/-}$ double-knockout mice, the differentiation of thymocytes from ISP to DP cells is completely arrested, and there is also a blockade at the $CD44^-CD25^+$ DN3 stage [57]. The requirement of β-catenin for intrathymic TCF-1 function, and therefore its connection with the Wnt cascade, has been demonstrated by Ioannidis *et al.* [52].

All the alterations seen in the absence of Wnt signalling could be explained by the reduction in cell survival and proliferation, as mentioned previously, and also by the block in T-cell differentiation at the ISP, $CD44^-CD25^+$DN and $CD44^+CD25^-$DN stages. Supporting the requirement of Wnt proteins during the earliest steps of thymocyte differentiation, TCF-$1^{-/-}$ haematopoietic progenitors are unable to differentiate into DP thymocytes when transferred to irradiated hosts or alymphoid FTOCs [56]. Similar blocks in T-cell differentiation at the DN stage are observed after transduction of foetal liver progenitor cells with a soluble form of Fz7 [55] and by the addition of antisense oligonucleotides for TCF-1 to foetal thymus lobes reconstituted with foetal liver cells [51].

The way in which Wnt proteins regulate different steps of T-cell maturation is unclear. In TCF-$1^{-/-}$ and TCF-$1^{-/-}$ LEF-$1^{-/-}$ thymocytes, the expression of specific genes, such as those encoding CD3ε, pTα, Lck, CD5 and Rag-1, is unaffected [57]. The transcriptional activities of TCF-1 and LEF-1 are not necessary for the rearrangement and expression of the TCRβ chain and only TCRα is affected in TCF-$1^{-/-}$ LEF-$1^{-/-}$ mice [57]. Nevertheless, recent data indicate that Wnt signalling must be switched-off to ensure the rearrangement and expression of the TCRβ chain before CD4/CD8 expression. The somatic activation of β-catenin induces a premature expression of CD4 and CD8 coreceptors, leading to the generation of DP and SP thymocytes that have not rearranged their TCRβ chain [53]. These cells are unable to expand or survive properly, indicating that the constitutive activation of the canonical Wnt pathway is not able to mimic completely the proliferation and survival signals derived from the pre-TCR [53]. p53 and Ikaros have been proposed to participate in the establishment of a refractory window to Wnt at the $CD25^+$DN stage while the TCRβ chain is being rearranged because Ikaros$^{-/-}$ mice show a similar phenotype to that produced after β-catenin stabilization [60] and p53 inactivation results in maturation of thymocytes to the DP stage in the absence of pre-TCR signalling [61–63]. Moreover, p53 is able to induce the proteasomal degradation of β-catenin [47]. Nevertheless, the possible participation of other mechanisms, such as the regulation of Fz/LRP-5/6 receptor expression or the autocrine production by $CD25^+$DN thymocytes of soluble molecules, which would block Wnt signalling, should be addressed. The stages in thymocyte development where Wnt signalling is required for differentiation, survival or proliferation are summarized in Fig. 2c.

Recently, Wnt proteins have been demonstrated to be involved in thymus organogenesis, by regulating the expression FoxN1/Whn, the transcription factor that is defective in athymic nude mice [54].

Interactions between Wnt, Hh and BMP2/4 signalling pathways

The three families of Wnt, Hh and BMP2/4 morphogens frequently interact and regulate one another's expression or function during the development of many tissues. In vertebrate development, there are examples where Hh is upstream of BMP2/4 (e.g. Ref. [21]) and downstream of BMP2/4 (e.g. Ref. [64]), and where Wnts are upstream of Hh (e.g. Ref. [65]) or BMP2/4 (e.g. Ref. [66]) and downstream of Hh (e.g. Ref. [67]) or BMP2/4 (e.g. Ref. [68]), in the regulation of their expression. There are also examples where one morphogen modulates the function of another by regulating the expression of an inhibitor protein, thereby altering local concentrations of the second morphogen (e.g. Refs [69,70]). In the thymus, it is not yet known if these three families of signalling protein modulate one another's expression or function but as the actions of BMP2/4 and Shh seem to oppose that of Wnt signalling at key developmental checkpoints, it will be interesting to understand the relationships between these different signalling pathways. To date, it is not clear if these molecules act as true morphogens in their regulation of thymocyte development, and it will be interesting to test the actions of different concentrations and of concentration gradients on thymocytes.

Conclusions

In summary, it has recently become clear that the Wnt, BMP and Hh families of intercellular signalling molecules have a role in the control of T-cell development in the thymus (Fig. 2). The Wnt signalling pathway has a positive role because its absence or inhibition leads to reduced proliferation and differentiation of DN thymocytes and survival of DP thymocytes [50,52,56,57], whereas increased Wnt signalling by stabilization of β-catenin enabled differentiation to DP cells in the absence of a pre-TCR signal [53]. By contrast, the Hh and BMP2/4 signalling pathways appear to function as negative regulators of T-cell development [7,22,23]. Shh, BMP2 and BMP4 are made by the thymic epithelium, suggesting that they provide a means for the epithelium to regulate T-cell development. Treatment of FTOCs with BMP4 *in vitro* inhibits thymocyte proliferation and arrests thymocyte development at the $CD44^+CD25^-$DN1 stage before T-cell lineage commitment [23], and at the transition from DN to DP cells [22], whereas treatment with BMP4 antagonists (Noggin or Chordin and Tsg) increases T-cell differentiation to DP cells [22,23]. BMP4 treatment enhances survival of $CD44^+CD25^-$DN1 cells, suggesting that the physiological role of BMP4 might be to maintain a pool of pluripotent thymocyte precursors and also to control thymic homeostasis and T-cell production. Treatment of FTOCs with Shh also arrests thymocyte development at the $CD25^+$DN stage after rearrangement of the

gene encoding the TCRβ chain. Pre-TCR signalling downregulates *smo*, which results in the differentiating thymocyte becoming refractory to Hh signalling. These data suggest that Hh signalling provides a break in thymocyte differentiation during rearrangement of the TCRβ chain gene.

Acknowledgements

A.V., R.S., A.V. and A.G.Z. are supported by grants PM99–0060 and BMC2001–2025 from Ministerio de Ciencia y Tecnología and CAM08.3/0041/2000 and CAM 08.3/0018.1/2001 from the Comunidad Autónoma de Madrid. A.L.H-T. and T.C. are supported by the Medical Research Council and the Wellcome Trust. This work was also supported by Acciones Integradas Hispano-Británicas. We thank David Bacon for preparation of figures.

References

1 Christian, J.L. (2000) BMP, Wnt and Hedgehog signals: how far can they go? *Curr. Opin. Cell Biol.* 12, 244–249
2 Gurdon, J.B. *et al.* (2001) Morphogen gradient interpretation. *Nature* 413, 797–803
3 Podos, S.D. *et al.* (1999) Morphogen gradients: new insights from DPP. *Trends Genet.* 15, 396–402
4 Ingham, P.W. *et al.* (2001) Hedgehog signaling in animal development: paradigms and principles. *Genes Dev.* 15, 3059–3087
5 Ruiz i Altaba, A. (1999) Gli proteins and Hedgehog signaling: development and cancer. *Trends Genet.* 15, 418–425
6 Koebernick, K. *et al.* (2002) Gli-type zinc finger proteins as bipotential transducers of Hedgehog signaling. *Differentiation* 70, 69–76
7 Outram, S.V. *et al.* (2000) Hedgehog signaling regulates differentiation from double-negative to double-positive thymocyte. *Immunity* 13, 187–197
8 Li, C.L. *et al.* (2002) Estrogen deficiency results in enhanced expression of Smoothened of the Hedgehog signaling in the thymus and affects thymocyte development. *Int. Immunopharmacol.* 2, 823–833
9 Li, C.L. *et al.* (2002) Thymosin α1 accelerates restoration of T cell-mediated neutralizing antibody response in immunocompromised hosts. *Int. Immunopharmacol.* 2, 39–46
10 Haks, M.C. *et al.* (1999) Cell-fate decisions in early T-cell development: regulation by cytokine receptors and the pre-TCR. *Semin. Immunol.* 11, 23–37
11 Wall, N.A. *et al.* (1994) TGF-β related genes in development. *Curr. Opin. Genet. Dev.* 4, 517–522
12 Winnier, G. *et al.* (1995) Bone morphogenetic protein-4 is required for mesoderm formation and patterning in the mouse. *Genes Dev.* 9, 2105–2116
13 Zhang, H. *et al.* (1996) Mice deficient for BMP2 are nonviable and have defects in amnion/chorion and cardiac development. *Development* 122, 2977–2986
14 von Bubnoff, A. *et al.* (2001) Intracellular BMP signaling regulation in vertebrates: pathway or network? *Dev. Biol.* 239, 1–14
15 Miyazono, K. *et al.* (2001) Divergence and convergence of TGF-β/BMP signaling. *J. Cell. Physiol.* 187, 265–276
16 Smith, W.C. (1999) TGF-β inhibitors. New and unexpected requirements in vertebrate development. *Trends Genet.* 15, 3–5
17 Chang, C. *et al.* (2001) Twisted gastrulation can function as a BMP antagonist. *Nature* 410, 483–487
18 Ross, J.J. *et al.* (2001) Twisted gastrulation is a conserved extracellular BMP antagonist. *Nature* 410, 479–483
19 Scott, I.C. *et al.* (2001) Homologues of Twisted gastrulation are extracellular cofactors in antagonism of BMP signalling. *Nature* 410, 475–478
20 Bhatia, M. *et al.* (1999) Bone morphogenetic proteins regulate the developmental program of human hematopoietic stem cells. *J. Exp. Med.* 189, 1139–1148
21 Bhardwaj, G. *et al.* (2001) Sonic hedgehog induces the proliferation of primitive human hematopoietic cells via BMP regulation. *Nat. Immun.* 2, 172–180
22 Graf, D. *et al.* (2002) The developmentally regulated expression of Twisted gastrulation reveals a role for bone morphogenetic proteins in the control of T-cell development. *J. Exp. Med.* 196, 163–171
23 Hager-Theodorides, A.L. *et al.* (2002) Bone morphogenetic protein 2/4 signaling regulates early thymocyte differentiation. *J. Immunol.* 169, 5496–5504
24 Dewulf, N. *et al.* (1995) Distinct spatial and temporal expression patterns of two type I receptors for bone morphogenetic proteins during mouse embryogenesis. *Endocrinology* 136, 2652–2663
25 Dick, A. *et al.* (1998) Expression of Smad1 and Smad2 during embryogenesis suggests a role in organ development. *Dev. Dyn.* 211, 293–305
26 Flanders, K.C. *et al.* (2001) Immunohistochemical expression of Smads 1–6 in the 15-day gestation mouse embryo: signaling by BMPs and TGF-β. *Dev. Dyn.* 220, 141–154
27 Graf, D. *et al.* (2001) Evolutionary conservation, developmental expression and genomic mapping of mammalian Twisted gastrulation. *Mamm. Genome* 12, 554–560
28 Takagi, T. *et al.* (2001) Murine Schnurri-2 is required for positive selection of thymocytes. *Nat. Immunol.* 2, 1048–1053
29 Takahama, Y. *et al.* (1994) Early progression of thymocytes along the CD4/CD8 developmental pathway is regulated by a subset of thymic epithelial cells expressing transforming growth factor β. *J. Exp. Med.* 179, 1495–1506
30 Xie, T. *et al.* (1998) decapentaplegic is essential for the maintenance and division of germline stem cells in the *Drosophila* ovary. *Cell* 94, 251–260
31 Miller, J.R. (2002) The Wnts. *Genome Biol.* 3 REVIEWS3001
32 Tamai, K. *et al.* (2000) LDL-receptor-related proteins in Wnt signal transduction. *Nature* 407, 530–535
33 Pandur, P. *et al.* (2002) Increasingly complex: new players enter the Wnt signaling network. *Bioessays* 24, 881–884
34 Niehrs, C. (1999) Head in the WNT: the molecular nature of Spemann's head organizer. *Trends Genet.* 15, 314–319
35 Leyns, L. *et al.* (1997) Frzb-1 is a secreted antagonist of Wnt signaling expressed in the Spemann organizer. *Cell* 88, 747–756
36 Wang, S. *et al.* (1997) Frzb, a secreted protein expressed in the Spemann organizer, binds and inhibits Wnt-8. *Cell* 88, 757–766
37 Piccolo, S. *et al.* (1999) The head inducer Cerberus is a multifunctional antagonist of Nodal, BMP and Wnt signals. *Nature* 397, 707–710
38 Wodarz, A. *et al.* (1998) Mechanisms of Wnt signaling in development. *Annu. Rev. Cell Dev. Biol.* 14, 59–88
39 Polakis, P. (2000) Wnt signaling and cancer. *Genes Dev.* 14, 1837–1851
40 Moon, R.T. *et al.* (2002) The promise and perils of Wnt signaling through β-catenin. *Science* 296, 1644–1646
41 Roose, J. *et al.* (1998) The *Xenopus* Wnt effector XTcf-3 interacts with Groucho-related transcriptional repressors. *Nature* 395, 608–612
42 Leiden, J.M. (1993) Transcriptional regulation of T cell receptor genes. *Annu. Rev. Immunol.* 11, 539–570
43 Clevers, H.C. *et al.* (1993) Transcription factors in early T-cell development. *Immunol. Today* 14, 591–596
44 Kuhl, M. *et al.* (2000) The Wnt/Ca^{2+} pathway: a new vertebrate Wnt signaling pathway takes shape. *Trends Genet.* 16, 279–283
45 Liu, T. *et al.* (2001) G protein signaling from activated rat frizzled-1 to the β-catenin–Lef–Tcf pathway. *Science* 292, 1718–1722
46 Adler, P.N. *et al.* (2001) Frizzled signaling and cell–cell interactions in planar polarity. *Curr. Opin. Cell Biol.* 13, 635–640
47 Matsuzawa, S.I. *et al.* (2001) Siah-1, SIP, and Ebi collaborate in a novel pathway for β-catenin degradation linked to p53 responses. *Mol. Cell* 7, 915–926
48 Oosterwegel, M. *et al.* (1991) Cloning of murine TCF-1, a T-cell-specific transcription factor interacting with functional motifs in the CD3-ϵ and T-cell receptor α enhancers. *J. Exp. Med.* 173, 1133–1142
49 Van de Wetering, M. *et al.* (1996) Extensive alternative splicing and dual promoter usage generate Tcf-1 protein isoforms with differential transcription control properties. *Mol. Cell. Biol.* 16, 745–752
50 Verbeek, S. *et al.* (1995) An HMG-box-containing T-cell factor required for thymocyte differentiation. *Nature* 374, 70–74
51 Hattori, N. *et al.* (1996) Involvement of transcription factors TCF-1 and GATA-3 in the initiation of the earliest step of T-cell development in the thymus. *J. Exp. Med.* 184, 1137–1147
52 Ioannidis, V. *et al.* (2001) The β-catenin–TCF-1 pathway ensures CD4(+)CD8(+) thymocyte survival. *Nat. Immun.* 2, 691–697
53 Gounari, F. *et al.* (2001) Somatic activation of β-catenin bypasses

pre-TCR signaling and TCR selection in thymocyte development. *Nat. Immun.* 2, 863–869
54 Balciunaite, G. *et al.* (2002) Wnt glycoproteins regulate the expression of FoxN1, the gene defective in nude mice. *Nat. Immunol.* 3, 1102–1108
55 Staal, F.J. *et al.* (2001) Wnt signaling is required for thymocyte development and activates Tcf-1 mediated transcription. *Eur. J. Immunol.* 31, 285–293
56 Schilham, M.W. *et al.* (1998) Critical involvement of Tcf-1 in expansion of thymocytes. *J. Immunol.* 161, 3984–3991
57 Okamura, R.M. *et al.* (1998) Redundant regulation of T-cell differentiation and TCRα gene expression by the transcription factors LEF-1 and TCF-1. *Immunity* 8, 11–20
58 Mulroy, T. *et al.* (2002) Wnt-1 and Wnt-4 regulate thymic cellularity. *Eur. J. Immunol.* 32, 967–971
59 Hsu, W. *et al.* (2001) Impaired mammary gland and lymphoid development caused by inducible expression of Axin in transgenic mice. *J. Cell Biol.* 155, 1055–1064
60 Winandy, S. *et al.* (1999) Pre-T cell receptor (TCR) and TCR-controlled checkpoints in T-cell differentiation are set by Ikaros. *J. Exp. Med.* 190, 1039–1048
61 Nacht, M. *et al.* (1996) Mutations in the p53 and SCID genes cooperate in tumourigenesis. *Genes Dev.* 10, 2055–2066
62 Jiang, D. *et al.* (1996) p53 prevents maturation to the $CD4^+CD8^+$ stage of thymocyte differentiation in the absence of T-cell receptor rearrangement. *J. Exp. Med.* 183, 1923–1928
63 Haks, M.C. *et al.* (1999) Pre-TCR signaling and inactivation of p53 induces crucial cell survival pathways in pre-T cells. *Immunity* 11, 91–101
64 Zhang, Y. *et al.* (2000) A new function of BMP4: dual role for BMP4 in regulation of Sonic hedgehog expression in the mouse tooth germ. *Development* 127, 1431–1443
65 Huelsken, J. *et al.* (2001) β-catenin controls hair follicle morphogenesis and stem-cell differentiation in the skin. *Cell* 105, 533–545
66 Kim, J.S. *et al.* (2002) Oncogenic β-catenin is required for bone morphogenetic protein 4 expression in human cancer cells. *Cancer Res.* 62, 2744–2748
67 Reddy, S. *et al.* (2001) Characterization of Wnt gene expression in developing and postnatal hair follicles and identification of Wnt5a as a target of Sonic hedgehog in hair follicle morphogenesis. *Mech. Dev.* 107, 69–82
68 Marcelle, C. *et al.* (1997) Coordinate actions of BMPs, Wnts, Shh and noggin mediate patterning of the dorsal somite. *Development* 124, 3955–3963
69 Lee, C.S. *et al.* (2001) Evidence that the WNT-inducible growth arrest-specific gene 1 encodes an antagonist of Sonic hedgehog signaling in the somite. *Proc. Natl. Acad. Sci. U. S. A.* 98, 11347–11352
70 Grotewold, L. *et al.* (2002) The Wnt antagonist Dickkopf-1 is regulated by Bmp signaling and c-Jun and modulates programmed cell death. *EMBO J.* 21, 966–975
71 van Genderen, C. *et al.* (1994) Development of several organs that require inductive epithelial–mesenchymal interactions is impaired in LEF-1-deficient mice. *Genes Dev.* 8, 2691–2703

Exhibit 3

Combinatorial Cassette Mutagenesis as a Probe of the Informational Content of Protein Sequences

John F. Reidhaar-Olson, Robert T. Sauer

Science, New Series, Volume 241, Issue 4861 (Jul. 1, 1988), 53-57.

Stable URL:
http://links.jstor.org/sici?sici=0036-8075%2819880701%293%3A241%3A4861%3C53%3ACCMAAP%3E2.0.CO%3B2-A

Research Articles

Combinatorial Cassette Mutagenesis as a Probe of the Informational Content of Protein Sequences

JOHN F. REIDHAAR-OLSON AND ROBERT T. SAUER

A method of combinatorial cassette mutagenesis was designed to readily determine the informational content of individual residues in protein sequences. The technique consists of simultaneously randomizing two or three positions by oligonucleotide cassette mutagenesis, selecting for functional protein, and then sequencing to determine the spectrum of allowable substitutions at each position. Repeated application of this method to the dimer interface of the DNA-binding domain of λ repressor reveals that the number and type of substitutions allowed at each position are extremely variable. At some positions only one or two residues are functionally acceptable; at other positions a wide range of residues and residue types are tolerated. The number of substitutions allowed at each position roughly correlates with the solvent accessibility of the wild-type side chain.

IT HAS BEEN MORE THAN 20 YEARS SINCE ANFINSEN AND HIS colleagues showed that the sequence of a protein contains all of the information necessary to specify the three-dimensional structure (*1*). However, the general problem of predicting protein structure from sequence remains unsolved. Part of the difficulty may stem from the complexity of protein structures. Although some 200 protein structures are known, no rules have emerged that allow structure to be related to sequence in any simple fashion (*2*). The problem is further complicated by the nonuniformity of the structural information encoded in protein sequences. Some residue positions are important, and changes at these positions can tip the balance between folding and unfolding (*3–7*). Other residues are relatively unimportant in a structural sense and a wide range of substitutions or modifications can be tolerated at these positions (*3, 7–9*).

If only a fraction of the residues in a protein sequence contribute significantly to the stability of the folded structure, then it becomes important to be able to identify these residues. We now describe the results of genetic studies that allow the importance of individual residues in protein sequences to be rapidly determined. Specifically, we determine the spectrum of functionally acceptable substitutions at residue positions near the dimer interface of the NH_2-terminal domain of phage lambda (λ) repressor (*10*). The NH_2-terminal domain binds to operator DNA as a dimer, with dimerization mediated by hydrophobic packing of α helix 5 of one monomer against α helix 5′ of the other monomer (*11*) (Fig. 1, A and B). Without helix 5 there are no contacts between the subunits (Fig. 1C). By applying combinatorial cassette mutagenesis to the helix 5 region, we find that the number and spectrum of allowable substitutions within helix 5 are extremely variable from residue to residue. In most cases, this variability can be rationalized in terms of the fractional solvent accessibility of the wild-type side chain.

General strategy. For our studies, we used a plasmid-borne gene that encodes a functional, operator-binding fragment (residues 1–102) of λ repressor (*12*). The binding of the 1–102 fragment to operator DNA depends on dimerization which, in turn, depends on the helix 5–helix 5′ packing interactions (*11, 13*). Thus, if a 1–102 protein retains normal operator-binding properties, we can infer that it is able to dimerize normally.

Mutagenesis of the helix 5 region was performed by a combinatorial cassette procedure. One example of this method, in which codons 85 and 88 are mutagenized, is illustrated in Fig. 2. On the top strand, the mutagenized codons are synthesized with equal mixtures of all four bases in the first two codon positions and an equal mixture of G and C in the third position. The resulting population of base combinations will include codons for each of the 20 naturally occurring amino acids at each of the mutagenized residue positions. On the bottom strand, inosine is inserted at each randomized position because it is able to pair with each of the four conventional bases (*14*). The two strands are then annealed and the mutagenic cassette is ligated into a purified plasmid backbone.

To identify plasmids encoding functional protein, we selected transformants for plasmid-encoded resistance to ampicillin and for resistance to killing by cI^- derivatives of phage λ. The latter selection requires that the cell express 1–102 protein that is active in operator binding (*15*). For each mutagenesis experiment, many independent transformants were chosen, single-stranded plasmid DNA was purified, and the relevant region of the 1–102 gene was sequenced. The resulting set of sequences provides a list of functionally acceptable helix 5 residues.

Substitutions in the helix 5 region. In separate experiments with different mutagenic cassettes, the codons for helix 5 residues 85 and 88; 86 and 89; 90 and 91; 84, 87, and 88; and 84, 87, and 91 were mutagenized, and genes encoding active 1–102 proteins were selected. In some cases, the survival frequency was low. For example, only 17 of 60,000 transformants passed the selection after randomization of codons 84, 87, and 88. In this case, each active candidate was sequenced. By contrast, 1,200 of 50,000 transformants passed the selection in the mutagenesis of positions 86 and 89 (*16*). In this case, we picked 50 candidates for sequence analysis. Overall, 150 active genes were sequenced (Table 1). In addition, we sequenced

The authors are in the Department of Biology, Massachusetts Institute of Technology, Cambridge, MA 02139.

approximately 40 genes that had been mutagenized, but not subjected to a functional selection. These serve as controls for the efficiency of mutagenesis and also provide examples of helix 5 mutations that result in inactive 1–102 proteins (Table 1).

Many of the active sequences contain at least two residue changes compared to wild type. In principle, some of these changes could be compensatory; for example, residue X might be functionally allowed at position 85 only in combination with residue Z at position 88. This cannot be generally true, however, because most residue changes at one position were recovered in combination with several different changes at the other position or positions. It is therefore likely that most substitutions that are functionally acceptable in multiply mutant backgrounds would also be allowed as single substitutions. In Fig. 3, we show the spectrum of functionally acceptable substitutions at residue positions 84 to 91.

From the list of allowed substitutions, several conclusions may be drawn concerning the structural requirements at various positions in helix 5. We now consider these residue positions in order of decreasing "informational content," where this term is roughly defined as a value that decreases as the number of allowed substitutions increases. Thus, the informational content of a residue position is highest if only the wild-type amino acid is allowed and is lowest if each of the 20 naturally occurring amino acids is allowed.

Positions 84 and 87 in particular stand out as having a high informational content. Ile appears to be the only acceptable residue at position 84. Both Met and Leu are residues of similar size and hydrophobicity, and are the only two residues that appear to be functional at position 87. The side chains of Ile^{84} and Met^{87} form a major part of the helix-helix packing interaction at the dimer interface, where Ile^{84} of one subunit packs against $Met^{87'}$ of the other subunit, and vice versa (Fig. 4). This cluster of four residues also contacts the globular portions of the domain. Solvent accessibility calculations by the method of Lee and Richards (*17*) show that the Ile^{84} and Met^{87} side chains are almost completely buried (92 to 98 percent solvent inaccessible) in the structure of the dimer. We assume that replacement of Ile^{84} or Met^{87} with smaller side chains would diminish dimerization because hydrophobic and van der Waals interactions would be lost. In fact, mutant repressors containing Ser^{84} or Thr^{87} are defective in dimerization (*13, 18*). Replacing Ile^{84} or Met^{87} with larger residues would also be expected to be detrimental because substantial structural rearrangements would be required to accommodate larger side chains.

Seven residues (Leu, Ile, Val, Thr, Cys, Ser, and Ala) are functionally acceptable at position 91. Aromatic residues, charged residues, and strongly hydrophilic residues are not found. The wild-type Val side chain is partially buried in the dimer structure, with the Cγ2 methyl group packing against the Cδ1 methyl group of the $Ile^{84'}$ side chain. Although some of the acceptable substitutions such as Ile and Thr could make equivalent packing contacts, others such as Ala and Ser could not.

Nine residues (Trp, His, Met, Gln, Leu, Val, Ser, Gly, and Ala) are acceptable at position 90. There is a surprisingly large range in both the acceptable size and hydrophilicity of these side chains. This is especially true as the Cβ methyl group of the wild-type Ala is almost completely buried in the structure of the dimer and, at first glance, it would appear that larger side chains could not be accommodated. However, the inaccessibility of the Cβ methyl group of Ala^{90} is largely caused by the $Lys^{67'}$ side chain, which packs against it. By rotating the $Lys^{67'}$ side chain away, we were able to introduce a Trp^{90} side chain by model-building without steric clashes. Rotation of the $Lys^{67'}$ side chain away from Ala^{90} should not be energetically costly and, in fact, is observed in crystals of the NH_2-terminal domain bound to operator DNA (*19*).

Nine different residues (Trp, Tyr, Phe, Met, Ile, Val, Cys, Ser, and Ala) are functionally acceptable at position 88. There are large variations in the sizes and volumes of the acceptable side chains, although most are relatively hydrophobic. Charged residues and other strongly hydrophilic residues are not observed. In the wild-type dimer (*11*), the aromatic ring of Tyr^{88} stacks against the ring of $Tyr^{88'}$. The side chains of Trp, Phe, Met, Ile, and Val could probably form some type of packing interaction at this position, although those of Ala and Ser could not. It is known that the presence of Cys at position 88 allows a stable Cys^{88}–$Cys^{88'}$ disulfide bond, which links the monomers in a conformation that is active in operator binding (*20*).

Positions 85, 86, and 89 show considerable variability. At each of these positions, 13 different amino acids were found to function. At positions 85 and 86, aromatic, hydrophobic, polar, and charged residues are all acceptable. At position 89, aromatic residues were not represented, but each of the remaining classes was observed. In

Table 1. Sequences for the helix 5 region of active and inactive mutants obtained by combinatorial cassette mutagenesis. Active mutants are resistant to phage λKH54; these are grouped by cassette, with the wild-type sequence at the top of each group and randomized positions in boldface. Asterisks indicate sequences of mutants obtained in the absence of a functional selection. The activity of these mutants was subsequently determined by a screen. Numbers next to sequences indicate the number of times particular mutant sequences were obtained. Numbers at the tops of the columns indicate amino acid positions. The one-letter abbreviations for the amino acids are: A, Ala; C, Cys; D, Asp; E, Glu; F, Phe; G, Gly; H, His; I, Ile; K, Lys; L, Leu; M, Met; N, Asn; P, Pro; Q, Gln; R, Arg; S, Ser; T, Thr; V, Val; W, Trp; and Y, Tyr.

Active

85 90		85 90		85 90		85 90	
IYEMYEAV		-L--V---		--Y--S--		--E--L--*	
I--MF---	2	-L--M---		--Y--T--		--E--E--	
I--MY---	4	-I--F---		--W--A--		--E--G--*	
I-AMA---		-I--A---		--W--C--		--G--E--	
I-DMY---		-I--S---		--W--Q--			
I--MA---	3	-Q--Y---		--W--S--	3	IYEMYEAV	
I--MI---		-S--Y---		--W--K--*		------WA	4
I--LF---		-S--W---		--W--D--		------WL*	
I--LW---		-T--Y---		--W--D--*		------WS	
		-T--W---		--W--E--		------HV	
IYEMYEAV		-T--A---		--W--G--	3	------AV	6
I--M---V		-R--F---		--A--E--	3	------AC	2
I--M---T		-R--W---	4	-SM--A--		------AL	4
I--L---T		-R--A---	3	--M--S--	3	------AI	
		-R--C---		--L--S--	2	------AT	2
IYEMYEAV		-E--F---		--L--T--		------VA	
-Y--F---		-G--Y---		--L--E--		------VC	2
-W--W---	2			--L--E--*		------MA	
-W--A---		IYEMYEAV		--I--S--		------LA*	
-A--Y---		--F--M--		--Q--S--		------QV	
-V--Y---	2	--F--L--		--S--Q--		------QT	
-V--A---	3	--F--I--		--S--E--		------SV	3
-C--F---	2	--F--Q--		--T--E--		------SC	2
-C--A---		--F--S--	3	--D--L--		------SL	5
-L--F---		--F--T--		--D--Q--		------ST	
-L--W---		--F--R--		--D--D--*		------GC	
-L--A---		--F--E--		--E--L--	2	------GI	
						------GT	

Inactive

85 90	85 90	85 90	85 90
A--VA---*	P--DS---*	Q--CS---*	------RN*
P--PL---*	R--TR---*	A--TP---*	------EA*
P--TN---*	T--TV---*	S--TK---*	------KV*
R--NP---*	R--VI---*	T--LN---*	------VM*
P--LL---*	L--PL---*	A--SL---*	------PA*
A--IL---*	I--LL---*	R--WS---*	------NQ*
T--KP---*	K-AIV---*	------PR*	------ME*
Q--RV---*	C--YT---*	------PP*5	------AY*
H-DVR---*			

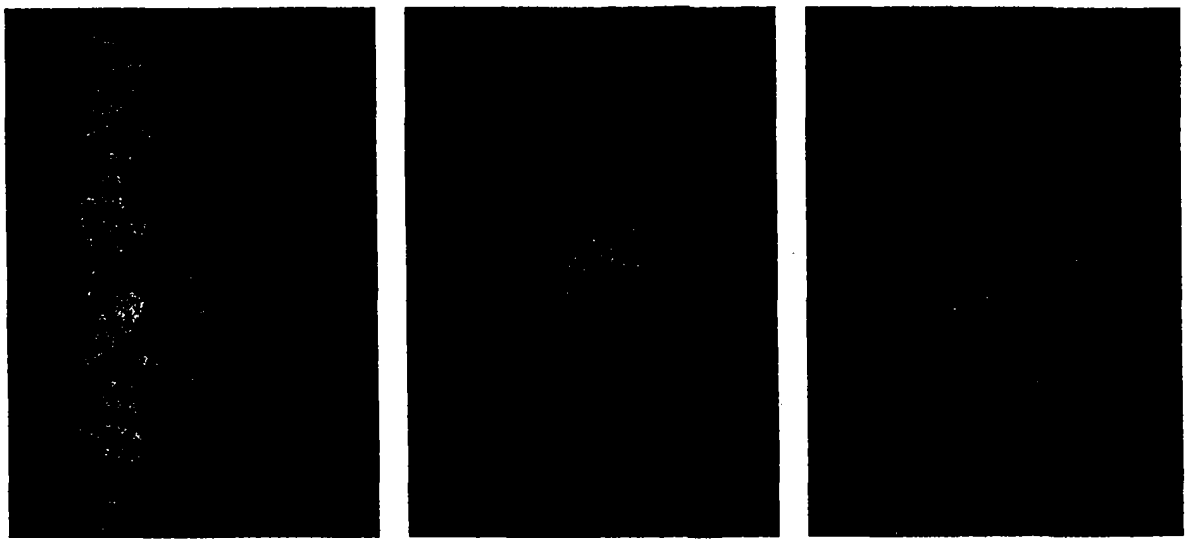

Fig. 1. Three views of the DNA-binding domain of λ repressor, showing the role of helix 5 in dimerization. (**A**) Proposed complex of repressor dimer with operator DNA (*11*). Helix 5 of each monomer is colored more lightly than the globular portion of that monomer. (**B**) Free repressor dimer, rotated 90° from the view in (A), to show the "back side" of the molecule. (**C**) Dimer with helix 5 of each monomer removed. This view illustrates the role helix 5 plays in mediating dimerization (*26*).

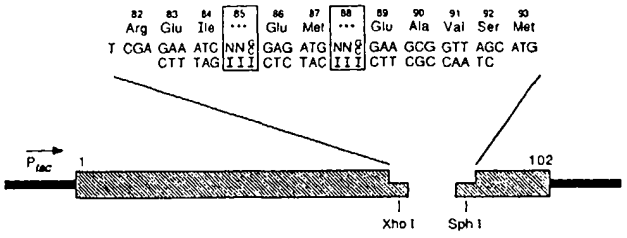

Fig. 2. Schematic diagram showing the combinatorial cassette mutagenesis procedure. At positions indicated as N, an equal mixture of A, G, C, and T was used during oligonucleotide synthesis. At positions indicated as I, inosine was used. After synthesis, the oligonucleotides were phosphorylated, annealed, and ligated into the Xho I–Sph I backbone of plasmid pJO103. Plasmid pJO103 is an M13 origin plasmid with the I–102 gene under control of a *tac* promoter; the region of the I–102 gene encoding residues 82–93 (the small Xho I–Sph I fragment) is replaced by an unrelated 1.9-kb Xho I–Sph I "stuffer" fragment. Ligated DNA was transformed into *Escherichia coli* strain X90 F'*lacI*^{Q} cells (*27*), and ampicillin-resistant colonies were selected in the presence or absence of phage λKH54. Candidates that survived the selection were cross-streaked against a series of virulent derivatives of phage λ to confirm their immunity properties [strains and methods are described in (*21*)]. Single-stranded plasmid DNA was purified from an M13RV1 transducing lysate as described (*28*), and DNA sequences were determined by the dideoxy method (*29*).

the wild-type dimer, the side chains of Tyr^{85}, Glu^{86}, and Glu^{89} are relatively solvent accessible.

Several amino acids are significantly underrepresented among the active sequences. For example, Pro is never found. This cannot be an artifact of our mutagenesis procedure because Pro is frequently observed among the unselected mutant sequences (Table 1). We conclude that Pro is not found among the functional sequences because it is selected against; its presence would presumably disrupt the α-helical structure and thereby the helix-helix packing at the dimer interface.

His, Asn, and Lys are also underrepresented among the functional helix 5 sequences. These residues are presumably not acceptable at positions 84 and 87, where the informational content is extremely high, and may not be acceptable at positions 88 and 91, where the functional substitutions are generally hydrophobic in character. The acceptability of these residues at positions such as 85 and 86 is difficult to assess from our experiments because the codons for these residues are present at reasonably low frequencies even among the unselected sequences. In these cases, we probably have not sequenced a large enough number of candidates to be confident that all acceptable substitutions have been identified. In fact, data from reversion studies (*21*) and suppressed amber studies (*22*) show that His^{85} and Lys^{86} are acceptable substitutions in the context of the intact λ repressor molecule.

Informational content and protein structure. We have combined an efficient combinatorial mutagenesis procedure and a functional selection to probe the informational content of the eight residues that form the major part of the dimerization interface of the NH_2-terminal, operator-binding domain of λ repressor. At two of these eight residue positions, the functionally acceptable choices are highly restricted. For example, we analyzed 17 functional genes in which codon 84 had been randomized and recovered the wild-type residue, Ile, in every case. This is clearly a position of high

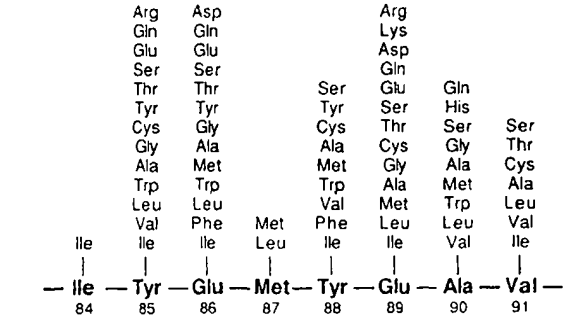

Fig. 3. Functionally acceptable residues in the helix 5 region. The amino acids are listed from top to bottom in order of increasing hydrophobicity according to the scale of Eisenberg *et al.* (*30*).

Fig. 4. Helix 5 residues high in informational content. The two isolated helix 5 regions of the protein are shown in green and blue. Ile^{84} and Met^{87} from the green helix are shown in yellow; Ile^{84} and Met^{87} from the blue helix are shown in red.

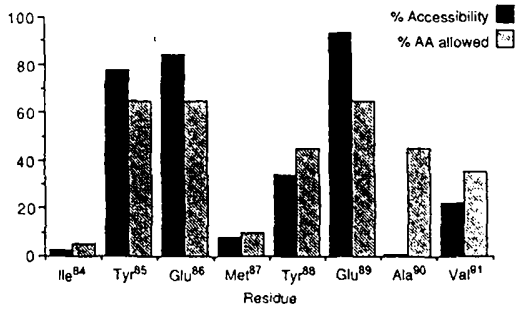

Fig. 5. Correlation between the solvent accessibility and the number of functionally acceptable substitutions. Hatched bars indicate the percentage of the 20 naturally occurring amino acids that are functionally acceptable at a residue position. Black bars indicate the fractional solvent accessibility of the wild-type side chain in the dimer. Solvent accessibilities for the NH_2-terminal domain dimer (*11*) were computed using a 1.4 Å probe by the method of Lee and Richards (*17*). Fractional accessibilities were obtained by dividing by the appropriate side chain accessibilities calculated for the monomer. The fractional accessibilities change only slightly if the side chain accessibilities in the reference tripeptide Ala-X-Ala (*17*) are used instead as the reference state.

informational content. The informational content is also high at position 87, where Met and Leu are the only acceptable residues. By contrast, the remaining positions have moderate to low informational contents. For example, among 38 functional genes in which codon 85 had been randomized, the wild-type residue was recovered only once, and 12 other residues, differing in size and chemical properties, were recovered in the remaining cases. This is clearly a position of low informational content. It is striking that most of the structural determinants of dimerization in this eight-residue segment reside in two residues only. The remaining positions are surprisingly tolerant of a wide range of substitutions. If this high level of tolerance is generally true of protein sequences, then the problem of understanding and predicting structure may rest largely on the ability to identify those few residues that are crucial.

The positional variability of the informational content in helix 5 can, in general, be rationlized in terms of the solvent accessibility of the wild-type residues in the crystal structure (*11*). There is a rough correlation between the number of acceptable substitutions and the fractional extent to which the wild-type side chain is solvent accessible (Fig. 5). At exposed surface positions such as 85, 86, and 89, we find that many different residues and residue types can be functionally accommodated. By contrast, at positions such as 84 and 87, where the wild-type side chain is almost completely buried, we find that the functionally acceptable residue choices are extremely restricted. There is one apparent exception to the simple rule that buried residues are high in informational content. Ala^{90} is inaccessible to solvent in the crystal structure, and yet we find that many substitutions are allowed at this position. However, the inacessibility of the Ala^{90} side chain to solvent is not due to close packing at the dimer interface, but rather to an interaction with a nearby surface side chain. This side chain can presumably move to allow larger side chains to be accommodated at position 90. Examples of this type demonstrate the need to distinguish between two types of buried side chains: those that can become exposed by relatively minor rearrangement of other side chains, and those that are tightly packed in the hydrophobic core.

There is no reason to assume that there should always be a strict correlation between the solvent accessibility of a residue and the structural informational content of that position. For one thing, the chemical properties of the 20 amino acids are not related in any simple linear fashion. Moreover, the structural importance of some residues in proteins almost certainly stems from interactions other than simple hydrophobic packing. Nevertheless, the closely packed nature of protein interiors (*23*) provides a simple molecular explanation for the structural importance of buried residues, and destabilizing mutations are commonly found to affect hydrophobic core residues (*3–7*). By contrast, missense mutations or chemical modifications that affect surface residues are often found to have little or no influence on protein stability (*3, 7, 8*). Thus, it is reasonable that solvent accessibility should be an extremely important determinant of the informational content of a residue position.

Our overall strategy for rapidly probing informational content should be broadly applicable to a wide range of protein structure-function problems in systems where genetic selections or screens can be devised. The method consists of three basic elements: (i) the use of cassette mutagenesis to introduce extremely high levels of targeted random mutagenesis; (ii) the use of a functional selection to identify genes encoding active proteins; and (iii) the use of rapid DNA sequencing methods to determine the spectrum of functionally acceptable residues in a relatively large number of candidates. Our method of combinatorial cassette mutagenesis (Fig. 2) allows several residue positions to be mutagenized at the same time and, in principle, generates a mutant population in which each of the 20 amino acids is represented at each mutagenized position (*24*). When two or three codons are mutagenized at the same time, the entire analysis is able to proceed more rapidly. Moreover, at this level of mutagenesis most two-residue and three-residue combinations should be present in the mutagenized population and should be recovered if they result in a functional protein. In our study of the packing of the 84 and 87 side chains, we recovered only two (Ile^{84} with Met^{87} and Ile^{84} with Leu^{87}) of the 400 possible residue combinations. Thus, because both positions were mutagenized in the same experiment, we are able to conclude that there are not significantly different ways of packing the dimer interface.

In principle, data like that shown in Fig. 3 could be generated for an entire protein sequence, and additional experiments could be devised to determine whether the positions of high informational content were important for structure or function. For proteins of unknown structure, such data might be quite useful for structural predictions. First, current predictive algorithms could be applied to the family of related sequences generated by our method, as each of these sequences is able to form the same basic structure. Second, because of their fundamental repeats, α-helical and β-strand regions might be recognized by characteristic patterns of high and low informational content. Third, the positions of highest structural informational content should include the residues involved in

formation of the hydrophobic core of the protein. This information might prove useful in combination with the tertiary template ideas recently proposed (*25*).

REFERENCES AND NOTES

1. C. J. Epstein, R. F. Goldberger, C. B. Anfinsen, *Cold Spring Harbor Symp. Quant. Biol.* **28**, 439 (1963); C. B. Anfinsen, *Science* **181**, 223 (1973).
2. T. E. Creighton, *Proteins: Structures and Molecular Properties* (Freeman, New York, 1983), chap. 6.
3. M. H. Hecht, H. C. M. Nelson, R. T. Sauer, *Proc. Natl. Acad. Sci. U.S.A.* **80**, 2676 (1983); M. H. Hecht, J. M. Sturtevant, R. T. Sauer, *ibid.* **81**, 5685 (1984); M. H. Hecht, K. M. Hehir, H. C. M. Nelson, J. M. Sturtevant, R. T. Sauer, *J. Cell. Biochem.* **29**, 217 (1985).
4. D. Shortle and B. Lin, *Genetics* **110**, 539 (1985); D. Shortle and A. K. Meeker, *Proteins* **1**, 81 (1986).
5. A. Pakula, V. Young, R. T. Sauer, *Proc. Natl. Acad. Sci. U.S.A.* **83**, 8829 (1986).
6. T. Alber, S. Dao-pin, J. A. Nye, D. C. Muchmore, B. W. Matthews, *Biochemistry* **26**, 3754 (1987).
7. G. Fermi and M. F. Perutz, *Haemoglobin and Myoglobin* (Clarendon, Oxford, 1981).
8. M. Hollacker and T. E. Creighton, *Biochem. Biophys. Acta* **701**, 395 (1982).
9. J. H. Miller, in *The Operon*, J. H. Miller and W. S. Reznikoff, Eds. (Cold Spring Harbor Laboratory, Cold Spring Harbor, NY, 1978), pp. 31–88.
10. λ repressor consists of an NH_2-terminal and COOH-terminal domain; each domain contains an independent set of dimerization contacts [C. O. Pabo, R. T. Sauer, J. M. Sturtevant, M. Ptashne, *Proc. Natl. Acad. Sci. U.S.A.* **76**, 1608 (1979); C. O. Pabo, thesis, Harvard University (1980)].
11. C. O. Pabo and M. Lewis, *Nature* **298**, 443 (1982).
12. The NH_2-terminal domain of λ repressor is minimally comprised of residues 1–92. This is the fragment for which the crystal structure is known. In our studies we use a slightly larger NH_2-terminal fragment consisting of repressor residues 1–102. Nuclear magnetic resonance studies show that the 1–92 and 1–102 fragments have the same basic structure and similar dimerization properties (*13*). The operator binding properties of the 1–92 and 1–102 fragments are also extremely similar (*20*).
13. M. A. Weiss, C. O. Pabo, M. Karplus, R. T. Sauer, *Biochemistry* **26**, 897 (1987); M. A. Weiss, M. Karplus, R. T. Sauer, *ibid.*, p. 890.
14. F. H. Martin, M. M. Castro, F. Aboul-ela, I. Tinoco, *Nucleic Acids Res.* **13**, 8927 (1985).
15. In control experiments, we found that cells containing at least 5 to 10 percent of the wild-type activity could survive the phage selection. This figure was determined by Western analysis of lysates of cells containing the wild-type 1–102 gene under control of the inducible *lac* promoter. When expression of 1–102 was induced to a level sufficient to make cells resistant to phage λKH54, the intracellular level of 1–102 was 5 to 10 percent of that produced from the *tac* promoter.
16. The survival frequency can be somewhat misleading, as some cells containing functional genes do not survive the selection. For example, by screening the unselected candidates in the mutagenesis of positions 86 and 89, we found that approximately 20 percent of the cells contained active protein. By contrast, only 2.4 percent of the cells survived the selection in this experiment.
17. B. Lee and F. M. Richards, *J. Mol. Biol.* **55**, 379 (1971); in our studies, accessible surface areas were calculated with the use of the ACCESS program written by T. Richmond.
18. F. S. Gimble and R. T. Sauer, *J. Mol. Biol.*, in press.
19. S. Jordan and C. Pabo, personal communication.
20. R. T. Sauer *et al.*, *Biochemistry* **25**, 5992 (1986); C. O. Pabo and E. G. Suchanek, *ibid.* **25**, 5987 (1986).
21. M. H. Hecht and R. T. Sauer, *J. Mol. Biol.* **186**, 53 (1985).
22. H. C. M. Nelson, M. H. Hecht, R. T. Sauer, *Cold Spring Harbor Symp. Quant. Biol.* **47**, 441 (1983).
23. F. M. Richards, *J. Mol. Biol.* **82**, 1 (1974); C. Chothia, *Nature* **254**, 304 (1975).
24. There are several methods, in addition to our own, that could be used for combinatorial cassette mutagenesis: A. R. Oliphant, A. L. Nussbaum, K. Struhl, *Gene* **44**, 177 (1986); K. M. Derbyshire, J. J. Salvo, N. D. F. Grindley, *ibid.* **46**, 145 (1986). The use of inosines, in our method, is convenient and efficient, but does lead to some bias in the frequency at which each base is recovered. For example, among the unselected candidates in the mutagenesis of positions 84, 87, and 88, the frequencies at which the four bases were recovered at the mutagenized positions were: 23 percent A, 35 percent C, 20 percent G, and 23 percent T. The methods cited above avoid a pairing bias by performing enzymatic second-strand synthesis.
25. J. W. Ponder and F. M. Richards, *J. Mol. Biol.* **193**, 775 (1987).
26. These graphics were produced with the Promodeber molecular graphics program (New England BioGraphics). Coordinates were provided by C. O. Pabo.
27. D. Hanahan, *J. Mol. Biol.* **166**, 557 (1983).
28. A. K. Vershon, K. Blackmer, R. T. Sauer, in *Protein Engineering: Applications in Science, Medicine, and Industry*, M. Inouye and R. Sarma, Eds. (Academic Press, Orlando, FL, 1986), pp. 243–256.
29. F. Sanger, S. Nicklen, A. R. Coulson, *Proc. Natl. Acad. Sci. U.S.A.* **74**, 5463 (1977).
30. D. Eisenberg, R. M. Weiss, T. C. Terwilliger, W. Wilcox, *Faraday Symp. Chem. Soc.* **17**, 109 (1982).

31. We thank R. Breyer for providing plasmids and antibodies required for the work, D. Vershon for suggesting the use of inosines for the combinatorial mutagenesis method, and J. Bowie for pointing out the potential uses of the method in structural prediction. We also thank C. Pabo and S. Jordan for providing the coordinates of the NH_2-terminal domain and its complex with operator DNA, and thank G. Quigley for help with the accessibility calculations. This work was supported by NIH grant AI-15706 and by a predoctoral grant (to J.R.-O.) from the National Science Foundation.

3 March 1988; accepted 18 May 1988

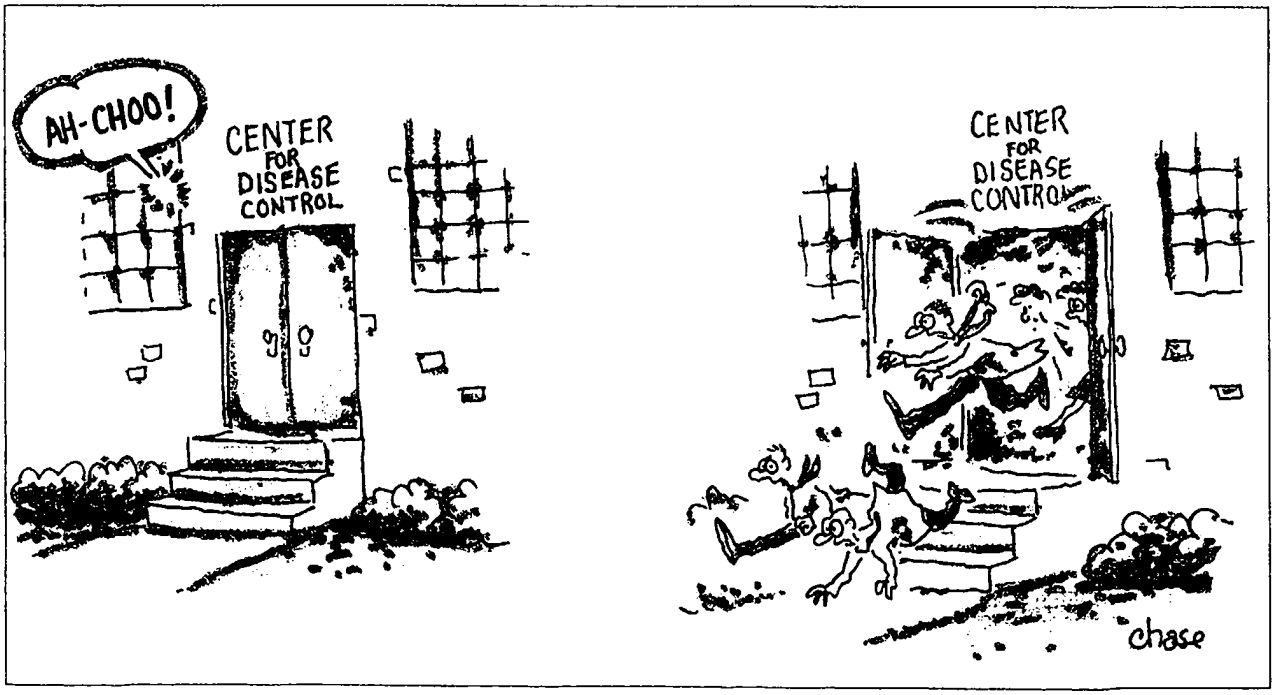

Exhibit 3

Development 120, 3339-3353 (1994)
Printed in Great Britain © The Company of Biologists Limited 1994

Products, genetic linkage and limb patterning activity of a murine *hedgehog* gene

David T. Chang[1], Alric López[2], Doris P. von Kessler[1], Chin Chiang[1], B. Kay Simandl[2], Renbin Zhao[1], Michael F. Seldin[3], John F. Fallon[2] and Philip A. Beachy[1]

[1]Howard Hughes Medical Institute, Department of Molecular Biology and Genetics, The Johns Hopkins School of Medicine, Baltimore, Maryland 21205, USA
[2]Department of Anatomy, Neuroscience Training Program, University of Wisconsin, Madison, Wisconsin 53706, USA
[3]Departments of Medicine and Microbiology, Duke University Medical Center, Durham, North Carolina 27710, USA

SUMMARY

The *hedgehog* (*hh*) segmentation gene of *Drosophila melanogaster* encodes a secreted signaling protein that functions in the patterning of larval and adult structures. Using low stringency hybridization and degenerate PCR primers, we have isolated complete or partial *hh*-like sequences from a range of invertebrate species including other insects, leech and sea urchin. We have also isolated three mouse and two human DNA fragments encoding distinct *hh*-like sequences. Our studies have focused upon *Hhg-1*, a mouse gene encoding a protein with 46% amino acid identity to *hh*. The *Hhg-1* gene, which corresponds to the previously described vhh-1 or sonic class, is expressed in the notochord, ventral neural tube, lung bud, hindgut and posterior margin of the limb bud in developing mouse embryos. By segregation analysis the *Hhg-1* gene has been localized to a region in proximal chromosome 5, where two mutations affecting mouse limb development previously have been mapped. In *Drosophila* embryos, ubiquitous expression of the *Hhg-1* gene yields effects upon gene expression and cuticle pattern similar to those observed for the *Drosophila hh* gene. We also find that cultured quail cells transfected with a *Hhg-1* expression construct can induce digit duplications when grafted to anterior or mid-distal but not posterior borders within the developing chick limb; more proximal limb element duplications are induced exclusively by mid-distal grafts. Both in transgenic *Drosophila* embryos and in transfected quail cells, the *Hhg-1* protein product is cleaved to yield two stable fragments from a single larger precursor. The significance of *Hhg-1* genetic linkage, patterning activity and proteolytic processing in *Drosophila* and chick embryos is discussed.

Key words: mouse, *hedgehog*, genetic linkage, limb development, gene expression, *Hammertoe*, *Hemimelic extra toes*

INTRODUCTION

Experimental manipulations of vertebrate embryos have revealed the existence of organizing centers that appear to function in the patterning of adjacent structures. The dorsal blastopore lip in *Xenopus*, for example, appears to control development of the major body axis (Spemann, 1933), while the posterior margin of the limb bud or ZPA (zone of polarizing activity or polarizing region) is capable of imposing pattern upon developing limbs (Saunders and Gasseling, 1968; Wolpert, 1969). Because these and other organizing centers contribute few of the cells that constitute the actual structure being formed, patterning activity is inferred to occur through the agency of molecules secreted from the organizing center. Until recently, however, little was known about the nature and identity of these molecules.

Drosophila development has long served as a model system for the study of molecules important in vertebrate developmental processes, including secreted signaling proteins. For example, the product of the *dpp* (*decapentaplegic*) gene, a member of the TGF-β super-family of signaling molecules which is expressed at the dorsal pole of the embryo, acts as a concentration-dependent factor capable of imposing pattern along the entire dorsal-ventral axis of the embryo (Ferguson and Anderson, 1992). The *wingless* (*wg*) segment polarity gene, a member of the *Wnt* super-family that also includes many vertebrate representatives (reviewed by Nusse and Varmus, 1992), encodes another signaling protein that acts at somewhat shorter range in segmentation and in patterning of the embryonic cuticle. Early expression of the *wg* gene in a stripe of cells bordering the parasegment boundary is required for maintenance of appropriate gene expression in an adjacent stripe of cells on the opposite side of the parasegment boundary (DiNardo et al., 1988; Martinez Arias et al., 1988); at a later stage, specification of appropriate differentiated fates depends upon expression of the *wg* product in neighboring cells (Baker, 1988; Bejsovec and Martinez-Arias, 1991; Dougan and DiNardo, 1992).

Another *Drosophila* segment polarity gene that has been implicated as encoding a signaling molecule with an important role in patterning is *hedgehog* (*hh*). Clones of mutant cells lacking *hh* function appear to affect adjacent structures in the

eye and cuticle of the *Drosophila* adult (Mohler, 1988; Heberlein et al., 1993; Ma et al., 1993). In the embryo, *hh* transcription is restricted to cells in a narrow stripe adjacent to and non-overlapping with the *wingless* stripe; *hh* mutations, however, affect gene expression and cuticle pattern elements in cells outside this zone of transcription (Mohler and Vani, 1992; Lee et al., 1992; Tabata et al., 1992; Tashiro et al., 1993). The notion that *hedgehog* encodes a secreted signaling molecule is also supported by other types of evidence – in vitro translated protein products can be secreted into microsomes (Lee et al., 1992) and immunostaining of *Drosophila* embryos shows that the *hh* protein is distributed in stripes that are broader than the stripes of *hh* transcription (Taylor et al., 1993; Tabata and Kornberg, 1994; von Kessler, D.V. and Beachy, P.A. unpublished observations). Molecular characterization of the *Drosophila hh* gene (Lee et al., 1992; Mohler and Vani, 1992; Tabata et al., 1992; Tashiro et al., 1993) revealed no sequence similarities to the products of other genes, despite the fact that many segment polarity genes do have homologues in other species (see Peifer and Bejsovec, 1992 for a review). More recently, however, several groups have demonstrated the existence of *hedgehog* homologs in chick, mouse, zebrafish and rat (Echelard et al., 1993; Krauss et al., 1993; Riddle et al., 1993; Roelink et al., 1994; S. C. Ekker and P. A. B., unpublished data).

Here we present evidence for broad evolutionary conservation of *hedgehog* sequences among invertebrate species. We also confirm the existence of a family of at least three mouse *hedgehog* homologues (Echelard et al., 1993) and demonstrate the existence of two new human *hedgehog* homologues. We show that *Hhg-1*, the mouse homologue which corresponds to the independently identified vhh-1 and sonic *hedgehog* genes in the rat and the mouse (Roelink et al., 1994; Echelard et al., 1993), is expressed in the notochord, ventral neural tube, lung bud, hindgut and posterior limb bud margin in developing mouse embryos. To elucidate *Hhg-1* function, we first demonstrated that *Hhg-1* yields effects upon gene expression and cuticle pattern similar to those of the *Drosophila hh* gene when ubiquitously expressed in *Drosophila* embryos. We also found that grafts of cells expressing *Hhg-1* can impose pattern upon the developing chick limb. In both of these systems, the *Hhg-1* protein product is cleaved to yield two stable fragments from a single larger precursor. Consistent with a role in limb patterning, we mapped *Hhg-1* by segregation analysis to a region of mouse chromosome five with tight linkage to two previously mapped limb mutants. Proteolytic processing of *Hhg-1* products and their ability to function in *Drosophila* embryos as well as in vertebrate limb patterning suggests widespread conservation of the fundamental mechanisms underlying function of the *hedgehog* multi-gene family.

MATERIALS AND METHODS

Isolation of *hedgehog* homologues

Genomic clones from *Drosophila hydei* and the mosquito *Anopheles gambiae* were isolated by low-stringency screening (hybridization at 52°C, 6× SSC; washes in 2× SSC) of a *D. hydei* genomic library in the EMBL4 lambda phage vector (a gift of M. Claudia and D. Sullivan) and of an *A. gambiae* genomic library in the lambda phage vector DASH 2 (kindly provided by J. Kassis). The initial probe for this screen corresponded to positions 389-1801 (numbering according to Lee et al., 1992), and further analysis of the *D. hydei* clone using exon-specific probes identified three hybridizing regions that corresponded to exons 1, 2 and 3 of *D. melanogaster hh*. The flour beetle (*Tribolium castaneum*; DNA a gift from Sue Brown), the leech (*Hirudo medicinalis*; DNA a gift from G. Aisemberg), the sea urchin (*Strongylocentrotus purpuratus*; DNA a gift from A. Cameron) and the mouse and human *hh*-like sequences were initially isolated by polymerase chain reaction (PCR) using primers degenerate for all possible coding combinations of the sequences underlined in Fig. 1. PCR amplifications contained from 100 ng to 2 μg genomic DNA (depending upon the genome size of the species), 2 μM of each primer, 200 μM dNTPs (Pharmacia), 1× reaction buffer (Boehringer-Mannheim) and 2.5 units Taq polymerase (Boehringer-Mannheim) in 50 μl reactions. Amplification was as follows: 94°C 5 minutes, addition of Taq polymerase at 75°C, followed by 94°C 1 minute, 52°C 1.5 minutes and 72°C 1 minute for 30 cycles and a final extension of 72°C for 5 minutes. All PCR products were cloned into pBluescript (Stratagene) prior to sequence determination. No *hh*-like sequences were obtained using DNA from *Dictyostelium* or from *C. elegans* using this approach.

Mouse clones obtained in this manner contained 144 bases of sequence between the primer ends and were labelled with [α-^{32}P]dATP and used for high stringency screens of mouse cDNA libraries made from whole 8.5 dpc embryonic RNA (Lee, 1990) and from 14.5 dpc embryonic brain in the λZAP vector (a gift from A. Lanahan). Several clones corresponding to *Hhg-1* were isolated and the largest, 2629 bp in length (pDTC8.0), was chosen for sequence analysis using dideoxy chain termination (Sanger et al., 1977) and Sequenase v2.0 (US Biochemicals). Compressions were resolved by using 7-deaza guanosine (US Biochemicals). Sequence analysis made use of the Geneworks 2.0 (IntelliGenetics) and MacVector 3.5 (IBI) software packages.

Analysis of RNA expression in mouse and *Drosophila* embryos

For northern blot analysis, RNA from mouse embryos and from mouse adult tissues was isolated, electrophoresed in 1.2% agarose, blotted and probed, essentially as described by Ausubel et al. (1993). The probe used was made by random hexamer primed synthesis using the pDTC8.0 insert as a template in the presence of [α-^{32}P]dATP. Hybridizations and washes were performed under standard high stringency conditions (Ausubel et al., 1993).

In situ hybridization to sections of mouse embryos was essentially as described Wilkinson (1992), except that [α-^{33}P]rUTP was substituted in place of [α-^{35}S]rUTP for riboprobe synthesis. Briefly, 7.5-10.5 dpc mouse embryos were harvested, fixed in ice-cold 4% paraformaldehyde in PBS, dehydrated through an ethanol series, cleared in xylene and embedded in paraffin. 6 μm sections were floated on a 48°C water bath, transferred to AAS (3-aminopropyltriethoxysilane, Sigma) subbed slides, dewaxed with xylene and hybridized overnight to riboprobe in the sense or antisense orientations. Slides were washed under high-stringency conditions, dipped in Kodak NTB-2 emulsion and developed after a 10 day exposure. All sections were then stained for 30 seconds with haematoxylin (Polysciences) and mounted with Permount (Fisher). Sense and antisense probes were synthesized using a riboprobe synthesis kit from Stratagene with a 249 bp *Bam*HI/*Sma*I fragment of pDTC8.0 that extends from residues 297 to 380 within the *Hhg-1* open reading frame (Fig. 1) subcloned into Bluescript as template (pDTC1.8). Adobe Photoshop was used for superimposition of bright-field and dark-field views, collected in digital form using a Sony 3 CCD camera attached to a Zeiss Axioplan microscope and transferred directly to a Macintosh Quadra 800 equipped with a Nuvista Video Capture Board.

In situ hybridization to *Drosophila* embryos was performed according to standard methods (Tautz and Pfeifle, 1989). The *wingless* (*wg*) probe was made by random hexamer primed synthesis (Feinberg and Vogelstein, 1983) using a 2.2 kb *Hin*dIII/*Xba*I fragment from a

wg cDNA (gift from R. Nusse; Rijsewijk et al., 1987) as template. Probe synthesis was carried out in the presence of digoxigenin-dUTP (Boehringer Mannheim).

Drosophila germ-line transformation and phenotypic analysis

The hs*hh* construct was made by inserting a blunted 1581 bp *MseI* fragment containing the full *hh* ORF (from 327 to 1908, Lee et al., 1992) into the *StuI* site of pCaSpeR-hs (Thummel et al., 1988; from C. Thummel, University of Utah, Salt Lake City). The hs*Hhg-1* construct was made by inserting a blunted 1330 bp *Bsu*36I/*Eco*57I fragment from pDTC8.0 that contained the entire *Hhg-1* open reading frame into the *StuI* site of pCaSpeR-hs. hs*hh* and hs*Hhg-1* each were coinjected with pπ25.2 wc into w^{1118} embryos using a standard protocol for P element-mediated transformation (Rubin and Spradling, 1982). Germ line transformants with P element integration on the third chromosome were isolated for each construct; hs*hh* was maintained as a homozygous stock and hs*Hhg-1* was maintained over the TM3 balancer chromosome.

Embryos for cuticle analysis were collected and aged at 25°C and heat shocked for 1 hour at 37°C. After further incubation for 24 hours at 25°C, embryos were dechorionated, transferred to Hoyer's mountant (Wieschaus and Nusslein-Volhard, 1986) and incubated at 65°C for 5 hours. For in situ hybridization, *Drosophila* embryos from the hs-*hh*, hs-*Hhg-1* and w^{1118} parent lines were collected for 5 hours at 25°C, aged an additional 5 hours at 25°C, heat shocked for 1 hour at 37°C and allowed to recover at 25°C for an additional hour before fixation.

Chick limb patterning assays

Isolation and characterization of the quail cell line QT6 has been described (Moscovici et al., 1977). QT6 cells were cultured on 3.5 cm uncoated plastic culture dishes (Falcon) in growth medium (M199 medium plus Earles balanced salt solution [Gibco, Grand Island, NY] supplemented with 10% tryptose phosphate broth, 5% fetal calf serum, 1% dimethylsulfoxide, 100 U/ml of penicillin and 100 μg/ml of streptomycin) in a 5% CO_2 atmosphere.

QT6 cells were transiently transfected by a modified calcium phosphate method (Chen and Okayama, 1987). In brief, after preincubation in transfection medium (DMEM plus 5% fetal calf serum + 1% DMSO) 20-25μg of precipitated DNA was added to 70-80% confluent QT6 cells in dishes. After overnight incubation, the DNA precipitate was removed and complete growth medium added. The pCIS plasmid, which carries a cytomegalovirus (CMV) promoter and SV40 intron and polyadenylation signal (Gorman, 1985), was used as the expression vector. Expression constructs included pCIS*lacZ* and pCIS*Hhg-1*, which contain *lacZ* and *Hhg-1* respectively under control of the CMV promoter. To assess transfection efficiency parallel plates were transfected with equimolar amounts of either pCIS-*lacZ* or pCIS*Hhg-1*.

For β-galactosidase activity staining, cells and limb buds were fixed 5 minutes and 1 hour, respectively, in PBS containing 2% formaldehyde and 0.2% glutaraldehyde. After rinsing in PBS, samples were incubated in X-gal cocktail (1 mg/ml X-gal (5-bromo-4-chloro-3-indolyl b-D-galactopyranoside), 2 mM $MgCl_2$, 16 mM $K_3Fe(CN)_6$, 16 mM $K_4Fe(CN)_6$) for 18-24 hours at 22°C.

Transiently transfected QT6 cells were scraped from tissue culture plates with a Teflon scraper (Falcon) and dissociated by repeated pipetting. Poly-D-lysine (Sigma, P1149) was added to the cell suspension to a concentration of 33 μg/ml. Cells were then pelleted by centrifugation at 1×10^3 revs/minute on a benchtop microfuge for 10 seconds. Wedge-shaped fragments were excised from the pelleted cells and grafted to anterior, mid-distal, or posterior slits made with fine forceps in stage 20-21 chick wing buds (Riley et al., 1993). Embryos harvested at day 10 were fixed overnight in 10% formaldehyde, stained with Victoria blue and cleared in methyl salicylate (see Riley et al., 1993).

Detection of *Hhg-1* protein

Region-specific antibodies were generated by immunization of New Zealand White rabbits with PCR-generated, His_6-tagged fusions (in the vector pTrcHis from InVitrogen, San Diego, CA) to residues 25-159 (N-terminal) and 202-389 (C-terminal) of the *Hhg-1* ORF (Fig. 1). Following repeated boosts, reactive sera were purified using affinity matrices carrying fusions of glutathione-S-transferase to the same portions of the *Hhg-1* ORF (in the vector pGEX from Amrad, Melbourne, Australia). Specific antibodies were eluted with a buffer containing 100 mM glycine-HCl at pH 2.5 (Harlow and Lane, 1988).

For immunodetection, samples of tranfected and untransfected QT6 cells and of heat-shocked wild-type and hs*Hhg-1* Drosophila embryos were suspended and boiled in sample loading buffer and electrophoresed in 12% polyacrylamide-SDS gels (Laemmli, 1970). Following transfer to nitrocellulose (Burnette, 1981), proteins were detected by chemiluminescence (with the ECL kit from Amersham), with affinity purified anti-*Hhg-1* antibodies at a dilution of 1/300 and HRP-conjugated goat anti-rabbit 2° antibody (Jackson ImmunoResearch, Baltimore MD) at a dilution of 1/10,000.

Chromosome localization of *Hhg-1*

C3H/HeJ-*gld* and *Mus spretus* (Spain) mice and [(C3H/HeJ-*gld* × Mus spretus)F_1 × C3H/HeJ-*gld*] interspecific backcross mice were bred and maintained as previously described (Seldin et al., 1988) *Mus spretus* was chosen as the second parent in this cross because of the relative ease of detection of informative restriction fragment length variants (RFLV) in comparison with crosses using conventional inbred laboratory strains.

DNA isolated from mouse organs by standard techniques was digested with restriction endonucleases and 10 μg samples were electrophoresed in 0.9% agarose gels. DNA was transferred to Nytran membranes (Schleicher & Schuell, Inc., Keene, NH), hybridized at 65°C and washed under stringent conditions, all as previously described (Sambrook et al., 1989). Clones used as probes in the current study included a ~500 bp 3'-UTR of *Hhg-1*, a quinoid dihydropteridine reductase (Qdpr) clone, DHPR13 (Lockyer et al., 1987) and an interleukin 6, (Il-6) specific clone, 27-4 (Mock et al., 1989).

Gene linkage was determined by segregation analysis (Green, 1981). Gene order was determined by analyzing all haplotypes and minimizing crossover frequency between all genes that were determined to be within a linkage group. This method resulted in determination of the most likely gene order (Bishop, 1985).

Characterization of *Hhg-1* sequences in *Hm* and *Hx* mutants

DNA from heterozygous *Hm* (AKR.C3H-*Ca Hm Sl*) and heterozygous *Hx* (B10.D2/nSn-*Hx*/+) mutant individuals were obtained from Jackson Laboratory and digested with *Eco*RI, *Bam*HI, *Taq*I, *Hin*dIII, *Alu*I, *Rsa*I, *Dpn*I, *Hin*fI and *Hin*pI. These digests were electrophoresed, blotted and probed as above with ^{32}P-labelled pDTC8.0 and compared to similarly digested and probed DNAs from parental strains. No differences in restriction fragment lengths were detected for either mutant. This analysis would have detected differences as small as 100 bp.

Hhg-1 coding sequences were isolated by PCR amplification from genomic DNA of individuals heterozygous for the *Hx* mutation (B10.D2/nSn-*Hx*/+; Jackson Labs). Analysis included eleven independent clones representing coding sequences from exon one, fourteen independent clones representing coding sequences from exon two and eight independent clones representing coding sequences from exon three.

RESULTS

Isolation of *hedgehog* homologues

As a first step toward isolation of *hedgehog* homologues from distant species, we used low-stringency hybridization to isolate

genomic *hh* clones from two other dipterans, *Drosophila hydei* and the mosquito *Anopheles gambiae*. We then used the polymerase chain reaction (PCR) with degenerate primers from conserved regions within the second exon (underlined regions in Fig. 1) to isolate single *hh*-like sequences from genomic DNA of the flour beetle, leech and sea urchin, and multiple sequences from mouse and man. No *hh*-like sequences were obtained using DNA from *Dictyostelium* or from *C. elegans* by this approach. From sequence comparisons, human PCR fragments 1 and 2 appear to correspond most closely to mouse fragments 1 and 2, respectively.

Our focus here is primarily upon one of the three mouse clones, *Hhg-1*, which when used as a probe yielded a 2.0 kb clone from a 8.5 dpc mouse embryonic cDNA library and a 2.7 kb clone from a 14.5 dpc embryonic cDNA library. The 2.7 kb cDNA appears to represent a nearly full-length mRNA because it corresponds to a 2.8 kb band detected by hybridization on a northern blot (see below). The largest methionine-initiated open reading frame within this cDNA encompasses 437 codons and is preceded by one in frame upstream stop codon (not shown). Sequence comparisons indicate that the protein encoded by *Hhg-1* is identical to the independently characterized mouse *Shh* (Echelard et al., 1993) except for an arginine to lysine difference at residue 122. *Hhg-1* also corresponds closely to the rat *vhh-1* gene (97% amino acid identity; Roelink et al., 1994), the chicken *Sonic hedgehog* (81% identity; Riddle et al., 1993) and *Shh* from the zebrafish (68% identity; Krauss et al., 1993; Roelink et al., 1994; S.C. Ekker and P.A.B., unpublished data). The PCR-generated fragments *Hhg-2* and *Hhg-3* appear to correspond to the *Indian* and *Desert* classes of mouse *hedgehog* genes, respectively (Echelard et al., 1993).

Alignment of the *Hhg-1* open reading frame with the two *Drosophila hh* sequences (Fig. 1) shows that all three proteins contain hydrophobic amino acid sequences near their amino-termini; the hydrophobic stretches within the *D. melanogaster* protein (residues 64 to 83) and within the mouse protein are known to act efficiently as signal sequences for cleavage (Lee et al., 1992, and J. J. Lee and P. A. B., unpublished data). Both *Drosophila* signal sequences are unusual in their internal locations, while the hydrophobic stretch of the mouse gene occurs at the extreme amino-terminus, a more conventional location for cleaved signal sequences. Although portions of

Fig. 1. Multiple mammalian and invertebrate *hedgehog*-like sequences. The *Drosophila melanogaster hedgehog* open reading frame is shown aligned with a complete *hedgehog* coding sequence deduced from genomic sequence for *Drosophila hydei* and a complete mouse coding sequence (*Hhg-1*) deduced from a cDNA clone. Amino acid identities between these complete sequences are boxed, Kyte-Dolittle hydrophobic domains are shaded, predicted signal sequence cleavage sites (von Heijne, 1986) are indicated by an arrow; and intron/exon boundaries are marked by triangles. Below these complete sequences are shown partial sequences deduced from cloned PCR products for two other mouse genes (*Hhg-2* and *Hhg-3*) and two human sequences (*HHG-1* and *HHG-2*). Sequences from invertebrate species above the complete sequence alignments include partial sequences for the mosquito *Anopheles gambiae* (from a genomic clone) and PCR-derived sequences from the flour beetle, *Tribolium castaneum*, the urchin, *Strongylocentrotus purpuratus* and the leech, *Hirudo medicinalis*. Degenerate primers used for PCR reactions incorporated sequence from the underlined portion of the *D. melanogaster* sequence.

sequence N-terminal to the *Drosophila* signal sequences are conserved, suggesting a functional role, the mouse mouse gene lacks this region.

The overall level of amino acid identity between *Hhg-1* and *hh* carboxy-terminal to the signal sequences is 46%. A closer examination shows that the amino terminal portion, from residues 25 to 187, displays 69% identity, while remaining residues in the carboxy-terminal portion display a much lower 31% identity. Like *hh*, the *Hhg-1* coding sequence is divided into three exons and the boundaries of these exons are at the same positions within coding sequence as those of the three *Drosophila hh* exons (see Fig. 1). Curiously, the boundary between coding sequences of the second and third exons occurs near the transition from high to low levels of overall sequence conservation. The coincidence of these two boundaries suggests a possible demarcation of functional domains within these proteins. This location within *Hhg-1* coding sequence also coincides approximately with the site of a presumed proteolytic cleavage (see below).

Expression of *Hhg-1* in mouse embryos

We began our analysis of *Hhg-1* expression by hybridization of a ^{32}P-labelled *Hhg-1* probe to a northern blot of RNA isolated from embryos ranging from 8.5 to 18.5 dpc. A band of ~2.8 kb was detected at each stage, with a peak at day 10.5 (Fig. 2). These results are similar to those reported by Echelard et al. (1993) for *Shh* except that we detect the 2.8 kb RNA throughout embryogenesis. To obtain more detailed spatial and temporal information regarding *Hhg-1* expression, sections from 7.5, 8.5, 9.5 and 10.5 dpc embryos were hybridized to a ^{33}P-labelled antisense RNA probe under stringent hybridization and wash conditions (see Materials and methods); the corresponding sense RNA probe was used as a control. Selected sections from these in situ hybridizations are presented in Figs 3-5 and described below.

In the 7.5 dpc embryo, *Hhg-1* expression is confined to anterior midline mesoderm. No expression is seen in the overlying ectoderm (Fig. 3B,C) or in other embryonic or extraembryonic tissue (data not shown). Transverse sections confirm restriction of expression in the early gastrula to axial mesoderm (Fig. 3D-F); this mesodermal expression extends caudally with retraction of the node and is maintained through to formation of the notochord by 8.5 dpc (data not shown).

At 9.5 dpc, well after neural tube formation, strong expression of *Hhg-1* is seen in the entire notochord and in the ventral midline of caudal portions of the neural tube. More rostrally within the neural tube, *Hhg-1* expression extends ventrolaterally to encompass ~40% of the ventral neural tube at its maximum extent in the midbrain. Even more rostrally in the midbrain, midline expression is lost but reappears in a portion of the diencephalon (Fig. 4B). Horizontal sections demonstrate that expression rostral to the midbrain (Fig. 4C) splits and extends bilaterally (Fig. 4D,E), finally re-uniting in the ventral

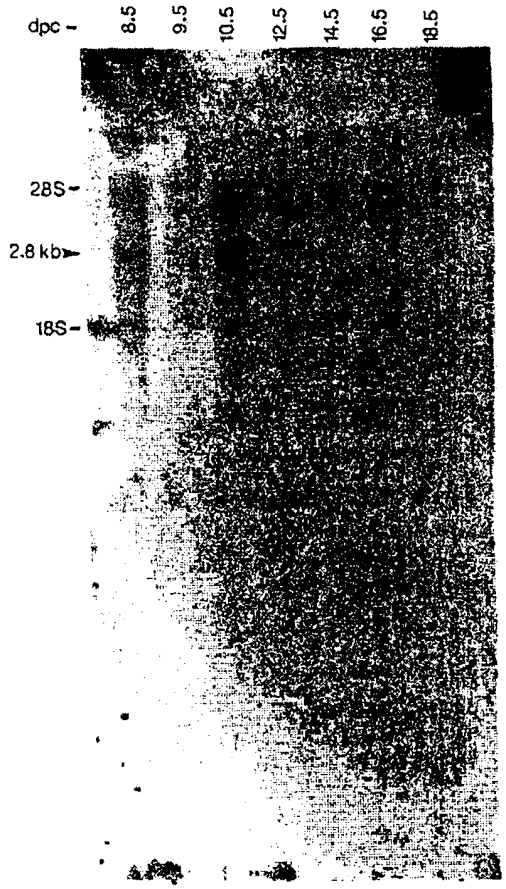

Fig. 2. Electrophoretic analysis of *Hhg-1* RNA. Each lane contains 10 μg total RNA from mouse embryos staged as indicated above the lanes (dpc, days post coitum). The probe, made from the full length *Hhg-1* cDNA, detected a ~2.8 kb band (indicated by arrowhead) in RNA from all stages of embryos examined. The upper band comigrates with the 28S RNA and is due to non-specific hybridization.

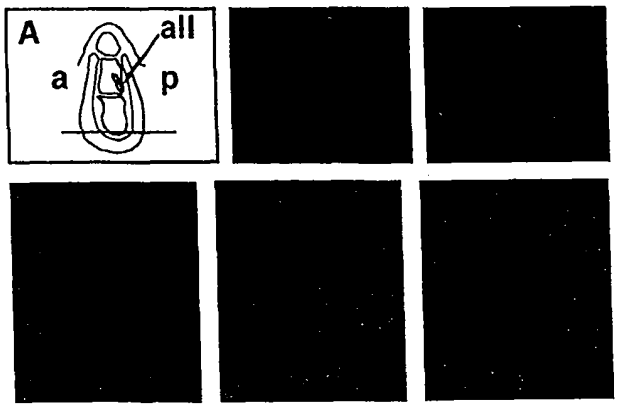

Fig. 3. *Hhg-1* expression at late gastrulation. (A) Schematic diagram showing 7.5 dpc mouse embryo, at late gastrulation. (B,C) Midsagittal sections through the egg cylinder showing hybridization in the axial mesoderm. (D-F) Adjacent horizontal sections through the egg cylinder at the level indicated in A. Note the hybridization in the midline mesoderm (asterisk). a, anterior; all, allantois; ect, ectoderm; mes, mesoderm; p, posterior.

midline of the diencephalon (Fig. 4B,E). *Hhg-1* expression thus is confined to a ring of cells in the ventral surface of the midbrain-diencephalic region. *Hhg-1* expression in the 10.5 dpc embryo is similar to that of the 9.5 dpc embryo, with strong expression in the notochord and most of the ventral neural tube and rostral neural tube expression remaining restricted to a ring of ventral cells. *Hhg-1* expression can also be observed in endoderm lining the future pharynx and foregut, with more intense expression occurring in the budding lungs; expression can also be detected in the hindgut. Finally, expression of *Hhg-1* in the limb buds at 10.5 dpc is restricted to the posterior margins of the forelimb (Fig. 5G-J) and hindlimb (data not shown). This expression clearly is restricted to the mesoderm and is absent from the overlying ectoderm, including the apical ridge. Our analysis of *Hhg-1* expression in the mouse embryo is consistent with that presented for *Shh* (Echelard et al., 1993) and for *vhh-1* in the rat embryo (Roelink et al., 1994).

Hhg-1 can function in *Drosophila* embryos

As a first step toward understanding the function of mouse *hedgehog* genes, we compared the effects of *Hhg-1* and *Drosophila hh* when ectopically expressed in *Drosopila* embryos under control of a heat inducible promoter. As described in Materials and Methods, germ-line insertions were made by P-element-mediated transformation of each gene cloned downstream of the *Drosophila* hsp70 promoter. Our analysis focused on one transformant line for each construct, designated hs*hh* and hs*Hhg-1*. Transcription of *hh* in the *Drosophila* embryo is normally restricted to a thin stripe of cells posterior to the parasegment boundary in each segment; expression of the *wingless* (*wg*) gene is normally restricted to a thin stripe of cells anterior and immediately adjacent to the *hh* stripe. Previous studies have demonstrated a dependence upon *hh* function for the maintenance of *wingless* expression (DiNardo et al., 1988; Martinez Arias et al., 1988); the spatial restriction of *wg* expression to this thin stripe is thought to result from limited diffusion of the signal encoded by *hh*. Ectopic expression of *hh* thus would be expected to cause an expansion in the domain of *wg* expression.

As shown in Fig. 6D,E, ubiquitous expression of *hh* induced by heat shock indeed causes an expansion in the extended germ band expression domain of the *wingless* gene, as has also been demonstrated by Ingham (1993). In addition, ectopic expression of *hh* produces consistent alterations in the size and orientation of denticles in the ventral cuticle (Fig. 6F; see Bejsovec and Wieschaus, 1993, for a description of the wild-type denticle pattern). The simplest interpretation of these changes is that bristle rows 4, 5 and 6 are replaced by bristles of size, shape and polarity normally associated with the denticles in rows 2 and 3, and our observations are again consistent with those of Ingham (1993). Neither of these changes occur in heat shocked wild-type embryos (Fig. 6A,C).

Similar analyses of ectopically expressed *Hhg-1* also reveal an expansion in the *wg* expression domain and effects upon the denticles in rows 4, 5 and 6 (Fig. 6G,I). The early effect on *wg*

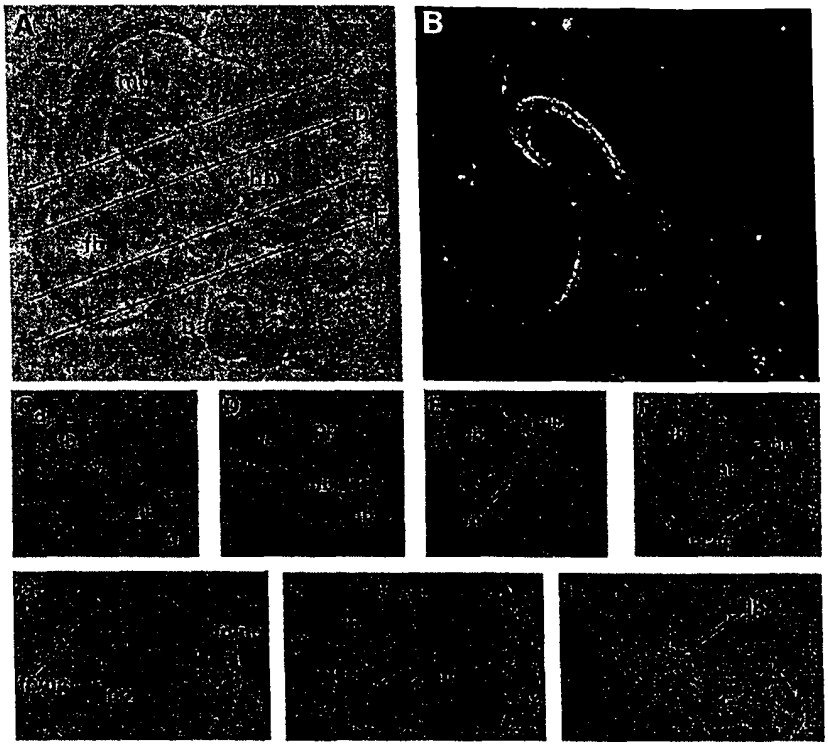

Fig. 4. *Hhg-1* expression in the 9.5 dpc embryo. (A,B) Bright and dark field views of a parasaggital section from a 9.5 dpc mouse embryo showing hybridization in the ventral midbrain and in a small patch of the ventral diencephalon. (C-F) Serial horizontal sections from superior to inferior levels in the head region of a 9.5 dpc mouse embryo. Broad, intense ventral hybridization is observed in the boundary region of the midbrain and forebrain (C). Rostrally, ventral-most expression is lost leaving two ventral/lateral domains of neural tube expression in cells adjacent to the optic vesicle. (D,E). Expression re-unites in a single midline domain of ventral neural tube cells overlying the pharyngeal lumen. Caudal to the hindbrain, neural tube expression is confined to the ventral midline (C-E) and expression is seen in the notochord beginning at its most rostral point (F). (G) Horizontal section at the level of the pericardiac region. The neural tube is cut twice in cross section at these levels and expression is likewise seen in floor plate and notochord of both cross sections. (H) Higher magnification view of G showing intense hybridization to floor plate and notochord. (I) Horizontal section at a lower level showing expression in the developing lung bud. In F, G and I, note the closer apposition of notochord to neural tube at more extreme rostral and caudal levels, indicative of an earlier stage of maturation relative to the intermediate level shown in H. ba, branchial arch; d, dorsal; fb, forebrain; fp, floor plate; lb, lung bud; mb, midbrain; nc, notochord; op, optic vesicle; pc, pericardiac region; ph, pharyngeal lumen; rp, Rathke's pouch; v, ventral.

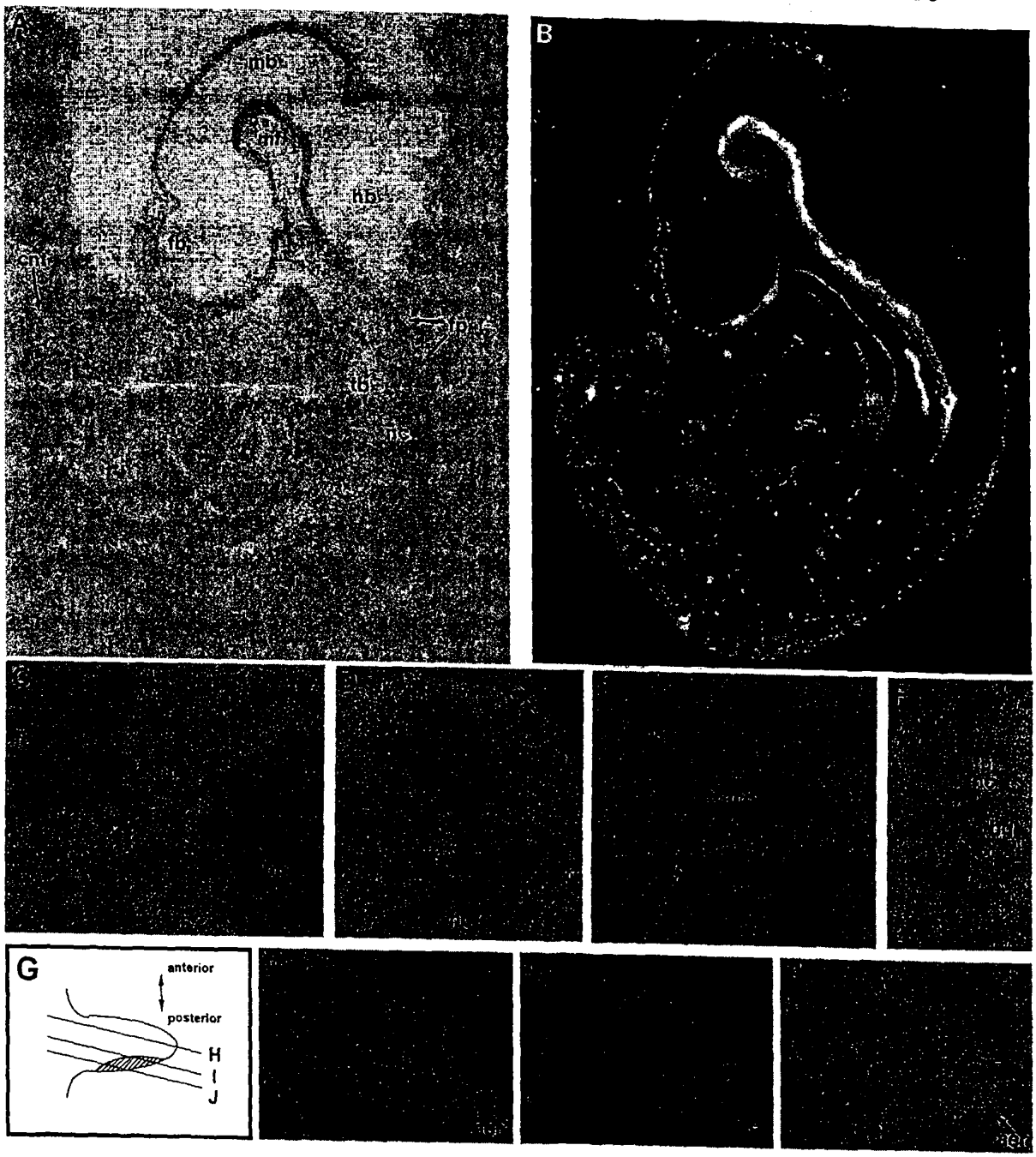

Fig. 5. *Hhg-1* expression in the 10.5 dpc embryo. (A,B) Bright-and dark-field views of a saggital section from a 10.5 dpc mouse embryo showing intense hybridization in the ventral neural tube and notochord, ventral diencephalic region (asterisk), and tracheal branch point. (C) Horizontal section showing hybridization in the ventral epithelium of the midbrain. (D) Horizontal section at lower level showing expression in floor plate and notochord. (E) Horizontal section showing hybridization in the epithelia of the tracheal lumen. (F) Horizontal section showing continued expression in the floor plate and notochord at caudal levels and expression in the epithelia of the hindgut. (G) Schematic diagram of developing limb, and reconstruction of expression from serial sections. Lines indicate approximate levels of sections shown in H-J. (H-J) Anterior to posterior sections of developing forelimb. Intense expression is observed in the posterior but not anterior mesoderm. No expression is observed in the apical ectodermal ridge. aer, apical ectodermal ridge; cnt, caudal neural tube; fb, forebrain; fp, floor plate; hb, hindbrain; hg, hindgut; mb, midbrain; mf, mesencephalic flexure; nc, notochord; tb, tracheal branch point; trach, tracheal lumen.

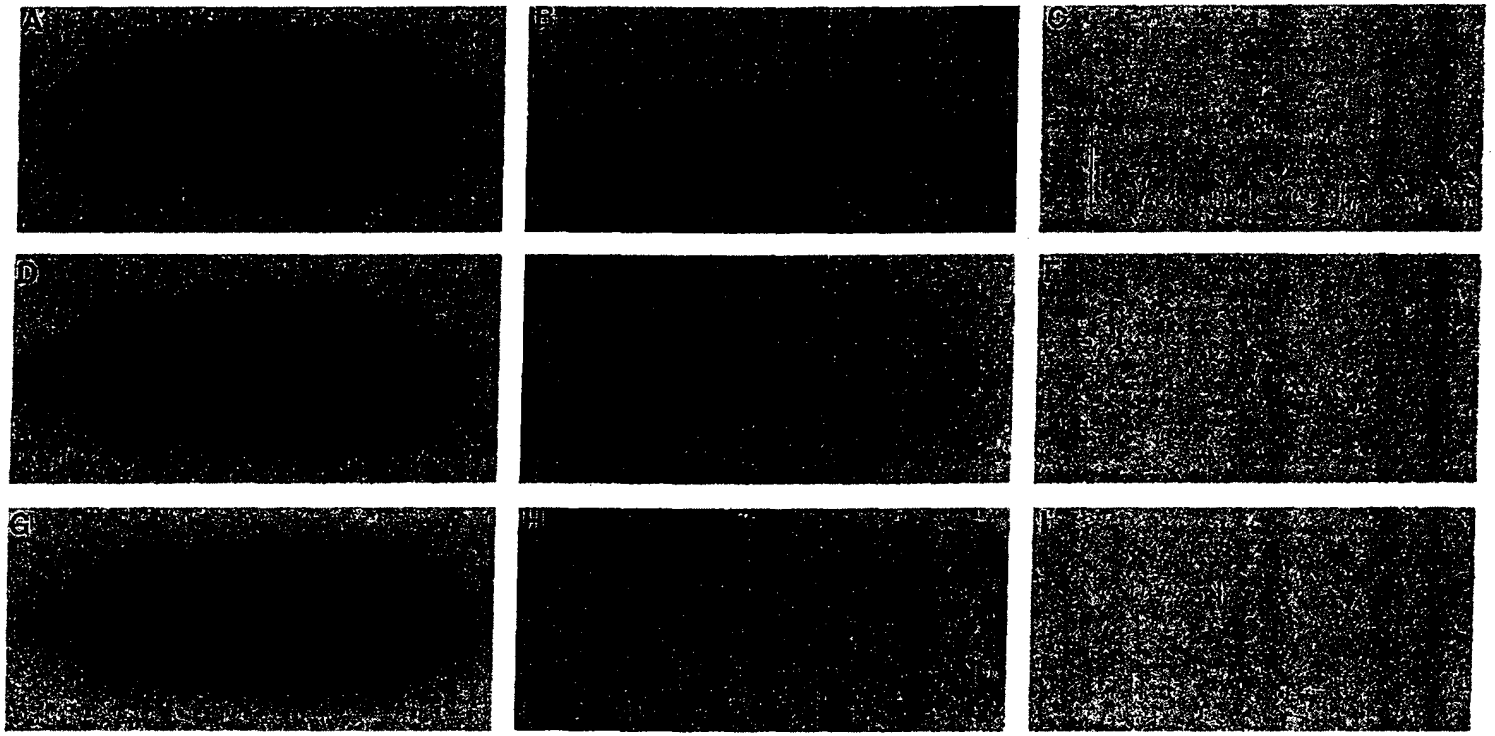

Fig. 6. Ectopic expression of *Hhg-1* in the *Drosophila* embryo. A,B,D,E,G and H show ventral views of germ-band-extended (A,D,G) and retracted (B,E,H) embryos which have been heat shocked and processed for in situ hybridization to detect *wingless* RNA expression. C, F and I show the pattern of ventral denticles within a single segment from heat-shocked embryos just prior to hatching. The genotypes of embryos in A-C are w^{1118} (wild-type control), while embryos in D-F and G-I, respectively, carry the hs*hh* and hs*Hhg-1* construct (see text). Note that, relative to wild type (A,B), the *wingless* stripes are expanded at the extended and retracted germ band stages for embryos carrying the hs*hh* (D,E) and hs*Hhg-1* (G,H) constructs. Note also that the wild-type polarity and character of the bristle rows 4-6 (bracketed portion of C; see text) are altered in F and I.

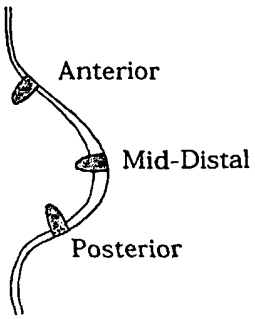

Fig. 7. Graft sites for limb patterning assays.

expression is indistinguishable from the *hh* effect. The denticles appearing in place of the posterior three denticle rows, however, appear more disorganized, with occasionally a missing denticle row and in some cases an unusual posterior row of anteriorly oriented denticles (Fig. 6I).

The patterns of *wg* expression thus far described pertain to the extended germ band stage. We also examined, however, the effects of ectopic *hh* and *Hhg-1* expression upon later stage embryos which had completed or nearly completed the process of germ band retraction. As shown in Fig. 6B,E,H, the *wg* expression domain is expanded relative to the wild type even at this later stage. The competence of cells in the expanded *wg* domain to respond to the ectopic *hh* signal at this late stage reveals a new requirement for temporal and spatial expression of candidate receptors for the *hh* signal (see Discussion).

Patterning activity of *Hhg-1* in the developing chick limb

Hhg-1 expression in mouse limb buds is restricted to mesoderm along the posterior margin of the limb bud (Fig. 5G-I), a location reminescent of the polarizing region in the chick limb bud. Given the ability of *Hhg-1* to function in as diverged a species as *Drosophila* (see above) and in light of previous reports of chick limb patterning activity present in grafts derived from mouse limb buds (Tickle et al., 1976; Fallon and Crosby, 1977), we tested the possibility that *Hhg-1* encodes an

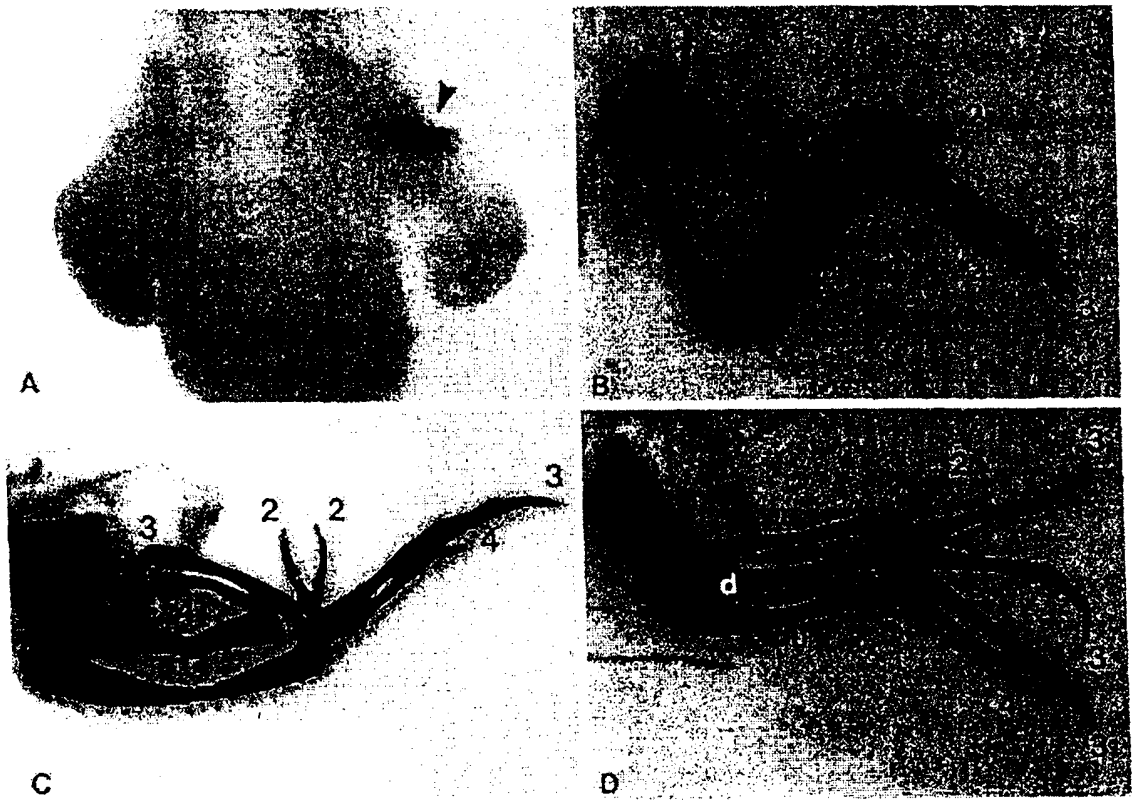

Fig. 8. Limb patterning activity of *Hhg-1*. Grafts of QT6 cells transfected with pCIS*lacZ* (A) or pCIS*Hhg-1* (B,C,D) were made to the anterior border (A,C) the posterior border (B) or to the mid-distal border (D) of forelimb buds within chick embryos at stage 20. The embryo in A was fixed 24 hours after grafting and stained for β-galactosidase activity (positive region indicated by arrowhead). Embryos in B-D were fixed, stained and cleared 7 days after grafting. The posterior border graft in B resulted in a normal limb skeleton (h, humerus; r, radius; u, ulna; 2,3 and 4 indicate digit identities). The anterior border graft in C caused a mirror image duplication of the manus with a digit pattern of 4-3-2-2-3-4. The mid-distal border graft in D induced skeletal duplications of digits and of the forearm: d indicates a duplicated forearm bone that probably is an ulna; the digit pattern from anterior is 2-3-3 followed by the normal 3-4.

activity capable of imposing pattern upon chick limbs. The strategy for these experiments involved high-efficiency transient transfection of the QT6 quail cell line (Moscovici et al., 1977), followed by grafting of wedge-shaped sections of transfected cell pellets to anterior, mid-distal or posterior borders of stage 20-21 chick wing buds (see Fig. 7). Initial transfections using the bacterial β-galactosidase expression gene in the vector pCIS (Gorman, 1985), which carries a cytomegalovirus promoter and an SV40 intron and polyadenylation signal, yielded expression in greater than 90% of the QT6 cells plated for transfection.

Fig. 8 shows that grafts of cells transfected with a *Hhg-1*-expression construct to anterior and mid-distal but not posterior locations within developing limb buds induced duplications of digits. Duplications induced by anterior border grafts were in mirror-image orientation relative to the normal pattern, with a typical sequence of digits shown in Fig. 8C (4-3-2-2-3-4). Mid-distal grafts commonly yielded digits in the sequence 2-3-3-3-4, with divergent curvature of adjacent third digits indicative of the location of the graft site (Fig. 8D). Grafts of β-galactosidase-expressing cells or posterior grafts of *Hhg-1*-expressing cells, in contrast, did not alter normal limb pattern (Fig. 8A,B). With respect to digit duplications and polarity, all grafts of *Hhg-1* expressing cells act as posterior organizing centers, much in the same manner observed for polarizing region grafts (Saunders and Gasseling, 1968).

Curiously, we observed duplications of proximal skeletal elements such as the humerus, radius and ulna at a frequency of 65% in mid-distal border grafts (Fig. 8D; see Table 1), but never with anterior border grafts (Fig. 8C; see Table 1). To our knowledge, a strong correlation between graft location and duplication of proximal skeletal elements has not been previously noted, although previously reported results are consistent with our observation (see Discussion). The overall level of proximal or distal element duplications in all limbs receiving anterior or mid-distal border grafts of *Hhg-1*-expressing cells was 86.5% (Table 1). These percentages are similar to those reported by Riddle et al. (1993) following anterior grafts of cells infected with a retrovirus carrying *Shh*, a *hedgehog* family member in the chicken that probably corresponds to *Hhg-1*.

Table 1. Skeletal element duplications induced by grafts of QT6 cells transfected with pCIS*Hhg-1*

Percentage of most posterior duplicated digit (*n*)				
Graft (*n*)	II	III	IV	Normal
Anterior hedgehog (29)	14% (4)	41% (12)	31% (9)	14% (4)
Mid-distal hedgehog (17)	17.5% (3)	65% (11)	0 (0)	17.5% (3)
β-galactosidase (11)	0	0	0	100% (11)
Posterior hedgehog (7)	0	0	0	100% (7)

Percentage of proximal element duplications* (*n*)				
Graft (*n*)	Radius	Ulna	Humerus	Normal
Anterior hedgehog (20)	0	0	0	100% (20)
Mid-distal hedgehog (17)	41% (7)	17.5% (3)	11.5% (2)	41% (7)
β-galactosidase (11)	0	0	0	100% (11)
Posterior hedgehog (7)	0	0	0	100% (7)

*A single specimen might contribute to more than one column.

Percentage of grafts that induced extra skeletal elements (*n*)		
Graft (*n*)	Duplications	Normal
Hedgehog (46)	87 % (40)†	13% (6)
β-galactosidase (11)	0	100% (11)
Posterior hedgehog (7)	0	100% (7)

†38 specimens showed digit duplications.

Qt6 cells transfected with either pCIS*Hhg-1* or pCIS*LacZ* were grafted to anterior, mid-distal or posterior borders of stage 20 chick limb buds. Embryos harvested at day 10 were fixed overnight in 10% formaldehyde, stained with Victoria Blue and cleared with methyl salicylate.

Proteolytic processing of the *Hhg-1* protein product

We have used affinity purified antibodies directed against epitopes from two distinct portions of the *Hhg-1* ORF (Fig. 9A) to confirm that *Hhg-1* encoded protein indeed is expressed in both systems where we have assayed for *Hhg-1* activity. As shown in the immunoblots of Fig. 9B, QT6 cells transfected with the pCIS*Hhg-1* expression vector produce a polypeptide species of ~45×10^3 M_r which is detected by both N- and C-terminal specific antibodies in transfected cells (lanes 1 and 3, respectively). In addition, a ~19×10^3 M_r species is specifically detected by the N-terminal antibody while the C-terminal antibody specifically detects a ~28×10^3 M_r species. Neither the

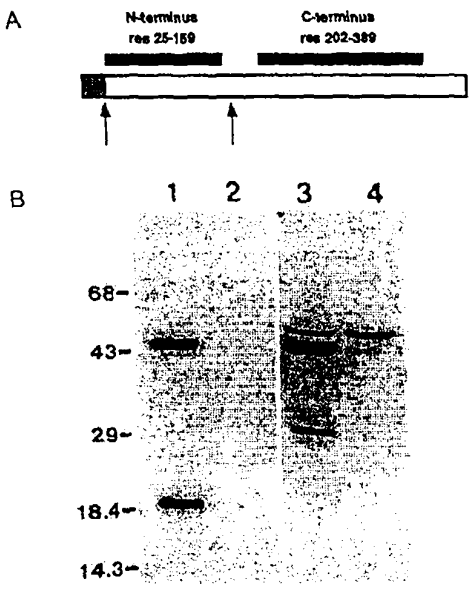

Fig. 9. Proteolytic processing of the *Hhg-1* protein. The filled boxes in A denote the portions of the *Hhg-1* ORF used to elicit antibodies, specific to the amino- and carboxy-terminal portions of the protein. The immunoblot in B illustrates the reactivity of amino-terminal (lanes 1 and 2) and carboxy-terminal (lanes 3 and 4) antibodies with species present in QT6 cells either transfected (lanes 1 and 3) or not transfected (lanes 2 and 4) with pCIS*Hhg-1*. Note the presence of a ~45×10^3 M_r transfection-dependent species detected by both antibodies. Each antibody also detects a single smaller species of ~19×10^3 M_r for the amino-terminal antibody and ~28×10^3 M_r for the carboxy terminal antibody. The slightly larger species detected in lanes 3 and 4 is not transfection dependent, but provides a control for the amount of protein loaded. The arrows in A denote a signal cleavage (following the shaded hydrophobic domain) and a proposed internal cleavage that can account for the observed species and their reactivities (see text).

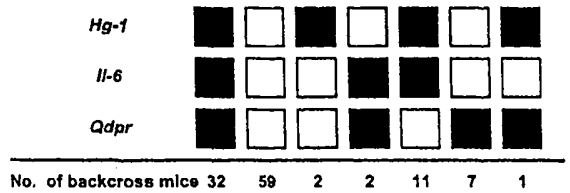

Fig. 10. Segregation of *Hhg-1* among proximal mouse chromosome 5 loci in [(C3H/HeJ-*gld* × *Mus spretus*)F1 × C3H/HeJ-*gld*] interspecific backcross mice Closed boxes represent the homozygous C3H pattern and open boxes the F_1 pattern. The number of mice with each haplotype is shown at the bottom of each column. The informative RFLV for *Hhg-1* is described in the text. The informative RFLVs for *Il-6* were generated by *Taq1* (C3H, 5.0 kb and 2.2 kb; *Mus spretus*, 8.6 kb and 1.9 kb) and for *Qdpr* were generated by *Eco*RI (C3H, 9.5 and 6.5 kb; *Mus spretus*, 8.2 kb).

large common species nor the smaller specific species are detected in untransfected cells (lanes 2 and 4). Essentially identical species were detected in protein extracts from heat shocked *Drosophila* embryos carrying the hs*Hhg-1* construct, but not in extracts from unshocked embryos (D. T. C. and P. A. B., data not shown).

The arrows in Fig. 9A denote cleavages of the primary protein product that could account for *Hhg-1* species of the observed size. The first of these occurs at the *Hhg-1* signal sequence and is observed in a microsome-dependent fashion in in vitro translation reactions (J. J. Lee and P. A. B., unpublished data). The second internal cleavage is proposed as a simple possibility that can account for the observed polypeptide species and is similar to an internal cleavage that occurs in the *Drosophila hedgehog* protein precursor (J. J. Lee, S. C. Ekker and P. A. B., unpublished; see Discussion).

Chromosomal localization and fine mapping of *Hhg-1*

In order to determine the chromosomal location of the *Hhg-1* gene and to assess potential linkage with mouse developmental mutants, we analyzed a panel of DNA samples from an interspecific cross that has been characterized for over 500 genetic markers throughout the genome. The genetic markers included in this map span between 50 and 60 centi-Morgans (cMs) on each mouse autosome and on the X Chromosome (for examples see Saunders and Seldin, 1990; Watson et al., 1992). Initially, DNA from the two parental mice [C3H/HeJ-*gld* and (c3H/HeJ-*gld* × *Mus spretus*)F_1] were digested with various restriction endonucleases and hybridized with *Hhg*-1 cDNA probe to determine restriction fragment length variants (RFLVs) thereby allowing haplotype analyses. Informative RFLVs were detected with *Msp*I restricted DNAs: C3H/HeJ-*gld*, 13.0 kb; *Mus spretus*, 5.0 kb. Comparison of the haplotype distribution of the *Hhg-1* indicated that in 109 of the 114 meiotic events examined, the *Hhg-1* locus cosegregated with Il-6 (Fig. 10), a locus previously mapped to proximal mouse Chromosome 5 (Mock et al., 1989; Kozak and Stephenson, 1993). The best gene order (Bishop, 1985) ± the standard deviation (Green, 1981) indicated the following gene order from proximal to distal: *Hhg-1* – 4.4 cM ± 1.9 cM – *Il-6* – 15.7 cM ± 3.5 cM – *Qdpr*.

DISCUSSION

Patterning functions of *Hhg-1*

The most remarkable feature of *Hhg-1* expression, which has also been noted for other closely related genes in multiple vertebrate species (Riddle et al., 1993; Echelard et al., 1993; Krauss et al., 1993; Roelink et al., 1994), is its occurrence in a number of embryonic tissues demonstrated to exert patterning influences on neighboring structures. The notochord and floor plate, for example, are capable of imposing ventral pattern upon the neural tube (reviewed in Jessell and Dodd, 1993), while the posterior margin of the vertebrate limb bud or polarizing region can function as a posterior organizing center when grafted to a developing limb. Grafting experiments also suggest that these organizing activities may be functionally related, since notochord and floor plate tissue can also function as posterior organizing centers when grafted to limb buds (Wagner et al., 1990).

Riddle et al. (1993) indeed showed that the chicken *Shh* gene encodes a product capable of imposing pattern upon developing chick limbs while Echelard et al. (1993) showed that ectopic expression of chicken *Shh* can induce inappropriate expression of ventral neural tube markers in the mouse; Krauss et al. (1993) also showed that ectopic expression of fish *shh* can induce inappropriate expression of ventral neural tube markers in fish embryos. Finally, Roelink et al. (1994) demonstrated that COS cells expressing the rat gene *vhh-1* can induce formation of floor plate and motor neurons when cocultured with lateral neural tube explants from rat.

The xenoplastic activities of *Hhg-1* described here represent the first direct assays of function for the mouse member of the *vhh-1* or *sonic* class of vertebrate *hh*-like sequences. Our results also demonstrate for the first time the activity of a mammalian *hh*-like gene in limb patterning. Consistent with the expression of *Hhg-1* in the posterior margin of mouse limb buds, polarizing activity previously has been identified in this location by grafting experiments (Tickle et al., 1976; Fallon and Crosby, 1977). In addition, preliminary results in the explant assay system suggest that the *Hhg-1* product can also induce floor plate formation in rat lateral neural tube (J. Dodd, D. T. C. and P. A. B., unpublished data). We thus conclude that the *Hhg-1* gene encodes patterning activities and that the expression of pattern of *Hhg-1* in the embryo could account, at least in part, for the patterning activities of specific tissues assayed by grafting experiments.

A noteworthy feature of our grafting operations was the high relative frequency of proximal skeletal element duplications in mid-distal grafts (65%) versus anterior grafts (0%). Although such a correlation between graft location and the occurrence of proximal duplications has not been previously noted, a cursory review of the literature from the first polarizing region grafts of Saunders and Gasseling (1968) onwards suggests that graft location indeed appears to operate as a determinant for formation of proximal element duplications. More recently, Riddle et al. (1993) reported proximal element duplications induced by anterior grafts of cells expressing the chicken *Shh* gene. In both cases of proximal element duplication depicted, however, the digit sequence indicated a location sufficiently posterior to allow formation at least one digit anterior to the graft, thus reinforcing the correlation between proximal

element duplications and a more posterior graft location (at least as far posterior as mid-distal). The significance of this observation remains to be investigated.

Genetic linkage of *Hhg-1*

Our segregation analysis of *Hhg-1* indicates a localization to the proximal region of mouse chromosome 5. Given the ability of *Hhg-1* to function in limb patterning, our attention was drawn to two mutations affecting limb development that also map to this region of mouse chromosome 5. One, *Hm* (hammertoe), is a semidominant mutation causing failure of normal programmed cell death in the webbing between toes during development, resulting in the formation of contractures in the second phalanx of all four limbs in the adult. This phenotype is somewhat more pronounced in homozygotes, which nevertheless remain viable and fertile. The second, *Hx* (Hemimelic extra toes), is also a dominant mutation associated with shortening or complete absence of tibia and talus in the hindlimbs and shortening of the radius in the forelimbs; in addition, metatarsals or metacarpals are duplicated giving a total of seven to eight digits per paw instead of the normal five (Dickie, 1968; Knudsen and Kochhar, 1981). The homozygous phenotype of *Hx* is an uncharacterized embryonic lethality (Knudsen and Kochhar, 1981). *Hx* and *Hm* are very closely linked but separate mutations, having been observed to recombine in only 1 of 3664 offspring from *trans*-heterozygous parents (Sweet, 1982). In addition to these mutations in the mouse, the syntenic region of human chromosome 7q has also been identified as the genetic locus for several developmental anomalies involving polydactyly (Tsukurov et al., 1994, Heutink et al., 1994).

In order to investigate the possibility that one or both of the mouse mutations affect the *Hhg-1* gene, we examined by Southern blotting the restriction pattern of DNA from both of these mutants. Using nine different restriction endonucleases for *Hx* and for *Hm*, we detected no differences between parental and mutant DNA (data not shown). Since the *Hx* phenotype suggests a defect in early limb patterning, as might be expected from a mutation in the *Hhg-1* gene, we attempted to discover alterations in *Hhg-1* coding sequences in the *Hx* mutant. Because only heterozygous *Hx* mutant DNA was available (from Jackson Labs), our conclusions depend upon analysis of multiple independently isolated clones. We examined eleven, fourteen and eight independent clones from the coding portions of exons one, two and three, respectively, without detecting any differences from wild type (see Materials and Methods). Since the clones for sequence determination were derived using the polymerase chain reaction, it is possible that a deletion(s) at the *Hhg-1* locus might have prevented amplification of the mutant allele. Given the uncertainty inherent in sampling from heterozygous DNA, it is also formally possible, although highly unlikely, that we could have missed a coding difference in the *Hhg-1* gene of *Hx* mutants.

In the absence of *Hx*- or *Hm*-associated alterations in *Hhg-1* coding sequence, another possibility to consider is that the *Hx* or *Hm* phenotypes could result from a mutation in *cis*-acting regulatory regions of *Hhg-1*, causing either a reduction of *Hhg-1* expression or inappropriate spatial localization of expression. Given our Southern blotting results, such a lesion could lie near the *Hhg-1* gene only if it is sufficiently subtle to escape detection by Southern blotting with our cDNA probe; alternatively, a *Hhg-1* regulatory lesion may have escaped detection because of a location distant from sequences represented within the *Hhg-1* cDNA.

With regard to potential mechanisms underlying genetic dominance for such a regulatory mutation, the dominant limb deformity mutation *Xt* (extra toes) may be informative. Like *Hx*, *Xt* causes polydactyly and is lethal when homozygous; mutations affect the gene GLI3, which encodes a zinc finger transcription factor. At least one allele of *Xt* appears to act simply by disrupting transcription of GLI3 (Schimmang et al., 1992), and thus, the genetic dominance of mutations at this locus is probably due to haploinsufficiency. The GLI3 gene is also interesting in that its close *Drosophila* relative, the gene *cubitus-interruptus*^{Dominant} (*ci*^{D}), functions downstream in the *hedgehog* signaling pathway (Forbes et al., 1993). If the GLI3 gene similarly functions downstream of *Hhg-1* in the mouse, and given that GLI3 function is haploinsufficient, it would not be surprising to find that partial loss of *Hhg-1* expression caused by a regulatory mutation might also have a dominant phenotype. Interestingly, a human polysyndactyly disease that maps to a region of human chromosome 7 syntenic to the region containing *Hhg-1* and *Hm* and *Hx* is also inherited in a dominant fashion (Tsukurov et al., 1994; Heutink et al., 1994). Alternatives to haploinsufficiency are that a regulatory mutation might cause *Hhg-1* mis-expression or that *Hx* and *Hm* are unrelated to *Hhg-1*.

Duplication and divergence of the *hedgehog* gene family in vertebrates

Our PCR-based search for vertebrate *hedgehog* homologues yielded the three distinct mouse and two distinct human sequences reported here, and five sequences each from the zebrafish *Brachydanio rerio* and the toad *Xenopus laevis* (S. C. Ekker, J. J. Lee, D.v.K. and P. A. B., unpublished data). In contrast, none of the invertebrate species to which our PCR-based method was applied yielded more than a single distinct *hh*-like sequence. For example, using various combinations of degenerate primers from conserved regions, eighteen independent *Drosophila melanogaster* clones identical to *hh* were isolated without encountering any diverged *hh*-like sequences. It is not yet possible to estimate accurately the total number of distinct vertebrate *hh*-like genes. The occurrence of multiple *hh*-like sequences in vertebrates but not invertebrates nevertheless suggests that at some point during evolution of the vertebrate lineage repeated duplication and divergence of a single ancestral *hedgehog* gene occurred, as has been proposed for the origin of multiple vertebrate HOM-C gene clusters from a single ancestral cluster (Schubert et al., 1993).

Broad evolutionary conservation of *hedgehog* protein function and proteolytic processing

The evolutionary conservation of *hh* extends beyond sequence to include function, as demonstrated by the ability of *Hhg-1* to encode a signal capable of inducing expansion of the *wingless* stripe of expression in *Drosophila* embryos. Similar results using a *hh*-like gene isolated from zebrafish were also reported by Krauss et al. (1993). If the proposal, based on genetic arguments, that the gene *patched* (*ptc*) encodes a *hh* receptor in *Drosophila* is correct (Ingham et al., 1991), the functional conservation of vertebrate *hedgehog* signals would suggest that *ptc*-like sequences and function should also be conserved in

vertebrates. With regard to the identity of a *hh* receptor, however, we observed that both *hh* and *Hhg-1* can induce broadening of the *wingless* stripe when ectopically expressed at the retracted germ band stage of *Drosophila* development. By this stage, the initially broad stripe of *ptc* mRNA and protein expression has split into two thinner stripes per segment by loss of expression from the cells in the middle of the broad stripe (Taylor et al., 1993). Expanded *wingless* expression in response to *hh* thus is occurring in interstripe cells that in normal embryos no longer express the *ptc* protein. Ingham (1993) has reported that *ptc* expression in these interstripe cells is also induced by ectopic *hedgehog*, but it is not known whether *ptc* induction in the interstripe precedes or follows *wg* induction in the interstripe cells. Whatever the sequence of induction, novel expression of *ptc* or *wg* represents a response to *hh* protein in interstripe cells, which do not express the *ptc* protein, thus suggesting that *ptc* does not encode the *hh* receptor, or at least not the only receptor.

The occurrence of multiple *Hhg-1* polypeptide species in *Drosophila* embryos as well as in avian cells raises a question as to the role of proteolytic processing in *hedgehog* protein function. We believe that the N- and C-terminally derived forms of the *Hhg-1* protein bear a product/precursor relationship to the larger form because the relative molecular masses of the smaller products sum to yield approximately the relative molecular mass of the larger product, and they could therefore be derived by a single internal cleavage as shown in the model in Fig. 9A. The location of this internal cleavage coincides approximately with an intron/exon boundary and with a sharp demarcation in the degree of sequence conservation (see Results). In addition, these smaller forms resemble smaller forms of the *hh* protein observed in *Drosophila* (Tabata and Kornberg, 1994; J. J. Lee and P. A. B., unpublished data), where an internal cleavage occurs and appears to be required for the *hh* signaling function (J. J. Lee, S. C. Ekker, D. P. von K. and P. A. B., unpublished data).

The existence of two distinct stable products derived from a single larger precursor may provide a clue to the apparent dual nature of *hedgehog* gene action in several developmental systems. In the *Drosophila* embryo, for example, the restriction of *wingless* gene expression to a narrow stripe within each segment is dependent upon the short-range nature of a *hedgehog* signaling activity (see above; Ingham, 1993); in contrast, the influence of a later-acting *hh*-encoded activity extends across most of the segment in imposing pattern upon the dorsal cuticle (Heemskerk and DiNardo, 1994). Similarly in ventral neural tube patterning, induction of floor plate occurs at short range and depends upon direct contact with notochord, floor plate, or COS cells expressing *vhh-1* (Placzek et al., 1993; Roelink et al., 1994). COS cells expresssing *vhh-1* also have motor neuron inducing activity (Roelink et al., 1994). This latter activity is found in diffusible form in supernatants from notochord and floor plate cultures (Yamada et al., 1993), although it is not yet clear that *vhh-1* directly encodes the diffusible activity. Long- and short-range *hedgehog* activities have not been definitively identified in the context of limb patterning, but such activities have been extensively discussed; dual modes of *hedgehog* action thus may yet emerge from studies of such apparently distinct activities as influences upon the apical ectodermal ridge and anterior/posterior patterning of the developing limb.

An alternative would be that only one of the smaller *hedgehog* protein species is biologically active, with the apparent dual nature of *hedgehog* action deriving from secondary effects. For example, restricted diffusion for the primary active species could produce apparent long-range effects by inducing expression of another diffusible molecule. Similarly, a diffusible or primarily long-range *hedgehog* signal could yield apparent short-range effects through threshhold-dependent responses of target cells. To resolve these questions, the structures and embryonic localizations of the *hedgehog*-encoded proteins must be determined and their patterning activities assayed. At another level, a true understanding of the functional roles of vertebrate *hedgehog* proteins requires a demonstration that patterning functions in vertebrate embryos actually are executed by the products of this class of genes; this would best be achieved through specific inactivation of *hedgehog* gene products by genetic or other means.

We gratefully acknowledge J. Gearhart, S.-J. Lee, C. Moore, C. Mjaatvedt and T. Huynh for instruction in handling of mice, manipulation of embryos, and advice on in situ hybridisation. We also thank A. Lanahan, J. Williams and S.-J. Lee for mouse cDNA libraries and RNA blots. K. Young, M. Claudia, D. Sullivan, J. Kassis, S. Brown, R. Denell, G. Aisenberg and A. Cameron generously provided genomic DNA and libraries from various species, and K. Young graciously assisted in the isolation and characterization of the mosquito and mouse sequences. We are indebted to N. Patel for equipment and help with dark field microscopy. We also thank J. Dodd, J. J. Lee and S. C. Ekker, for sharing unpublished data, and S.C. Ekker for help with figures. T. Vogt and S.-J. Lee provided useful comments on the manuscript. This work was supported by the Howard Hughes Medical Institute, an NIH MSTP award to D. T. C., NIH awards HD20743 and 5T32GM07507 to J. F. F. and A. L., and NIH award HG00734 to M. F. S.

REFERENCES

Ausubel, F. M., Brent, R., Kingston, R. E., Moore, D. D., Seidman, J. G., Smith, J. A. and Struhl, K. (1993). *Current Protocols in Molecular Biology*. New York: Greene Publishing Associates and Wiley-Interscience.

Baker, N. E. (1988). Embryonic and imaginal requirements for *wingless*, a segment polarity gene in *Drosophila*. *Dev. Biol.* **125**, 96-108.

Bejsovec, A. and Martinez-Arias, A. (1991). Roles of *wingless* in patterning the larval epidermis of *Drosophila*. *Development* **113**, 471-485.

Bejsovec, A. and Wieschaus, E. (1993). Segment polarity gene interactions modulate epidermal patterning in *Drosophila* embryos. *Development* **119**, 501-517.

Bishop, D. T. (1985). The information content of phase-known matings for ordering genetic loci. *Genet. Epidemiol.* **2**, 349-361.

Burnette, W. N. (1981). Western blotting: electrophoretic transfer of proteins from sodium dodecyl sulfate-polyacrylamide gels to unmodified nitrocellulose and radiographic detection with antibody and radio-iodinated Protein A. *Anal. Biochem* **112**, 195-203.

Chen, C. and Okayama, H. (1987). High-efficiency transformation of mammalian cells by plasmid DNA. *Molecular & Cellular Biology* **7**, 2745-2752.

Dickie, M. M. (1968). *Mouse News Lett.* **38**, 24.

DiNardo, S., Sher, E., Heemskerk-Jongens, J., Kassis, J. A. and O'Farrell, P. H. (1988). Two-tiered regulation of spatially patterned *engrailed* gene expression during *Drosophila* embryogenesis. *Nature* **332**, 604-609.

Dougan, S. and DiNardo, S. (1992). *Drosophila wingless* generates cell type diversity among *engrailed* expressing cells. *Nature* **360**, 347-50.

Echelard, Y., Epstein, D. J., St-Jacques, B., Shen, L., Mohler, J., McMahon, J. A. and McMahon, A. P. (1993). Sonic hedgehog, a member of a family of putative signaling molecules, is implicated in the regulation of CNS polarity. *Cell* **75**, 1417-1430.

Fallon, J. F. and Crosby, G. M. (1977). Polarizing zone activity in limb buds

of amniotes. In *Vertebrate Limb and Somite Morphogenesis*. (ed. D. A. Ede, J. R. Hinchliffe and M. Balls), pp 55-70. Cambridge: England.

Feinberg, A. and Vogelstein, B. (1983). A technique for radiolabeling DNA restriction endonuclease fragments to high specific activity. *Anal. Biochem.* **132**, 6-13.

Ferguson, E. L. and Anderson, K. V. (1992). Decapentaplegic acts as a morphogen to organize dorsal-ventral pattern in the Drosophila embryo. *Cell* **71**, 451-461.

Forbes, A. J., Nakano, Y., Taylor, A. M. and Ingham, P. W. (1993). Genetic analysis of *hedgehog* signalling in the *Drosophila* embryo. *Development* **1993 Supplement**, 115-124.

Gorman, C. (1985). High efficiency gene transfer into mammalian cells. In *DNA cloning*. (ed. D. M. Glover). pp 143. Oxford.

Green, E. L. (1981). Linkage, recombination and mapping. In *Genetics and Probability in Animal Breeding Experiments*. (ed. E. Green), pp 77-113. New York.

Harlow, E. and Lane, D. (1988). *Antibodies: A Laboratory Manual*. Cold Spring Harbor, New York: Cold Spring Harbor Publications.

Heberlein, U., Wolff, T. and Rubin, G. M. (1993). The TGF beta homolog *dpp* and the segment polarity gene *hedgehog* are required for propagation of a morphogenetic wave in the Drosophila retina. *Cell* **75**, 913-926.

Heemskerk, J. and DiNardo, S. (1994). Drosophila *hedgehog* acts as a morphogen in cellular patterning. *Cell* **76**, 449-460.

Heutink, P., Zguricas, J., Oosterhout, L. v., Breedveld, G. J., Testers, L., Sandkuijl, L. A., Snijders, P. J. L. M., Weissenbach, J., Lindhout, D., Hovius, S. E. R. and Oostra, B. A. (1994). The gene for triphalangeal thumb maps to the subtelomeric region of chromosome 7q. *Nature Genetics* **6**, 287-292.

Ingham, P. W. (1993). Localized *hedgehog* activity controls spatial limits of wingless transcription in the *Drosophila* embryo. *Nature* **366**, 560-562.

Ingham, P. W., Taylor, A. M. and Nakano, Y. (1991). Role of the *Drosophila patched* gene in positional signalling. *Nature* **353**, 184-187.

Jessell, T. M. and Dodd, J. (1993). Control of neural cell identity and pattern by notochord and floor plate signals. In *Cell-Cell Signaling in Vertebrate Development*. (ed. E. J. Robertson, F. R. Maxfield and H. J. Vogel), pp 139-155. Sand Diego.

Knudsen, T. B. and Kochhar, D. M. (1981). The role of morphogenetic cell death during abnormal limb-bud outgrowth in mice heterozygous for the dominant mutation *Hemimelia-extra toe* (*Hmx*). *J. Embryol. Exp. Morphol* **65 (Supplement)**, 289-307.

Kozak, C. A. and Stephenson, D. A. (1993). Mouse chromosome 5. *Mammalian Genome* **4**, s72-87.

Krauss, S., Concordet, J.-P. and Ingham, P. W. (1993). A functionally conserved homolog of the Drosophila segment polarity gene *hh* is expressed in tissues with polarizing activity in zebrafish embryos. *Cell* **75**, 1431-1444.

Laemmli, U. K. (1970). Cleavage of structural proteins during the assembly of the head of bacteriophage T4. *Nature* **227**, 680-685.

Lee, J. J., von Kessler, D. P., Park, S. and Beachy, P. A. (1992). Secretion and localized transcription suggest a role in positional signaling for products of the segmentation gene hedgehog. *Cell* **71**, 33-50.

Lee, S. J. (1990). Identification of a novel member (GDF-1) of the transforming growth factor-β superfamily. *Mol. Endocrinol.* **4**, 1034-1040.

Lockyer, J., Cook, R. G., Milatien, S., Kaufman, S., Woo, S. L. C. and Ledley, F. D. (1987). Structure and expression of human dihydropteridine reductase. *Proc. Natl. Acad. Sci. USA* **84**, 3329-3333.

Ma, C., Zhou, Y., Beachy, P. A. and Moses, K. (1993). The segment polarity gene *hedgehog* is required for progression of the morphogenetic furrow in the developing *Drosophila* eye. *Cell* **75**, 927-938.

Martinez Arias, A., Baker, N. E. and Ingham, P. W. (1988). Role of segment polarity genes in the definition and maintenance of cell states in the *Drosophila* embryo. *Development* **103**, 157-170.

Mock, B. A., Nordan, R. P., Justice, M. J., Kozak, C., Jenkins, N. A., Copeland, N. G., Clark, S. C., Wong, G. G. and Rudikoff, S. (1989). The murine Il-6 gene maps to the proximal region of Chromosome 5. *Journal of Immunology* **142**, 1372-1376.

Mohler, J. (1988). Requirements for *hedgehog*, a segmental polarity gene, in patterning larval and adult cuticle of *Drosophila*. *Genetics* **120**, 1061-1072.

Mohler, J. and Vani, K. (1992). Molecular organization and embryonic expression of the hedgehog gene involved in cell-cell communication in segmental patterning in Drosophila. *Development* **115**, 957-971.

Moscovici, C., Moscovici, M. G., Jimenez, H., Lai, M. M., Hayman, M. J. and Vogt, P. K. (1977). Continuous tissue culture cell lines derived from chemically induced tumors of Japanese quail. *Cell* **11**, 95-103.

Nusse, R. and Varmus, H. E. (1992). *Wnt* genes. *Cell* **69**, 1073-1087.

Peifer, M. and Bejsovec, A. (1992). Knowing your neighbors: cell interactions determine intrasegmental patterning in Drosophila. *Trends in Genetics* **8**, 243-249.

Placzek, M., Jessell, T. M., and Dodd, J. (1993). Induction of floor plate differentiation by contact-dependent homeogenetic signals. *Development* **117**, 205-218.

Riddle, D. R., Johnson, R. L., Laufer, E. and Tabin, C. (1993). Sonic hedgehog mediates the polarizing activity of the ZPA. *Cell* **75**, 1401-1416.

Rijsewijk, F., Schuermann, M., Wagenaar, E., Parren, P., Weigel, D. and Nusse, R. (1987). The Drosophila homolog of the mouse mammary oncogene *int-1* is identical to the segment polarity gene *wingless*. *Cell* **50**, 649-657.

Riley, B. B., Savage, M. P., Simandl, B. K., Olwin, B. B. and Fallon, J. F. (1993). Retroviral expression of FGF-2 (bFGF) affects patterning in chick limb bud. *Development* **118**, 95-104.

Roelink, H., Augsburger, A., Heemskerk, J., Korzh, V., Norlin, S., Ruiz i Altaba, A., Tanabe, Y., Placzek, M., Edlund, T., Jessell, T. M. and Dodd, J. (1994). Floor plate and motor neuron induction by *vhh-1*, a vertebrate homolg of *hedgehog* expressed by the notochord. *Cell* **76**, 761-775.

Rubin, G. M. and Spradling, A. C. (1982). Genetic transformation of Drosophila with transposable element vectors. *Science* **218**, 348-353.

Sambrook, J., Fritsch, E. F. and Maniatis, T. (1989). Molecular Cloning: A Laboratory Manual. 2nd edition Cold Spring Harbor, Cold Spring Harbor Laboratory Publications.

Sanger, F., Nicklen, S. and Coulson, A. R. (1977). DNA sequencing with chain-terminating inhibitors. *Proc. Natl. Acad. Sci. USA* **74**, 5463-5467.

Saunders, A. M. and Seldin, M. F. (1990). A molecular genetic linkage map of mouse chromosome 7. *Genomics* **8**, 524-535.

Saunders, J. W. and Gasseling, M. (1968). Ectodermal-mesenchymal interaction in the origin of limb symmetry. In *Epithelial-Mesenchymal Interaction*. (ed. R. Fleischmayer and R. E. Billingham), pp 78-97. Baltimore.

Schimmang, T., Lemaistre, M., Vortkamp, A. and Ruther, U. (1992). Expression of the zinc finger gene *Gli3* is affected in the morphogenetic mouse mutant *extra-toes* (*Xt*). *Development* **116**, 799-804.

Schubert, F. R., Nieselt-Struwe, K. and Gruss, P. (1993). The Antennapedia-type homeobox genes have evolved from three precursors separated early in metazoan evolution. *Proc. Natl. Acad. Sci. USA* **90**, 143-147.

Seldin, M. F., Morse, H. C., Reeves, J. P., Scribner, J. P., LeBoeuf, R. C. and Steinber, A. D. (1988). Genetic analysis of autoimmune *gld* mice I. Identification of a restriction fragment length polymorphism closely linked to the *gld* mutation within a conserved linkage group. *J. Exp. Med.* **167**, 688-693.

Sweet, H. O. (1982). *Mouse News Lett.* **66**, 66.

Tabata, T., Eaton, S. and Kornberg, T. (1992). The Drosophila *hedgehog* gene is expressed specifically in posterior compartment cells and is a target of *engrailed* regulation. *Genes Dev.* **6**, 2635-2645.

Tabata, T. and Kornberg, T. B. (1994). *Hedgehog* is a signaling protein with a key role in patterning *Drosophila* imaginal discs. *Cell* **76**, 89-102.

Tashiro, S., Michiue, T., Higashijima, S., Zenno, S., Ishimaru, S., Takahashi, F., Orihara, M., Kojima, T. and Saigo, K. (1993). Structure and expression of *hedgehog*, a *Drosophila* segment polarity gene required for cell-cell communication. *Gene* **124**, 183-189.

Tautz, D. and Pfeifle, C. (1989). A non-radioactive *in situ* hybridization method for the localization of specific RNAs in the *Drosophila* embryo reveals translational control of the segmentation gene *hunchback*. *Chromosoma* **98**, 81-85.

Taylor, A. M., Nakano, Y., Mohler, J. and Ingham, P. W. (1993). Contrasting distributions of *patched* and *hedgehog* proteins in the *Drosophila* embryo. *Mech. Dev.* **42**, 89-96.

Thummel, C. S., Boulet, A. M. and Lipshitz, H. D. (1988). Vectors for *Drosophila* P-element-mediated transformation and tissue culture transfection. *Gene* **74**, 445-456.

Tickle, C., Shellswell, G., Crawley, A. and Wolpert, L. (1976). Positional signalling by mouse limb polarising region in the chick wing bud. *Nature* **259**, 396-397.

Tsukurov, O., Boehmer, A., Flynn, J., Nicolai, J.-P., Hamel, B. C. J., Traill, S., Zaleske, D., Mankin, H. J., Yeon, H., Ho, C., Tabin, C., Seidman, J. G. and Seidman, C. (1994). A complex bilateral polysyndactyly disease locus maps to chromosome 7q36. *Nature Genetics* **6**, 282-286.

von Heijne, G. (1986). A new method for predicting signal sequence cleavage sites. *Nucl. Acids Res.* **14**, 4683-4690.

Wagner, M., Thaller, C., Jessell, T. and Eichele, G. (1990). Polarizing activity and retinoid synthesis in the floor plate of the neural tube. *Nature* **345**, 819-822.

Watson, M. L., D'Eustachio, P. D., Mock, B. A., Steinberg, A. D., Morse, H. C. I., Oakey, R. J., Howard, T. A., Rochelle, J. M. and Seldin, M. F. (1992). A linkage map of mouse chromosome 1 using an interspecific cross segregating for the gld autoimmunity mutation. *Mammalian Genome* **2**, 158-171.

Wieschaus, E. and Nusslein-Volhard, C. (1986). Looking at embryos. In *Drosophila: A Practical Approach.* (ed. D. B. Roberts), pp 199-227. Oxford: England.

Wilkinson, D. G. (1992). Whole mount *in situ* hybridization of vertebrate embryos. In *In situ hybridization: A practical approach.* (ed. D. G. Wilkinson), pp 75-83. Oxford.

Wolpert, L. (1969). Positional information and the spatial pattern of cellular differentiation. *Journal of Theoretical Biology* **25**, 1-47.

Yamada, T., Pfaff, S. L., Edlund, T., and Jessell, T. M. (1993). Control of cell pattern in the neural tube: motor neuron induction by diffusible factors from notochord and floor plate. *Cell* **73**, 673-686.

(Accepted 12 August 1994)

Exhibit 4

ELSEVIER

Mechanisms of Development 106 (2001) 107–117

www.elsevier.com/locate/modo

Comparative biological responses to human Sonic, Indian, and Desert hedgehog

Suji Pathi[a,1], Sylvia Pagan-Westphal[a,1], Darren P. Baker[b], Ellen A. Garber[b], Paul Rayhorn[b], David Bumcrot[c], Clifford J. Tabin[a], R. Blake Pepinsky[b], Kevin P. Williams[b,*]

[a]*Department of Genetics, Harvard Medical School, Boston, MA, USA*
[b]*Biogen Inc., 14 Cambridge Center, Cambridge, MA, USA*
[c]*Curis Inc., 45 Moulton Street, Cambridge, MA, USA*

Received 29 March 2001; received in revised form 8 May 2001; accepted 15 May 2001

Abstract

A comprehensive comparison of Sonic (Shh), Indian (Ihh), and Desert (Dhh) hedgehog biological activities has not previously been undertaken. To test whether the three higher vertebrate Hh proteins have distinct biological properties, we compared recombinant forms of the N-terminal domains of human Shh, Ihh, and Dhh in a variety of cell-based and tissue explant assays in which their activities could be assessed at a range of concentrations. While we observed that the proteins were similar in their affinities for the Hh-binding proteins; Patched (Ptc) and Hedgehog-interacting protein (Hip), and were equipotent in their ability to induce Islet-1 in chick neural plate explant; there were dramatic differences in their potencies in several other assays. Most dramatic were the Hh-dependent responses of C3H10T1/2 cells, where relative potencies ranged from 80 nM for Shh, to 500 nM for Ihh, to >5 μM for Dhh. Similar trends in potency were seen in the ability of the three Hh proteins to induce differentiation of chondrocytes in embryonic mouse limbs, and to induce the expression of *nodal* in the lateral plate mesoderm of early chick embryos. However, in a chick embryo digit duplication assay used to measure polarizing activity, Ihh was the least active, and Dhh was almost as potent as Shh. These findings suggest that a mechanism for fine-tuning the biological actions of Shh, Ihh, and Dhh, exists beyond the simple temporal and spatial control of their expression domains within the developing and adult organism.

Keywords: Sonic; Indian; Desert; Hedgehog; Patched; C3H10T1/2; Nodal; Digit duplication; Chondrocyte differentiation

1. Introduction

Hedgehog (Hh) proteins are involved in many important developmental processes in vertebrates and invertebrates. In contrast to the single *hh* gene present in *Drospohila*, higher vertebrates have three *hh* genes, *Sonic* (*Shh*), *Indian* (*Ihh*), and *Desert* (*Dhh*) *hedgehog*, and additional family members are present in zebrafish and Xenopus. Each of the vertebrate *hh* appears to have a unique set of roles as first suggested by their distinct expression domains (Bitgood and McMahon, 1995), and subsequently by various functional studies, reviewed in Hammerschmidt et al. (1997). Whether these genes also encode proteins with distinct bioloogical properties is unknown. Shh, of the higher vertebrates homologs, is the most well-studied and has been implicated in the establishment of the early left–right (L–R) axis in the chick embryo (Levin et al., 1995; Tsukui et al., 1999), the regulation of ventral cell fates in the central nervous system (CNS) (Echelard et al., 1993; Ericson et al., 1996, 1997; Roelink et al., 1994, 1995), and the specification of antero-posterior (A-P) axis in the limb (Riddle et al., 1993). Ihh has been implicated in modulating chondrogenesis in the appendicular skeleton, and acts as a negative regulator of the differentiation of proliferating chondrocytes (Vortkamp et al., 1996). Dhh is implicated in germ-cell proliferation, the development of germ cells toward the later stages of spermatogenesis, in nerve–Schwann cell interactions (Bitgood and McMahon, 1995), and in signaling peripheral nerve ensheathment (Parmantier et al., 1999). Mice null for Shh (Chiang et al., 1996), Ihh (St.-Jacques et al., 1999), and Dhh (Bitgood et al., 1996) have further defined key developmental roles.

The mature amino terminal domain of Hh (Bumcrot et al., 1995; Lee et al., 1994) has been shown to be sufficient for all the known long- and short-range activities of this protein. Further biochemical studies have shown that Shh is modi-

* Corresponding author. Tel.: +1-617-679-3341; fax: +1-617-679-3148.
E-mail address: kevin_williams@biogen.com (K.P. Williams).
[1] S. Pathi and S. Pagan-Westphal contributed equally to this article.

0925-4773/01/$ - see front matter
PII: S0925-4773(01)00427-0

fied with a C-terminal cholesterol moiety (Porter et al., 1996), and an N-terminal palmitic acid group (Pepinsky et al., 1998) that serve to tether the protein to the cell surface of the expressing cell resulting in a lipid-modified Hh protein that is 30-fold more potent than the unmodified protein (Pepinsky et al., 1998). While short-range effects can be mediated by such a tethered protein, the mechanism by which this tethered signal is released or transported to mediate long-range effects is currently unclear, although a number of mechanisms have been proposed (reviewed in Christian, 2000; Chuang and Kornberg, 2000).

Vertebrate Hh proteins appear to be processed by the same mechanism (reviewed in Johnston and Scott, 1998) and use the same receptors and signal transduction pathway (Hammerschmidt et al., 1996; Johnston and Scott, 1998; Carpenter et al., 1998). The transmembrane protein Patched (Ptc) is required for cellular responsiveness to Hh, and is highly expressed in all cells known to be actively responding to any of the vertebrate Hh proteins, reviewed in Tabin and McMahon (1997). Ptc is also a receptor for the Hh protein (Ingham et al., 1991; Marigo et al., 1995; Stone et al., 1996). In the absence of Hh, Ptc represses the signaling activity of a second transmembrane protein Smoothened (Smo) (Alcedo et al., 1996; van den Heuvel and Ingham, 1996) by indirectly destabilizing Smo (Denef et al., 2000). Hh binding to Ptc causes Ptc to be removed from the cell surface (Denef et al., 2000), directing it to a distinct subcellular compartment and thereby relieving the repression of Smo signaling. Ptc itself is also an important transcriptional target of Hh signaling, activated downstream of Smo. Because of its ability to bind to Hh, the high levels of Ptc induced by Hh have the effect of acting as a sink, binding additional Hh molecules and thus limiting the range of Hh action (Chen and Struhl, 1996). Vertebrates have at least two *Ptc* genes: *Ptc* (also referred to as *Ptc-1*) and *Ptc-2* (Goodrich et al., 1996; Marigo et al., 1996; Motoyama et al., 1998; Takabatake et al., 1997). Vertebrates also have another Hh-binding protein, hedgehog-interacting protein (Hip), which is also inducible by Hh (Chuang and McMahon, 1999). Zinc-finger transcription factors of the *Gli* family also play critical roles in mediating Hh signaling (reviewed in Ruiz i Altaba, 1999).

A number of assays have been established to assess the effects of the Hh proteins in vitro and in vivo including those assessing alkaline phosphatase induction in C3H10T1/2 cells (Day et al., 1999; Katsuura et al., 1999; Kinto et al., 1997; Nakamura et al., 1997; Pepinsky et al., 1998; Williams et al., 1999), lateralizing activity (Levin et al., 1995; Pagan-Westphal and Tabin, 1998), digit duplication (Riddle et al., 1993; Wada et al., 1999; Yang et al., 1997), motor neuron induction (Roelink et al., 1995), and chondrocyte proliferation (Vortkamp et al., 1996). To determine whether the three forms of vertebrate Hh have an equivalent capacity to induce specific biological responses in vivo, we compared the human forms of Shh, Ihh, and Dhh in these assays over a range of concentrations. We find that all three proteins can elicit similar biological responses, but that their relative potencies differ in an assay-dependent manner.

2. Results

2.1. Structural and functional characterization of human Shh, Ihh, and Dhh

The mature forms of human Shh, Ihh, and Dhh, encoding residues 24–197, residues 28–202, and residues 23–198, respectively (Fig. 1), were expressed in *E. coli* and purified by conventional chromatography. The recombinant proteins were tested for their ability to bind the Hh-binding proteins Ptc and Hip: Shh, Ihh, and Dhh bound Ptc with comparable IC_{50} values, in the 3–7 nM range (Fig. 2) and bound Hip with comparable IC_{50} values, in the 6–15 nM range. Structural characteristics of Shh, Ihh, and Dhh were assessed by thermal denaturation using circular dichroism as a measure of secondary and tertiary structures. The proteins all showed cooperative unfolding and gave comparable T_m values (Shh = 58°C, Ihh = 58°C, and Dhh = 57°C). These analyses indicate that the recombinant proteins are functional and have similar structure.

2.2. Comparative assessment of human Shh, Ihh, and Dhh in cell-based assays

Shh, Ihh, and Dhh were next subjected to analysis in a number of Hh-responsive cell lines. The Hh-responsive cell line C3H10T1/2 has been used to assess the activity of a range of Hh protein forms (Day et al., 1999; Katsuura et al., 1999; Kinto et al., 1997; Nakamura et al., 1997; Pepinsky et al., 1998; Williams et al., 1999). Human Shh produced a dose-dependent response in the C3H10T1/2 alkaline phosphatase (AP) induction assay, with an EC_{50} of 80 nM (Fig. 3A) consistent with our previous observations (Pepinsky et al., 1998; Williams et al., 1999). In the same assay, recom-

```
          * ****  *  **  * * * ******  *  * ******  **  * **
Shh   C'GPGRGF-G- KRRHPKK-LTP LAYKQFIPNV AEKTLGASGR YEGKISRNSE
Ihh   C'GPGRV-VGS RRRPPRK-LVP LAYKQFSPNV PEKTLGASGR YEGKIARSSE
Dhh   C'GPGRGPVG- RRRYARKQLVP LLYKQFVPGV PERTLGASGP AEGRVARGSE

          **  * **** ********** ******* * **   * ***  *** ****
Shh   RFKELTPNYN PDIIFKDEEN TGADRLMTQR CKDKLNALAI SVMNQWPGVK
Ihh   RFKELTPNYN PDIIFKDEEN TGADRLMTQR CKDRLNSLAI SVMNQWPGVK
Dhh   RFRDLVPNYN PDIIFKDEEN SGADRLMTER CKERVNALAI AVMNMWPGVR

          ********** ***  **** **** ***** **** ** * **********
Shh   LRVTEGWDED GHHSEESLHY EGRAVDITTS DRDRSKYGML ARLAVEAGFD
Ihh   LRVTEGWDED GHHSEESLHY EGRAVDITTS DRDRNKYGLL ARLAVEAGFD
Dhh   LRVTEGWDED GHHAQDSLHY EGRALDITTS DRDRNKYGLL ARLAVEAGFD

          ******  *  * ***  *  *  **
Shh   WVYYESKAHI HCSVKAENSV AAKSGG'"
Ihh   WVYYESKAHV HCSVKSEHSA AAKTGG'"
Dhh   WVYYESRNHV HVSVKADNSL AVRAGG'"
```

Fig. 1. Sequence alignment of human Shh, Ihh, and Dhh N-terminal domain sequences. Protein sequences for human Shh (residues 24–197), human Ihh (residues 28–202) and human Dhh (residues 23–198) are shown. Gaps introduced to facilitate alignment are represented by dashes. Residues conserved in all three proteins are shown with asterisks above. Shh has 91% identity with Ihh (one extra residue in Ihh + 17 amino acid differences); Shh has 76% identity with Dhh (two extra residues in Dhh + 42 amino acid differences); Ihh has 80% identity with Dhh (one extra residue in Ihh + 36 amino acid differences).

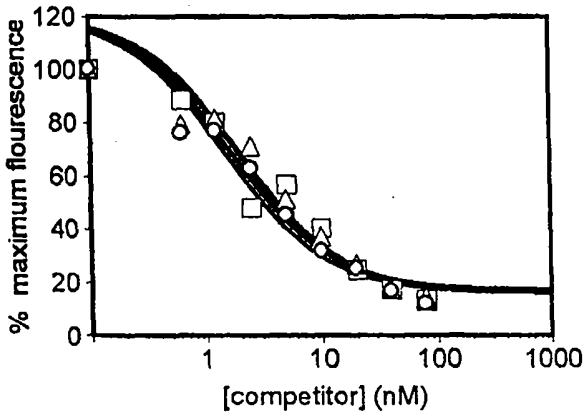

Fig. 2. Comparison of human Shh, Ihh, and Dhh binding to Ptc. The relative potency of human Shh (□), Ihh (Δ), and Dhh (○) for binding to Ptc was assessed on *ptc*-transfected EBNA-293 cells by FACS analysis. Serial dilutions of the test samples were incubated with the *ptc*-transfected EBNA-293 cells and washed, and then the percent binding was measured by the ability of the proteins to compete with Shh-Fc for binding to the cells. Bound Shh-Fc was quantified by mean fluorescence. The data were fitted to a hyperbolic curve by non-linear regression.

binant human Ihh and Dhh have lower potencies (Fig. 3A) with EC_{50} values of 500 nM and >5 μM, respectively, and corresponding lower efficacies, as assessed by the maximal AP response. Despite the large differences in potency, the three Hh proteins exhibited similar induction time courses, with maximal AP response at 5 days (data not shown). Furthermore, these differences in potency could not be accounted for by differences in solubility or stability in the assay medium (data not shown).

Since C3H10T1/2 is a mesenchymal stem cell line (Reznikoff et al., 1973) that can differentiate into a number of different lineages, including osteoblasts, chondrocytes, adipoycytes, and myoblasts, depending on the factor added and the conditions of incubation (Ibric et al., 1988; Katagiri et al., 1990; Taylor and Jones, 1979; Wang et al., 1993), we tested the possibility that Ihh and Dhh might induce differentiation into different cell types, thus accounting for the differences in AP responsiveness observed in this assay. However, when compared to Shh, the reduced potency of Ihh and Dhh for osteoblast induction (as assessed by histochemical detection of AP), was not reflected in the appearance of any other cell types such as adipocytes (as detected by Oil red staining, data not shown). In turn, because the AP induction assay takes 5 days to develop a maximal response, another possibility was that the observed differences in potency might reflect differences in downstream AP signaling events rather than more upstream Hh signaling events. To test this possibility, we assayed Shh, Ihh, and Dhh in C3H10T1/2 cells transfected with a Hh-responsive promoter-luciferase construct, *gli-luc*, where the Hh signaling response is coupled to activation of a known Hh-responsive gene (*gli-1*) and maximal activity is observed within 1 day by measuring luciferase activity. In the 18-h C3H10T1/2 *gli-luc* assay, we observed the same rank and range of potencies for Shh, Ihh, and Dhh as in the AP induction assay, with EC_{50} values of 80 nM, 500 nM, and 5 μM, respectively, suggesting that the differences in potency are at the level of Hh signaling and not further downstream. As an independent measure of Hh-dependant signaling, we also evaluated the ability of the Hh proteins to induce *gli-1*, *ptc*, *ptc-2*, and *hip* mRNA using RT-PCR assays in C3H10T1/2 cells. Shh, Ihh, and Dhh had the same dose responses for each gene, with Shh being more potent than Ihh with Dhh the weakest. Representative data for *gli-1* mRNA induction, as measured by RT-PCR, are shown in Fig. 3B. These findings were confirmed by quantitative PCR studies (data not shown).

2.3. The effects of Ihh, Dhh, and Shh on chondrocyte differentiation in cultured mouse limbs

When proliferating chondrocytes commit to the differentiation pathway, they transiently express Ihh as pre-hypertrophic cells, which leads to a signaling cascade that prevents further cells from entering the pathway toward hypertrophy. This has been demonstrated in vivo, but can also be recapitulated in vitro by directly adding Ihh protein to bone explant cultures (Vortkamp et al., 1996). We compared the relative potencies of the three Hh proteins

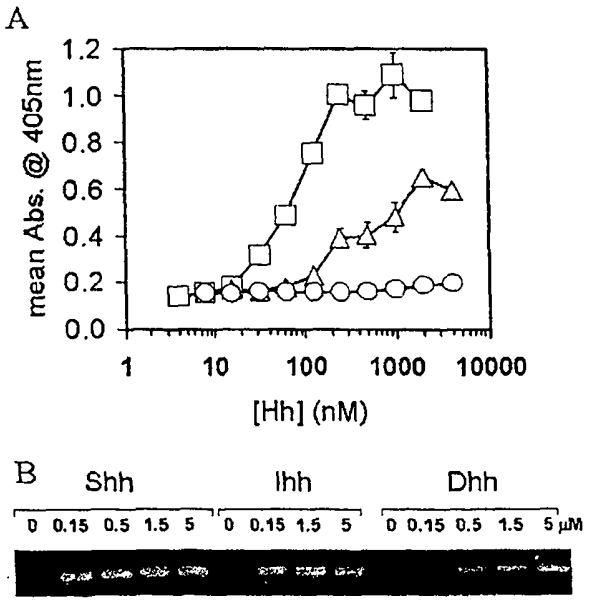

Fig. 3. Human Shh, Ihh, and Dhh have different potencies on C3H10T1/2 cells. (A) The relative activities of Shh, Ihh, and Dhh were assessed in the C3H10T1/2 AP induction assay. Serial two-fold dilutions of Shh (□), Ihh (Δ), and Dhh (○) were incubated with the cells for 5 days and the resulting levels of AP activity measured at 405 nm using the AP chromogenic substrate *p*-nitrophenyl phosphate. (B) Induction of *gli-1* mRNA by Shh, Ihh, and Dhh in C3H10T1/2 cells. RT-PCR for *gli-1* was carried out on total RNA extracted from C3H10T1/2 cells that were incubated for 5 days with the indicated concentrations of Shh, Ihh, and Dhh. Loadings were normalized to actin levels.

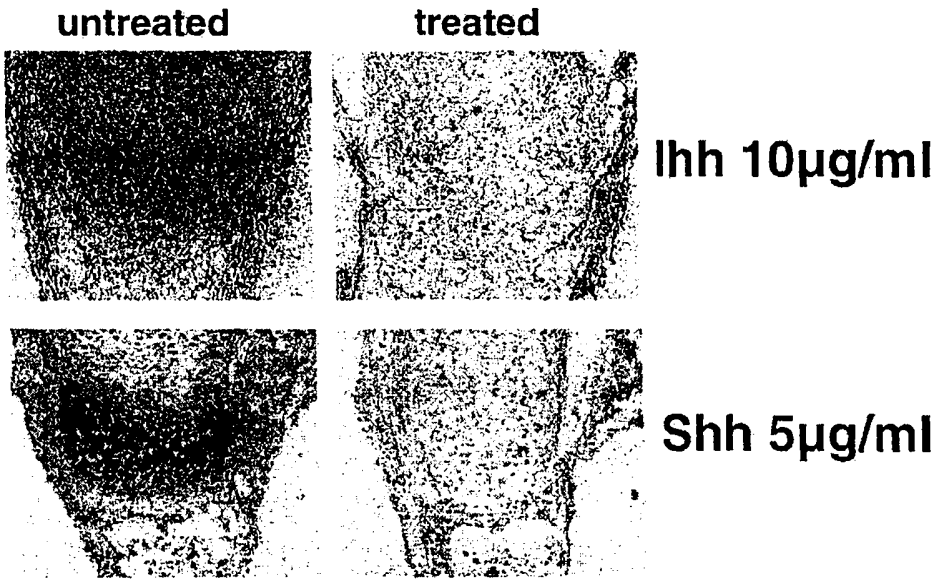

Fig. 4. Examples of total suppression of *Collagen X* expression. E16.5 mouse proximal tibial growth plates were hybridized to a mouse *Collagen X* riboprobe. The examples shown are the lowest concentrations at which Ihh and Shh can completely suppress hypertrophic differentiation of chondrocytes. Treated limbs show a near absence in the expression of *Collagen X* as displayed by the lack of silver grains above background levels. Each protein and concentration was tested in five independent cultures. Dhh was not able to fully suppress *Collagen X* expression at any of the protein concentrations tested.

in suppressing hypertrophic chondrocyte differentiation, a role played by Ihh during normal bone development. Shh, Ihh, and Dhh proteins were added to E16.5 mouse tibia organ cultures as described in Section 4 (Experimental procedures). Section in situ hybridization of the treated and untreated contralateral control limbs revealed differences in the ability of the three proteins to suppress the hypertrophic differentiation of chondrocytes, as measured by the marker for hypertrophic chondrocytes, *Collagen X*. The activities of the three Hh proteins were compared in two ways by determining (i) the lowest concentration at which the exogenous protein totally suppresses *Collagen X* expression (Fig. 4), and (ii) the lowest concentration at which the exogenous protein causes a difference between the treated and untreated contralateral limbs as measured by decreased density of *Collagen X* expression (Fig. 5). Shh completely suppressed *Collagen X* expression at a concentration of 5 µg/ml (Fig. 4). At this concentration, Ihh was not as effective; however, there was a decrease in the amount and density of silver grains in the treated limbs as compared to the untreated contralateral control (data not shown). With Ihh, near total suppression of *Collagen X* expression was achieved at a concentration of 10 µg/ml (Fig. 4), Dhh was unable to fully suppress *Collagen X* expression at any of the protein concentrations tested. The lowest Shh concentration at which treated limbs were noticeably different from their contralateral controls, in terms of *Collagen X* expression, was 0.5 µg/ml (Fig. 5). At this concentration, the Shh-treated limbs showed a decreased density of silver grains as compared to the controls. Ihh and Dhh consistently showed less dense *Collagen X* expression at concentrations of 5 and 20 µg/ml, respectively (Fig. 5). Thus, in this in vitro organ culture assay, Shh appears to be the most potent suppressor

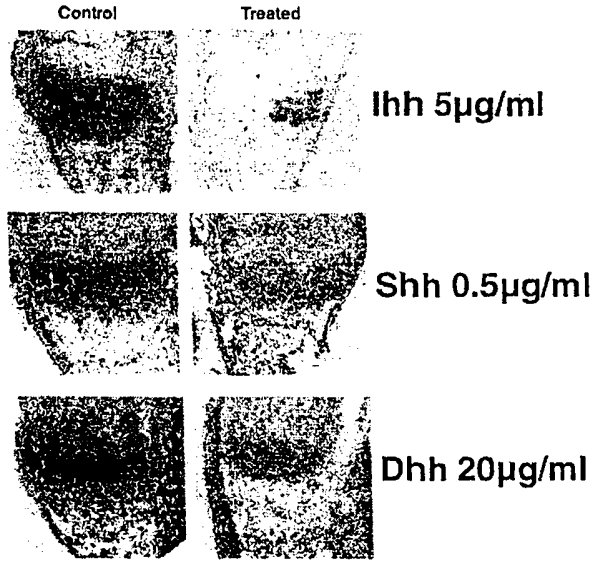

Fig. 5. Examples of cultures showing decreased density of *Collagen X* expression. E16.5 mouse proximal tibial growth plates were hybridized to a mouse *Collagen X* riboprobe. Treated limbs show a decrease in the expression of *Collagen X* as displayed by the decreased density of silver grains. Examples shown correspond to the lowest concentration where a reproducible effect was seen for each. Limbs treated with lower concentrations of their respective proteins have virtually no discernible differences from their untreated contralateral controls. Each protein and concentration was tested in five independent cultures.

of chondrocyte hypertrophy, followed by Ihh, with Dhh having the weakest potency.

2.4. Lateralizing activity of human Shh, Ihh, and Dhh

We next compared the relative potencies of the three Hh proteins in assays based on the early embryonic roles of Shh. The earliest known function of Shh in the chick embryo is in the establishment of left–right asymmetry. Shh, produced exclusively by cells on the left side of Hensen's node, triggers a cascade of signals leading to the expression of several left-side-specific genes, including the transforming growth factor (TGF)-β family member *nodal*, in the lateral plate mesoderm (LPM) (Levin et al., 1995). This lateralizing activity can be assessed by adding Shh protein to the right side of the node, causing *nodal* to be ectopically induced on the right side and resulting in the randomizing of heart sidedness (Levin et al., 1995; Pagan-Westphal and Tabin, 1998). At Shh concentrations of 0.1 mg/ml or greater, *nodal* was activated in a domain identical to that normally seen on the left (Fig. 6A), while at lower concentrations (0.05 mg/ml), *nodal* was activated in a more limited domain and/or in a smaller percentage of embryos (Fig. 6B,C). We used this as an assay to test the relative ability of the different Hh proteins to induce the left-sided signaling cascade, scoring the percentage of embryos displaying any ectopic *nodal* expression following implantation of a protein-laden Affigel-Blue bead (Fig. 6D). While Shh induced *nodal* in 100% of the embryos at 1, 0.5, and 0.1 mg/ml, Ihh required at least 0.5 mg/ml to achieve this effect, only inducing *nodal* in 60% of the embryos at 0.1 mg/ml. Dhh was even less potent in this assay, inducing *nodal* in only 75% of the embryos at 0.5 mg/ml. Thus, the relative potencies of the Hh proteins at inducing the left-sided cascade was the same as in the chondrocyte differentiation, with Shh being the most potent, followed by Ihh, and then by Dhh.

2.5. Polarizing activity of human Shh, Ihh, and Dhh

We next compared the relative potencies of the Hh proteins in causing digit duplications in chick wing buds. In the vertebrate limb, Shh is responsible for A-P patterning as well as supporting the regulation of the proximo-distal (P-D) outgrowth of the limb. During the limb bud stages, Shh is expressed in a subset of posterior mesenchymal cells known as the zone of polarizing activity (ZPA) (Riddle et al., 1993). When Shh-expressing cells or beads containing Shh are implanted into the anterior portion of the limb, a mirror image duplication of the digits results (Riddle et al., 1993; Wada et al., 1999). The degree of digit duplication is Hh-concentration dependent and thus serves as an assay for Shh polarizing activity (Yang et al., 1997). Chicks have three wing digits, referred to as digits 4, 3, and 2 (from posterior to anterior). High levels of Shh ectopically released in the anterior causes a full mirror-image duplication, resulting in a 4-3-2-2-3-4 pattern. Lower levels of Shh result in a less complete duplication. Since a higher level of polarizing activity is required to duplicate a digit 4 than a digit 3, and still less is required to duplicate a digit 2, a quantitative score of polarizing activity can be assigned to a given limb skeletal pattern based on the types of ectopic digits that form (Fig. 7A). Different concentrations of each Hh protein were loaded onto Affigel-Blue beads (as used in the *nodal* induction assay above) and the data are shown in Fig. 7B. Shh showed strong polarizing activity, with an average score of four or higher at 8, 2, and 0.5 mg/ml. Dhh also produced duplications scored at four or higher at 8 and 2 mg/ml, but dropped down to a score of two at 0.5 mg/ml. In contrast, Ihh did not give rise to duplications with an average score above two even at 8 mg/ml. Thus, although the same batches of protein and same beads for delivery were used in the lateralizing and polarizing assays, the relative order of potency in the latter assay was different from the two previous assays for chondrocyte differentiation and lateralizing activity. Shh was still the most potent, but Dhh was significantly better than Ihh at eliciting digit duplications.

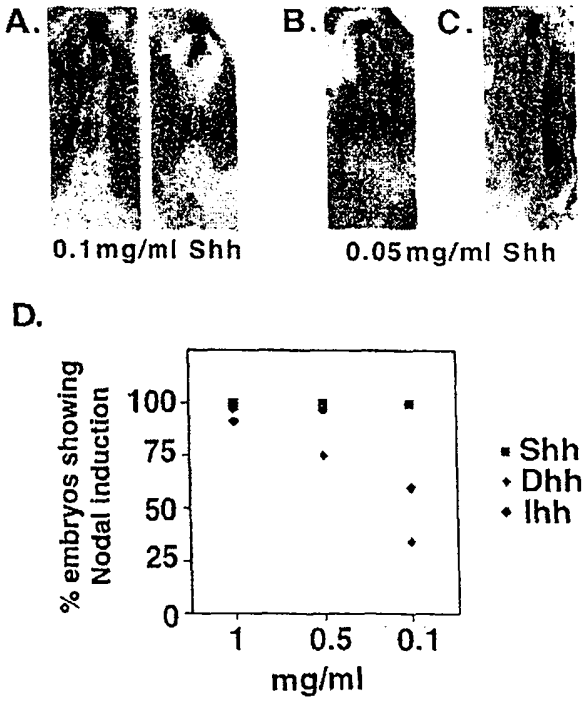

Fig. 6. *Nodal* induction in the right LPM in response to human Hh proteins. Beads soaked in Hh protein were implanted to the right of Hensen's node in stage 4 chick embryos in New culture. At stage 8, the embryos were harvested and *nodal* expression was examined by whole mount in situ hybridization. (A) In response to beads soaked in 0.1 mg/ml Shh, all embryos (two examples are shown) showed bilateral *nodal* expression. (B) At 0.05 mg/ml Shh, many embryos have only partial *nodal* induction, or (C) fail to show any *nodal* expression on the right side. (D) Percent *nodal* induction in the left LPM following Hh protein application. Affigel-Blue beads were soaked in the Hh protein concentrations shown and implanted into gastrulating chick embryos. Each symbol represents the percent *nodal* induction from 10 embryos. Shh (black ■); Ihh (green); Dhh (red ◆).

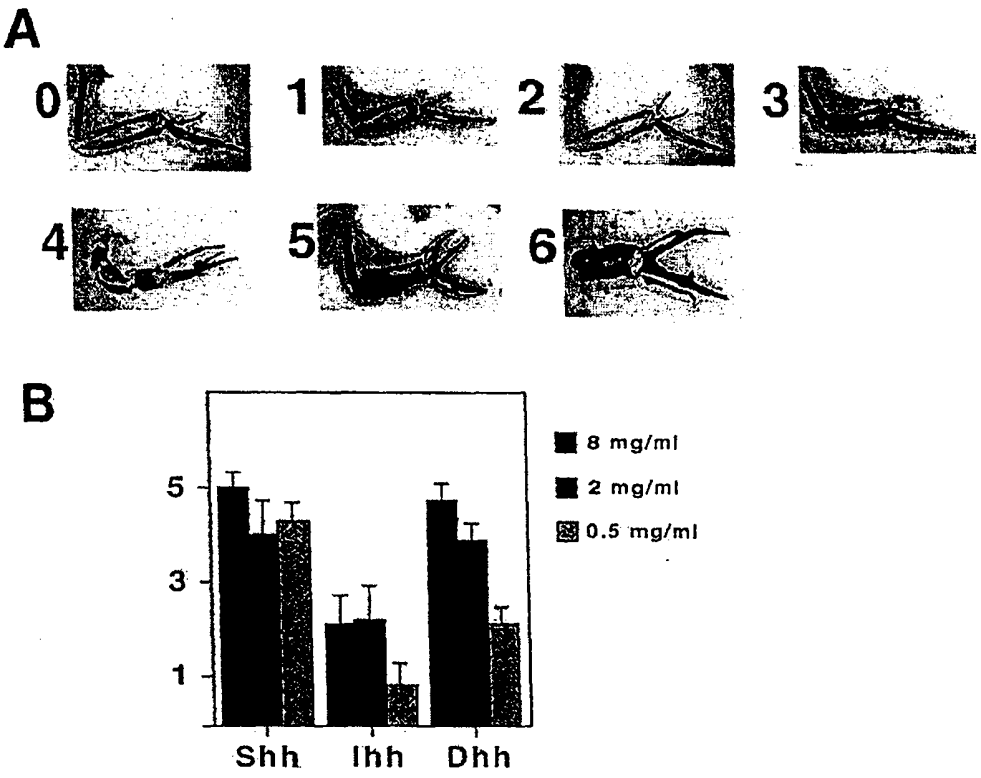

Fig. 7. Relative potencies of human Shh, Ihh, and Dhh in causing digit duplications in chick wing buds. (A) Assay for polarizing activity. Shh protein was loaded onto Affigel-Blue beads and implanted into stage 22 limb buds. In response to different concentrations of Shh protein, a variety of skeletal phenotypes are induced in the limb. A numerical score for the level of polarizing activity is assigned based on the type of ectopic digits produced (0 = no duplication; 1, a partial ectopic digit; 2, a full ectopic digit; 3, an ectopic digit 2 plus an additional partial digit; 4, an ectopic digit 3; 5, an ectopic digit 3 plus an additional partial digit; 6, an ectopic digit 4). Examples of each phenotype and the score assigned are shown. (B) Polarizing activity was scored on the six-point scale following implantation of Affigel-Blue beads soaked in hedgehog protein at 8 (red bar), 2 (blue bar) or 0.5 mg/ml (green bar). Average polarizing activity scores are shown.

2.6. Motor neuron-inducing activity of Shh, Ihh, and Dhh proteins

As an independent measure of function, we also tested the ability of each Hh protein to induce motor neurons in lateral neural tube explants. The induction of neural cell types in response to Shh secreted from the notochord and floor plate in vivo is dose-dependent and can be recapitulated in vitro with explants of lateral neural tube, which have not been exposed to Shh. The induction of motor neurons in such explants can be assayed by antibodies specific to the marker Islet-1 (Roelink et al., 1995). In this assay, Shh, Ihh, and Dhh were equipotent in their Islet-1-inducing activity, with an EC_{50} value of 2 nM.

3. Discussion

A comprehensive comparison of the biological activities of Shh, Ihh, and Dhh hedgehog has not previously been undertaken. To test whether the three higher vertebrate Hh proteins have distinct biological properties, we compared recombinant forms of the N-terminal domains of human Shh, Ihh, and Dhh in a variety of cell-based and tissue explant assays. The highly conserved sequences of Shh, Ihh, and Dhh (Fig. 1) would suggest that they could have overlapping or identical activities (Kumar et al., 1996; Shimeld, 1999). Thus, their activities might be expected to be similar to one another. However, the comparative data for all the assays, summarized in Table 1, does not support this notion. While the three proteins bind the receptor Ptc and Hip with similar affinity and were equipotent in their ability to induce Islet-1 in neural plate explants, in other in vitro assays, large differences in their potency was observed. The rank order of potency was generally Shh > Ihh > Dhh, with Shh and Ihh more closely related in terms of potency than Shh and Dhh, or Ihh and Dhh. Only in the digit duplication assay was the rank order of potencies different; Shh was again the most potent, but in this assay, Dhh was more potent than Ihh. Previous studies have shown that Ihh at sufficient dosage can cause digit duplications (Yang et al., 1998). One possible reason that Ihh may not have been as effective as Shh or Dhh at inducing digit duplication is that its activity was manifested in additional effects such as

Table 1
Differences in the responsiveness of biological systems to human Shh, Ihh, and Dhh

Protein[a]	Shh	Ihh	Dhh
Ptc binding (IC_{50})	3.7 nM	7.1 nM	6.8 nM
Hip binding (IC_{50})	6 nM	15 nM	9 nM
C3H10T1/2 AP induction (EC_{50})	80 nM	500 nM	> 5 μM
C3H10T1/2 gli-luc induction (EC_{50})	80 nM	500 nM	> 5 μM
TM3 gli-luc induction (EC_{50})	80 nM	320 nM	800 nM
Islet-1 induction (EC_{50})	2 nM	2 nM	2 nM
Chondrocyte differentiation	++++	++	+
Left/right nodal induction	++++	++	+
Digit duplication	++++	+	+++

[a] Proteins were generated and assays carried out as described in Section 4 (Experimental procedures).

increasing the thickness of the bones (data not shown). However, even in systems that might be expected to be Ihh-responsive, such as those involved in bone development (chondrocyte differentiation and osteoblast induction in C3H10T1/2 cells), Shh was still the most potent of the three Hh proteins and had an even greater effect on bone thickness than Ihh. It is unclear whether the quantitative differences seen here for the three human Hh proteins are a reflection of differing biological activities, of unidentified components that can modulate their responses dependent on the context of the assay system or from sequence differences for the different proteins.

Nevertheless, there is evidence from zebrafish that under physiological conditions, not all Hh proteins function equivalently. In particular, the zebrafish genes *echidna hedgehog* (*Ehh*), an Ihh homolog, and *Shh*, have been shown to have distinct biological roles: induction of muscle pioneer (MP) cells specifically requires *Ehh* in conjunction with *Shh* (Currie and Ingham, 1996), and micro-injection of *Ehh*, but not *Shh*, can restore MP cells in mutants which have a disrupted notochord. This strongly indicates that the two proteins have distinct biological activities. Conversely, *netrin-1a* expression in zebrafish somites is induced by *Shh* but not by *Ehh* (Lauderdale et al., 1998). We do not know whether these differences are a consequence of true independent activities, or whether it is an assay-dependent effect. It would be interesting to assay the purified zebrafish Ehh and Shh proteins in vitro to determine whether they have overlapping or independent activities.

The differences in potency of human Shh, Ihh, and Dhh described in this study (Table 1) are unlikely to be a consequence of differences in the structural integrity of the three Hh proteins, as they all appear to be folded similarly and can bind the receptor Ptc and Hip with comparable affinities (Table 1). Published studies (Carpenter et al., 1998) demonstrate that in addition to Hip and Ptc, all three mammalian Hh proteins bind with comparable affinities to Ptc-2. Moreover, we also found that Shh, Ihh, and Dhh had comparable activities in the neural plate explant assay (Table 1), indicating that the recombinant forms of Ihh and Dhh can be as functional as Shh in at least one biological system.

Previously, we observed that N-terminally truncated (Williams et al., 1999) and lipid-modified (Pepinsky et al., 1998) forms of Shh bound Ptc with comparable affinities and induced Islet-1 with comparable potencies, but had a wide range of potencies in the C3H10T1/2 assay, with the truncated form being inactive and the lipid-modified form being 30-fold more potent than the unmodified protein. In addition, we found that the activity of Shh in C3H10T1/2 cells, but not in the neural plate explant or Ptc-binding assays, was highly dependent on the N-terminal region of the protein (Williams et al., 1999).

To further investigate whether the differences in relative potencies of the three Hh proteins could be ascribed to effects mediated by the N-terminal region, we have generated chimeras of Shh and Dhh with the first 10 residues of the N-terminal domains swapped (K.P. Williams, E.A. Garber, and P. Rayhorn, unpublished data). Substituting the first 10 residues of Shh with those from Dhh substantially reduced the activity of this chimera (EC_{50} = 400 nM) compared to wild type Shh (EC_{50} = 80 nM), confirming the importance of the N-terminal region of Shh for activity in the C3H10T1/2 assay. The reverse experiment in which we replaced the first 10 residues of Dhh with those of Shh led to a modest increase in potency of this chimera (EC_{50} ≈ 2 μM) compared to wild type Dhh (EC_{50} > 5 μM), suggesting that the inability to regain full activity is not simply due to differences in sequence in this region. These changes in activity are probably not due to gross changes in structure at the N-terminus, since in the X-ray structure of Shh (Pepinsky et al., 2000), this region is extended from the core and is presumably not important for the correct folding of the core protein. Furthermore, circular dichroism of wild type Shh and the N-terminally truncated form of Shh had comparable spectra (Williams et al., 1999). Although the N-terminal portion of the Hh genes are highly conserved in particular the first five amino acid residues which are absolutely conserved in all Hh proteins found to date (Kumar et al., 1996); there is an additional residue for Dhh within the N-terminal region which may result in spatial differences in this region.

An additional observation that we have made in the course of purifying these proteins is that all three Hh proteins bind to heparin. Significantly, Shh- and Ihh-binding were comparable, whereas Dhh appeared to have a much tighter interaction, as assessed by the sodium chloride concentration required for elution. In this regard, one intriguing possibility is that differences in the N-terminal region for the three Hh proteins, though not affecting their ability to bind Ptc, affect their interactions with accessory molecules on the cell surface that in turn modulate their activity. A role for accessory molecules in mediating Hh activity has been implicated previously, particularly the role of proteoglycans in mediating Hh long-range signaling, although a number of

other mechanisms have been proposed, including those mediated by lipid rafts (reviewed in Christian, 2000; Chuang and Kornberg, 2000) and by the Hh receptors themselves (Incardona et al., 2000). Although Shh, Ihh, and Dhh bind Ptc, Ptc-2, and Hip with comparable affinities when the receptors are overexpressed on cells, it may be that in their natural settings these binding events are modified by additional interactions with accessory molecules. Such differences in cellular context may explain the differences in potency of Dhh in C3H10T1/2 cells versus the Leydig cell line TM3, where we observed a substantial increase in the potency of Dhh compared to its potency in C3H10T1/2 cells, although it was still less potent than Shh or Ihh (Table 1). Significantly, Dhh is expressed in Sertoli cells and Leydig cells have been identified as the responding cell type (Bitgood et al., 1996; Clark et al., 2000). Furthermore, Ptc-2, but not Ptc, has been localized to Leydig cells, and Ptc-2 has been proposed to be the endogenous receptor for Dhh (Carpenter et al., 1998). Thus, in TM3 cells with Ptc-2 but not Ptc present, the repertoire of accessory molecules on these cells may act to increase the interaction of Dhh with Ptc-2.

The multiple *hh* genes of vertebrates have presumably arisen by duplication and subsequent divergence of a single ancestral *hh* gene. Although Shh, Ihh, and Dhh are highly homologous, Shh is much closer to Ihh than Dhh in sequence identity (Fig. 1). Our findings in a range of biological systems supports this notion, since Shh and Ihh appear to be closer in potency and function than Dhh in the majority of assays. It has been postulated that *Shh* has maintained essential ancestral roles in midline patterning, leaving *Ihh* and *Dhh* genes free to diverge and take on new roles (Kumar et al., 1996; Shimeld, 1999). Consistent with this is the observation that the *Shh* gene knockout in mice is embryonic lethal (Chiang et al., 1996), while the *Dhh* knockout animals survive to adulthood with only minor defects (Bitgood et al., 1996). Here we show that the three Hh proteins have the potential to function similarly, although in certain assays they have different potencies. These differences in the ability to elicit specific biological responses may reflect unknown control mechanisms for modulating Hh activity during development. Whether they represent the presence of additional unidentified factors on the pathway or result from sequence differences for Shh, Ihh, and Dhh remains to be determined.

4. Experimental procedures

4.1. Preparation of Hh

Recombinant human Shh (residues 24–197) was expressed in *E. coli* and purified as described previously (Pepinsky et al., 1998; Williams et al., 1999). cDNAs encoding human Ihh (residues 28–202) and human Dhh (residues 23–198) (Curis Inc., Cambridge, MA, USA) were subcloned into the pET11d expression vector (Novagen) as His-tagged constructs with an enterokinase cleavage site engineered into the constructs adjacent to the N-terminal cysteine, and transformants were grown as described previously for His-tagged human Shh (Williams et al., 1999). Ihh and Dhh were purified following the protocol described previously for the purification of human Shh (Williams et al., 1999).

4.2. Hedgehog cell-based assays

Ptc binding and C3H10T1/2 AP induction assays were performed as described previously (Pepinsky et al., 1998; Williams et al., 1999). For Ptc-binding experiments, EBNA 293 cells transiently transfected with a Myc-tagged, C-terminally truncated murine *ptc* cDNA construct (a gift of Matt Scott, Stanford University) were titrated with serial two-fold dilutions of each test compound in the presence of 5 nM Shh-IgG_1 fusion protein reporter (Shh-Fc) (Williams et al., 1999). Cells were washed, fixed, and read on a fluorescence-activated cell sorter. Binding constants were calculated from single determinants for each sample. Shh-Fc was observed to bind to Ptc directly with a K_D value of 3 nM. An assay to measure Hh binding to Hip was performed by transiently transfecting a *Hip* cDNA construct (a gift of Andy McMahon, Harvard University) into EBNA 293 cells and measuring Hh binding as described for the Ptc binding assay above. For this assay, Shh-Fc was observed to bind to Hip directly with a K_D value of 10 nM.

For assessing activity, C3H10T1/2 cells (ATCC) were incubated for 5 days with serial dilutions of each Hh protein. The cells were lysed and assayed for AP activity using the chromogenic substrate *p*-nitrophenyl phosphate (read at 405 nm). Each sample was analyzed in duplicate, and EC_{50} values were measured from the mean data values. Samples were also tested for function on C3H10T1/2 and TM3 cells (murine Leydig cell, ATCC) transfected with a luciferase reporter under the control of the *gli-1* promoter. Details of this assay will be published elsewhere (J.A. Porter, D. Bumcrot, and G.S.B. Horan, unpublished data).

The induction of *gli-1*, *ptc*, *ptc-2*, and *hip* mRNA by Hh in C3H10T1/2 and TM3 cells was measured by RT-PCR as described previously (Williams et al., 1999). Total RNA was extracted from the cells with Trizol (Life Technologies, Gaithersburg, MD, USA) and subjected to RT-PCR. Primer sequences for *gli-1* were: 5′-CGGGGTCTCAAACTGCC-CAGCTT-3′, and 5′-GGCTGGGTCACTGGCCCTC-3′.

4.3. Chondrocyte differentiation assay

The ability of the different Hh proteins to block chondrocyte differentiation was assessed by culturing E16.5 mouse hindlimbs with different concentrations of human Shh, Ihh, or Dhh proteins. Hindlimbs were severed at mid-femur, deskinned, and cultured as described previously (Vortkamp et al., 1996). Treated hindlimbs were cultured with either 20, 10, 5, 1, or 0.5 μg/ml of Hh protein, while the contralateral

hindlimb was cultured as an untreated control. After 4 days in culture, limbs were fixed in 4% paraformaldehyde/PBS. The state of chondrocyte differentiation was compared by detecting *Collagen X* mRNA expression in the growth plate of the proximal tibia. In situ hybridizations (5 μm serial sections) were performed using ^{33}P-UTP-labeled riboprobes as described previously (Vortkamp et al., 1996). Hybridizations were performed at 70°C in 50% formamide, and post-hybridization washes were carried out at 55°C in 50% formamide/2 × SSC. For serial sections, three successive sections were collected.

4.4. Left/right assay

Hamburger–Hamilton (HH) stage 4 chick embryos were processed for New culture (New, 1955) and implanted with protein-soaked beads as described previously (Levin et al., 1995). Affigel-Blue beads were soaked in either 1, 0.5, or 0.1 mg/ml of Hh protein. Protein-soaked beads were implanted on the right side of Hensen's Node. Embryos were harvested at stage 8, fixed in 4% paraformaldehyde/PBS, and processed for whole-mount in situ hybridization using a probe for *nodal*, as described previously (Levin et al., 1995).

4.5. Digit duplication assay

Fertilized chicken eggs (Spafas) were incubated at 38°C until the embryos reached HH stage 21. Protein-soaked beads were then placed in the anterior region of the right-side wing bud as described previously (Riddle et al., 1993). Beads were soaked in either 8, 2, or 0.5 mg/ml of Hh protein. Embryos were harvested at stage 36, fixed in 4% paraformaldehyde/PBS, and stained with Alcian blue. Polarizing activity was assessed by scoring for the degree of digit duplication.

4.6. Neural plate explant assay

The motor neuron-inducing activity of the Hh proteins was assessed in a neural plate explant assay as described previously for human Shh (Williams et al., 1999). Intermediate neural plate explants dissected from the caudal region of stage 10 chick embryos were embedded in a collagen gel, Hh protein was added, and the explants were cultured for 60 h in N2 medium. After fixing with 1% paraformaldehyde, Islet-1-positive nuclei were detected with an anti-Islet-1 mAb (Developmental Studies Hybridoma Bank, University of Iowa; deposited by Dr T. Jessell, Columbia University) and counted using a microscope equipped with fluorescence optics.

Acknowledgements

The authors thank Amie Carmillo, Eric Day, Sarah Bixler, Jennifer Reilly, Dingyi Wen, Xiaoping Hronowski, Susan Foley, Stephan Miller and Weihong Shen for their contributions to this work, and Alphonse Galdes of Biogen, Inc. and Kyle Vogan of Harvard Medical School for valuable discussions and comments on the manuscript. This work was partially funded by a grant to C.J.T. from the National Institutes of Health.

References

Alcedo, J., Ayzenzon, M., Von Ohlen, T., Noll, M., Hooper, J.E., 1996. The *Drosophila* smoothened gene encodes a seven-pass membrane protein, a putative receptor for the hedgehog signal. Cell 86, 221–232.

Bitgood, M.J., McMahon, A.P., 1995. Hedgehog and Bmp genes are coexpressed at many diverse sites of cell–cell interaction in the mouse embryo. Dev. Biol. 172, 126–138.

Bitgood, M.J., Shen, L., McMahon, A.P., 1996. Sertoli cell signaling by Desert hedgehog regulates the male germline. Curr. Biol. 6, 298–304.

Bumcrot, D.A., Takada, R., McMahon, A.P., 1995. Proteolytic processing yields two secreted forms of Sonic hedgehog. Mol. Cell. Biol. 15, 2294–2303.

Carpenter, D., Stone, D.M., Brush, J., Ryan, A., Armanini, M., Frantz, G., Rosenthal, A., de Sauvage, F.J., 1998. Characterization of two patched receptors for the vertebrate hedgehog protein family. Proc. Natl Acad. Sci. USA 95, 13630–13634.

Chen, Y., Struhl, G., 1996. Dual roles for patched in sequestering and transducing Hedgehog. Cell 87, 553–563.

Chiang, C., Litingtung, Y., Lee, E., Young, K., Corden, J.L., Westphal, H., Beachy, P.A., 1996. Cyclopia and defective axial patterning in mice lacking Sonic hedgehog gene function. Nature (London) 383, 407–413.

Christian, J.L., 2000. BMP, Wnt and hedgehog signals: how far can they go? Curr. Opin. Cell. Biol. 12, 244–249.

Chuang, P.T., Kornberg, T.B., 2000. On the range of hedgehog signaling. Curr. Opin. Genet. Dev. 10, 515–522.

Chuang, P.T., McMahon, A.P., 1999. Vertebrate hedgehog signaling modulated by induction of a Hedgehog-binding protein. Nature 397, 617–621.

Clark, A.M., Garland, K.K., Russell, L.D., 2000. Desert hedgehog (Dhh) gene is required in the mouse testis for formation of adult-type Leydig cells and normal development of peritubular cells and seminiferous tubules. Biol. Reprod. 63, 1825–1838.

Currie, P.D., Ingham, P.W., 1996. Induction of a specific muscle cell type by a hedgehog-like protein in zebrafish. Nature 382, 452–455.

Day, E.S., Wen, D., Garber, E.A., Hong, J., Avedissian, L.S., Rayhorn, P., Shen, W., Zeng, C., Bailey, V.R., Reilly, J.O., Roden, J.A., Moore, C.B., Williams, K.P., Galdes, A., Whitty, A., Baker, D.P., 1999. Zinc-dependent structural stability of human Sonic hedgehog. Biochemistry 38, 14868–14880.

Denef, N., Neubuser, D., Perez, L., Cohen, S.M., 2000. Hedgehog induces opposite changes in turnover and subcellular localization of patched and smoothened. Cell 102, 521–531.

Echelard, Y., Epstein, D.J., St.-Jacques, B., Shen, L., Mohler, J., McMahon, J.A., McMahon, A.P., 1993. Sonic Hedgehog, a member of a family of putative signaling molecules, is implicated in the regulation of CNS polarity. Cell 75, 1417–1430.

Ericson, J., Morton, S., Kawakami, A., Roelink, H., Jessell, T.L., 1996. Two critical periods of Sonic hedgehog signaling required for the specification of motor neuron identity. Cell 87, 661–673.

Ericson, J., Briscoe, J., Rashbass, P., van Heyningen, V., Jessell, T.M., 1997. Graded sonic hedgehog signaling and the specification of cell fate in the ventral neural tube. Cold Spring Harbour Symp. Quant. Biol. 62, 451–466.

Goodrich, L.V., Johnson, R.L., Milenkovic, L., McMahon, J.A., Scott, M.P., 1996. Conservation of the hedgehog/patched signaling pathway from flies to mice: induction of a mouse patched gene by Hedgehog. Genes Dev. 10, 301–312.

Hammerschmidt, M., Bitgood, M.J., McMahon, A.P., 1996. Protein kinase

A is a common negative regulator of Hedgehog signaling in the vertebrate embryo. Genes Dev. 10, 647–658.

Hammerschmidt, M., Brook, A., McMahon, A.P., 1997. The world according to hedgehog. Trends Genet. 13, 14–21.

Ibric, L.L., Benedict, W.F., Peterson, A.R., 1988. Simultaneous determination of ascorbic acid and dehydroascorbic acid in cultures of C3H/10T1/2 cells. In Vitro Cell Dev. Biol. 24, 669–676.

Incardona, J.P., Lee, J.H., Robertson, C.P., Enga, K., Kapur, R.P., Roelink, H., 2000. Receptor-mediated endocytosis of soluble and membrane-tethered Sonic hedgehog by Patched-1. Proc. Natl Acad. Sci. USA 97, 12044–12049.

Ingham, P.W., Taylor, A.M., Nakano, Y., 1991. Role of the *Drosophila* patched gene in positional signalling. Nature 353, 184–187.

Johnston, R.L., Scott, M.P., 1998. New players and puzzles in the hedgehog signaling pathway. Curr. Opin. Genet. Dev. 8, 450–456.

Katagiri, T., Yamaguchi, A., Ikeda, T., Yoshiki, S., Wozney, J.M., Rosen, V., Wang, E.A., Tanaka, H., Omura, S., Suda, T., 1990. The non-osteogenic mouse pluripotent cell line, C3H10T1/2, is induced to differentiate *into* osteoblastic cells by recombinant human bone morphogenetic protein-2. Biochem. Biophys. Res. Commun. 172, 295–299.

Katsuura, M., Hosono-Sakuma, Y., Wagatsuma, M., Yanagisawa, S., Okazaki, M., Kimura, M., 1999. The NH2-terminal region of the active domain of sonic hedgehog is necessary for its signal transduction. FEBS Lett. 447, 325–328.

Kinto, N., Iwamoto, M., Enomoto-Iwamoto, M., Noji, S., Ohuchi, H., Yoshioka, H., Kataoka, H., Wada, Y., Yuhao, G., Takahashi, H.E., Yoshiki, S., Yamaguchi, A., 1997. Fibroblasts expressing Sonic hedgehog induce osteoblast differentiation and ectopic bone formation. FEBS Lett. 404, 319–323.

Kumar, S., Balczarek, K.A., Lai, Z.C., 1996. Evolution of the hedgehog gene family. Genetics 142, 965–972.

Lauderdale, J.D., Pasquali, S.K., Fazel, R., van Eeden, F.J., Schauerte, H.E., Haffter, P., Kuwada, J.Y., 1998. Regulation of netrin-1a expression by hedgehog proteins. Mol. Cell. Neurosci. 11, 194–205.

Lee, J.J., Ekker, S.C., von Kessler, D.P., Porter, J.A., Sun, B.I., Beachy, P.A., 1994. Autoproteolysis in hedgehog *protein biogenesis. Science* 266, 1528–1537.

Levin, M., Johnson, R.L., Stern, C.D., Kuehn, M., Tabin, C., 1995. A molecular pathway *determining left–right* asymmetry in chick embryogenesis. Cell 82, 803–814.

Marigo, V., Roberts, D.J., Scott, M.K.L., Tsukurov, O., Levi, T., Gastier, J.M., Epstein, D.J., Gilbert, D.J., Copeland, N.G., Seidman, C.E., Jenkins, N.A., Seidman, J.G., McMahon, A.P., Tabin, C., 1995. Cloning, expression, and chromosomal location of Shh and Ihh: two human *homologues of the Drosophila* segment polarity gene hedgehog. Genomics 28, 44–51.

Marigo, V., Davey, R.A., Zuo, Y., Cunningham, J.M., Tabin, C.J., 1996. Biochemical evidence that patched is the hedgehog receptor. Nature 384, 176–179.

Motoyama, J., Takabatake, T., Takeshima, K., Hui, C., 1998. Ptch2, a second mouse Patched gene is co-expressed with Sonic hedgehog. Nat. Genet. 18, 104–106.

Nakamura, T., Aikawa, T., Iwamoto-Enomoto, M., Iwamoto, M., Higuchi, Y., Maurizio, P., Kinto, N., Yamaguchi, A., Noji, S., Kurisu, K., Matsuya, T., 1997. Induction of osteogenic differentiation by hedgehog proteins. Biochem. Biophys. Res. Commun. 237, 465–469.

New, D.A.T., 1955. A new technique for the cultivation of the chick embryo in vitro. J. Embroyol. Exp. Morphol. 3, 326–331.

Pagan-Westphal, S.M., Tabin, C.J., 1998. The transfer of left–right positional information during chick embryogenesis. Cell 93, 25–35.

Parmantier, E., Lynn, B., Lawson, D., Turmaine, M., Namini, S.S., Chakrabarti, L., McMahon, A.P., Jessen, K.R., Mirsky, R., 1999. Schwann cell-derived Desert hedgehog controls the development of peripheral nerve sheaths. Neuron 23, 713–724.

Pepinsky, R.B., Zeng, C., Wen, D., Rayhorn, P., Baker, D.P., Williams, K.P., Bixler, S.A., Ambrose, C.M., Garber, E.A., Miatkowski, K., Taylor, F.R., Wang, E.A., Galdes, A., 1998. Identification of a palmitic acid-modified *form of human Sonic* hedgehog. J. Biol. Chem. 273, 14037–14045.

Pepinsky, R.B., Rayhorn, P., Day, E.S., Dergay, A., Williams, K.P., Galdes, A., Taylor, F.R., Boriack-Sjodin, P.A., Garber, E.A., 2000. Mapping sonic hedgehog–receptor interactions by steric interference. J. Biol. Chem. 275, 10995–11001.

Porter, J.A., Ekker, S.C., Park, W.J., von Kessler, D.P., Young, K.E., Chen, C.H., Ma, Y., Woods, A.S., Cotter, R.J., Koonin, E.V., Beachy, P.A., 1996. Hedgehog patterning activity: role of a lipophilic modification mediated by the carboxy-terminal autoprocessing domain. Cell 86, 21–34.

Reznikoff, C.A., Brankow, D.W., Heidelberger, C., 1973. Establishment and characterization of a cloned line of C3H mouse embryo cells sensitive to postconfluence inhibition of division. Cancer Res. 33, 3231–3238.

Riddle, R.D., Johnson, R.L., Laufer, E., Tabin, C., 1993. Sonic hedgehog mediates the polarising activity of the ZPA. Cell 75, 1401–1416.

Roelink, H., Augsburger, A., Heemskerk, J., Korzh, V., Norlin, S., Ruiz i Altaba, A., Tanabe, Y., Placzek, M., Edlund, T., Jessell, T.M., Dodd, J., 1994. Floor plate and motor neuron induction by vhh-1, a vertebrate *homolog of hedgehog* expressed by the notochord. Cell 76, 761–775.

Roelink, H., Porter, J.A., Chiang, C., Tanabe, Y., Chang, D.T., Beachy, P.A., Jessell, T.M., 1995. Floor plate and motor neuron induction by different concentrations of the amino-terminal cleavage product of Sonic hedgehog autoproteolysis. Cell 81, 445–455.

Ruiz i Altaba, A., 1999. Gli proteins and Hedgehog signaling: development and cancer. Trends Genet. 15, 418–425.

Shimeld, S.M., 1999. The evolution of the hedgehog gene family in chordates: insights from amphioxus hedgehog. Dev. Genes. Evol. 209, 40–47.

St.-Jacques, B., Hammerschmidt, M., McMahon, A.P., 1999. Indian hedgehog signaling regulates proliferation and differentiation of chondrocytes and is essential for bone formation. Genes Dev. 13, 2072–2086.

Stone, D.M., Hynes, M., Armanini, M., Swanson, T.A., Gu, Q., Johnson, R.L., Scott, M.P., Pennica, D., Goddard, A., Phillips, H., Noll, M., Hooper, J.E., de Sauvage, F., Rosenthal, A., 1996. The tumour-suppressor gene product *Patched* encodes a candidate receptor for Sonic hedgehog. Nature 384, 129–134.

Tabin, C.J., McMahon, A.P., 1997. Recent advances in hedgehog signalling. Trends Cell. Biol. 7, 442–446.

Takabatake, T., Ogawa, M., Takahashi, T.C., Mizuno, M., Okamoto, M., Takeshima, K., 1997. Hedgehog and patched gene expression in adult ocular tissues. FEBS Lett. 410, 485–489.

Taylor, S.M., Jones, P.A., 1979. Multiple new phenotypes induced in 10T1/2 and 3T3 cells treated with 5-azacytidine. Cell 17, 771–779.

Tsukui, T., Capdevila, J., Tamura, K., Ruiz-Lozano, P., Rodriguez-Esteban, C., Yonei-Tamura, S., Magallon, J., Chandraratna, R.A., Chien, K., Blumberg, B., Evans, R.M., Belmonte, J.C., 1999. Multiple left–right asymmetry defects in Shh(-/-) mutant mice unveil a convergence of the shh and retinoic acid pathways in the control of Lefty-1. Proc. Natl Acad. Sci. USA 96, 11376–11381.

van den Heuvel, M., Ingham, P.W., 1996. Smoothened encodes a receptor-like serpentine protein required for hedgehog signaling. Nature 382, 547–551.

Vortkamp, A., Lee, K., Lanske, B., Segre, G.V., Kronenberg, H.M., Tabin, C.J., 1996. Regulation of rate of cartilage differentiation by Indian hedgehog and PTH-related protein. Science 273, 613–622.

Wada, N., Kawakami, Y., Nohno, T., 1999. Sonic hedgehog signaling during digit pattern duplication after application of recombinant protein and expressing cells. Dev. Growth Differ. 41, 567–574.

Wang, E.A., Israel, D.I., Kelly, S., Luxenberg, D.P., 1993. Bone morphogenetic protein-2 causes commitment and differentiation in C3H10T1/2 and 3T3 cells. Growth Factors 9, 57–71.

Williams, K.P., Rayhorn, P., Chi-Rosso, G., Garber, E.A., Strauch, K.L., Horan, G.S., Reilly, J.O., Baker, D.P., Taylor, F.R., Koteliansky, V., Pepinsky, R.B., 1999. Functional antagonists of sonic hedgehog reveal

the importance of the N terminus for activity. J. Cell Sci. 112, 4405–4414.

Yang, Y., Drossopoulou, G., Chiang, P.-T., Duprez, D., Marti, E., Bumcrot, D., Clarke, J., Niswander, L., McMahon, A., Tickle, C., 1997. Relationship between dose, distance and time in Sonic hedgehog-mediated regulation of anteroposterior polarity in the chick limb. Development 124, 4393–4404.

Yang, Y., Guillot, P., Boyd, Y., Lyon, M.F., McMahon, A.P., 1998. Evidence that preaxial polydactyly in the Doublefoot mutant is due to ectopic Indian hedgehog signaling. Development 125, 3123–3132.